THESIS

AUTHOR - N. G. PATEL

SUPERVISOR - K. H. GRIFFIN

DEPARTMENT OF AIRCRAFT DESIGN

BUCKLING OF CORRUGATED CORE SANDWICH PANELS.

1968/1969

19th SEPTEMBER 1969.

31 M

SUMMARY

A computer program is developed to determine the buckling stresses and deflections of symmetric corrugated core sandwich panels. In the program freedom for lateral deflections at core to face-plate junction is allowed for. Provision is also made to study the effect of variation of core bend radius.

A range of test specimens using four basic core configurations is designed to assess the effect of core bend radius on the buckling stress of the panel.

The computer program indicates that above a certain value of core bend radius there is a marked drop in the value of critical buckling stress and a change in buckling mode.

The values of deflections at core to face-plate junctions at low buckling wave-lengths are not reliable.

Due to the limited range of the experimental work, it is not possible to draw any conclusions on the effect of core bend radius on the buckling stress.

The method used for determining the experimental buckling load is somewhat subjective in application, and its accuracy is difficult to assess.

In general, the experimental values of buckling stresses are 15% higher than those predicted by the computer program. These discrepancies are not large when dimensional and material property variations are considered and indicate that the computer results are giving the correct trend and are conservative.

Recommendations are made for:

(i) Investigation of the buckling deflections at low values of buckling wave-lengths for specimens with high face-plate-to-core thickness ratio.

(ii) A test programme covering a wider range of specimens than that covered by the test programme in this study.

and (iii) Trying out the other two methods of determining the buckling load.

ACKNOWLEDGEMENTS.

The Author wishes to express his thanks to Mr. K.H.Griffin, Mr.T.Borthwick and the Technical Staff for their helpful advice and co-operation.

LIST OF CONTENTS :

.........(/continued.)...

.........(/continuation.)

LIST OF CONTENTS. Page No.

SECTION 1.

THE PROBLEM

1. THE PROBLEM.

The Royal Aeronautical Society Data Sheets in 02.01.28 series deal with the local instability of bonded corrugated-core sandwich panels under longitudinal compression. The theoretical values calculated from the data sheets are compared with the Handley Page test data. (Ref.2).

Large unexplained discrepancies are apparent between the test results and the theoretical values.

Work done by Wittrick at the University of Birmingham concluded that the analysis in Data Sheets 02.01.28 which is based upon the movement of the core to face-plate junctions and buckling modes which are repeated every pitch is substantially correct. Further, in cases of specimens which buckled well below the values predicted by the data sheets, probability of bond failure or some similar event was suggested.

The purpose of this work is to investigate several factors which could explain the discrepancy between the theoretical and test values.

SECTION 2.

THEORETICAL ANALYSIS

2. THEORETICAL ANALYSIS

2.1 Review of Previous Study.

Wittrick has devised a computer program which determines the buckling characteristics of the test specimens and accounts for the effects of panel edge restraint, core (transverse) stiffness, the movement of core to face plate junctions, overall buckling effects and transverse buckling modes extending over 1 or 2 pitches. The results of the computer program indicate that the theoretical basis of the Data Sheets is sound, even when overall displacement of the panel is allowed. (Ref.4).

2.2 Line of Action of this Study.

The basic theoretical approach used so far has assumed perfect connection at intersections of centre-line of flats.

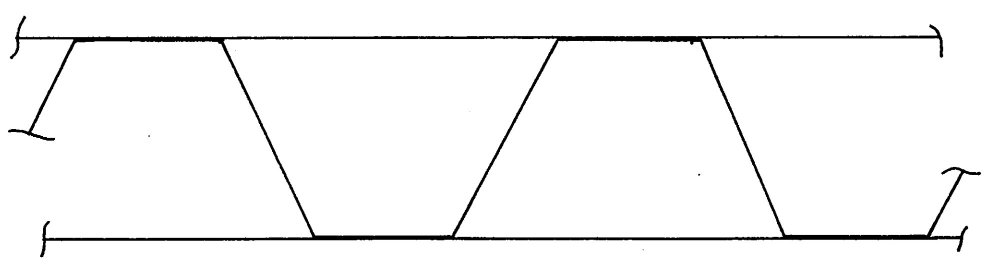

In the theoretical analysis described below, a computer program is developed to examine the effect on buckling stress of the radiused corners of the corrugation, both from the point of the flexibility of the curved corner and of the modification of the effective point of attachment.

In addition, several transverse buckling modes repeating over 1 or 2 pitches are considered.

2.3 Preliminary Studies.

2.3.1 Estimation of the stiffness of the corrugated core.

Preliminary work is done to estimate the stiffness of the corrugated core. The Handley Page specimen 37 (see Section 3) is considered.

The core 'flat' is assumed to be pin-jointed at 'a' and 'd'.

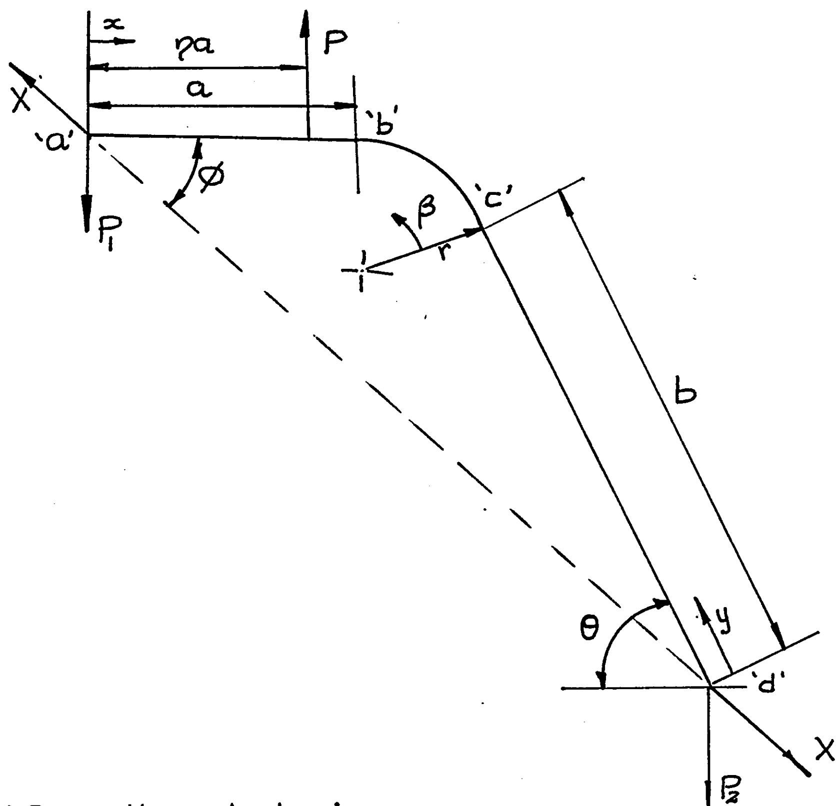

X and P are the redundancies.

Geometrical properties of the core.

(4:1 Scale)

p, pitch = 4.4"

r, bend radius = 0.48"

a, half-flat width = 0.8"

θ, = 61^o

ϕ = 41^o

b = 1.8"

<u>Case 1.</u> P is considered to act at $x = a$.

$$P_1 = \left(\frac{b \cos\theta + r \sin\theta}{a + b\cos\theta + r\sin\theta} \right) P = 0.6176\, P \qquad \ldots(1)$$

$$P_2 = \left(\frac{a}{a + b\cos\theta + r\sin\theta} \right) P = 0.3824\, P \qquad \ldots(2)$$

<u>Between 'd' and 'c'</u>

Bending moment,

$$M = \left\{ P_2 \cos\theta - X \sin(\theta - \phi) \right\} y$$

+ve

$$= (.1853P - .342X)y \qquad \ldots(3)$$

<u>Between 'b' and 'c'</u>

$$M = \left\{ P_2 \sin\theta + X \cos(\theta-\phi) \right\} r(1 - \cos\beta) \qquad \left(\begin{array}{c} \text{For} \\ 0 \leq \beta \leq \theta \end{array} \right)$$

$$+ \left\{ P_2 \cos\theta - X \sin(\theta-\phi) \right\} (b + r\sin\beta)$$

$$= (.0889P - .1641X)\sin\beta - (.1605P + .451X)\cos\beta$$

$$+ (.4924P - .1646X) \qquad \ldots(4)$$

<u>Between 'a' and 'b'</u>

$$M = (P_1 - X\sin\phi)\, x$$

+ve

$$= (.6176P - .6561X)\, x \qquad \ldots(5)$$

The Strain Energy,

$$\delta U^* = \int_0^l \frac{M \,\partial M}{EI}\, ds$$

$$EI\,\delta U^* = (.1853P - .342X)(.1853\,\delta P - .342\,\delta X)\int_0^b y^2 dy$$

$$+ \left\{(.0889P - .1641X)\mathrm{Sin}\beta - (.1605P + .451X)\mathrm{Cos}\beta + (.4924P - .1646X)\right\}$$

$$\left\{(.0889\,\delta P - .1641\,\delta X)\int_0^\theta \mathrm{Sin}\,\beta\, r\, d\beta - (.1605\,\delta P + .451\,\delta X)\int_0^\theta \mathrm{Cos}\,\beta\; r\; d\beta + (.4942\delta P - .646\delta X)\int_0^\theta r d\beta\right\}$$

$$+ (.6176P - .6561X)(.6176\delta P - .6561\delta X)\int_0^a x^2\, dx$$

Integrating and simplifying,

$$\begin{aligned}
EI\,\delta U^* = & \ (.3602P - .6648X)\ (.1853\,\delta P - .342\,\delta X) \\
+ & \ (.0136P - .0252X)\ (.0889\,\delta P - .1641\delta X) \\
+ & \ (.0572P + .1608X)\ (.1605\,\delta P - .4510\delta X) \\
+ & \ (.2525P - .0841X)\ (.4942\,\delta P - .1646\delta X) \\
- & \ (.0163P - .0301X)\ (.1605\,\delta P + .4510\delta X) \\
- & \ (.0294P + .0827X)\ (.0889\,\delta P - .1641\delta X) \\
+ & \ (.0219P - .0405X)\ (.4942\,\delta P - .1646\delta X) \\
- & \ (.0673P + .1893X)\ (.4942\,\delta P - .1646\delta X) \\
+ & \ (.1221P - .0406X)\ (.0889\,\delta P - .1641\delta X) \\
- & \ (.2074P - .0690X)\ (.1605\,\delta P + .4510\delta X) \\
+ & \ (.1503P - .1119X)\ (.6176\,\delta P - .6561\delta X)
\end{aligned}$$

Comparing with

$$EI\,\delta U^* = f_{pp}\,P^2 + f_{PX}\,PX + f_{xx}\,X^2 \quad ,$$

$$f_{pp} = +.2167$$

$$f_{PX} = -.3187$$

$$f_{xx} = +.4935$$

Flexibility,

$$f = \frac{1}{EI}\left(f_{pp} - \frac{(f_{px})^2}{f_{xx}} \right)$$

$$= \frac{1}{EI}\left(.2167 - \frac{(-.3187)^2}{.4935} \right)$$

$$f = \frac{1}{EI}\ (.0111) \qquad \text{(in./lb.)}$$

<u>Case 2.</u> P is considered to act at $x = \frac{3}{4}a$

Repeating the procedure as before,

$$f = \frac{1}{EI}\ (.0196) \quad \text{(in./lb.)}$$

The above calculations were made for quadruple linear dimensions, therefore, for real dimensions

$$f = \frac{.0196}{64\ EI} \qquad \text{(in./lb.)}$$

Case 2 is now considered as it indicates greater flexibility.

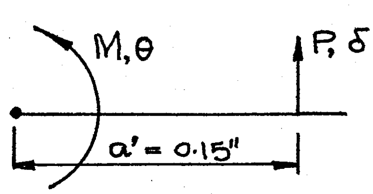

$$M = a'P$$

$$\theta = \delta/a'$$

$\therefore$ Stiffness, $M/\theta = (a')^2 \frac{P}{\delta}$ lbf. in./in.

where $P/\delta = \frac{1}{f}$

$$\therefore \frac{M}{\theta} = \frac{(.15)^2\ 64 \times 9.3 \times 10^6 \times .9 \times (.036)^3}{12 \times .0196}$$

$$= 2400 \ \ lb_f\ \text{in./in.}$$

This indicates a very great stiffness compared with the stiffness required to give consistency with the experimental results in Ref.2.

For further investigation, modes of skin deformation which would allow a greater basic panel width are considered.

2.3.2 Estimate of Edge Couple Restraint.

Estimate of edge couple restraint for a plate at a buckling stress of 30,800 lb./in.^{2}. (Buckling stress of HP 37 specimen).

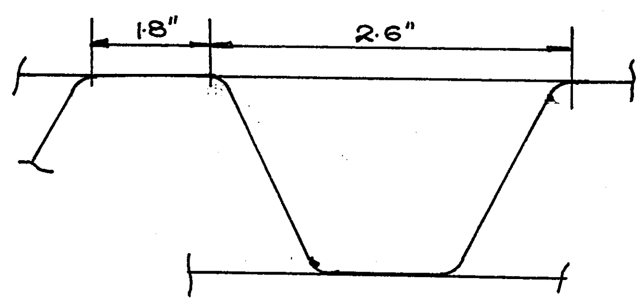

t_s = .064"

(Scale 4:1)

f_o , buckling stress of plate assuming simply supported edges,

f_x , longitudinal compressive stress in the plate.

for b = 1.8 ins.

$$\frac{fx}{fo} = \frac{30{,}800}{9.3 \times 10^6 \times 3.62 \times \left(\frac{0.064}{1.8}\right)^2}$$

$$= 0.72$$

for b = 2.6 ins.

$$\frac{f_x}{f_o} = 1.5$$

From R.Ae.S.D.S. 02.01.31,

for b = 1.8 ins. $\mu_2 = \dfrac{0.45 \times 9.3 \times 10^6 \times (.064)^3}{.91 \times 3 \times 1.8}$

$= + 224$ lb.in./in. (minimum value)

for b = 2.6 ins., μ_2 = -1550 lb.in./in. (minimum value)

where μ_2 is stiffness of the strip.

Combined edge stiffness for a pair of plates 2.6 ins and 1.8 ins. wide.

$$\text{Combined } \mu_2 = \frac{9.3 \times 10^6 \times (.064)^3}{0.91 \times 3} \left(\frac{A_1}{2.6} + \frac{A_2}{1.8} \right)$$

$$= 895 \left(\frac{A_1}{2.6} + \frac{A_2}{1.8} \right)$$

where A_1 and A_2 are the parameters from the Data Sheet 02.01.31 for 2.6 in. and 1.8 in wide plates respectively. Values of μ_2 for various values of half-buckling wave-length, λ, are obtained. Plotting μ_2 versus λ, minimum value of μ_2 is -1300 lb.in./in. at λ of 1.8 ins.

This again indicates a greater stiffness than the one required to give consistency with the experimental results in Ref.2.

2.3.3 Component flat edge support.

Test results from Ref.2 are examined. Using the test buckling stress equivalent component flat widths assuming simply supported edges and clamped edges are calculated. These are then compared with actual component flat widths. See Table 2.1.

It can be seen that, in general, component flat edges have 'less' support than the simple support.

2.4 Final Study.

The theory is developed along the path outlined in para.2.2. Reference 1 is extensively used. For the theoretical analysis the corrugated core sandwich panel is idealized into component flats as shown in Fig.2.1.

2.4.1 The out-of-plane stiffness matrix, $\underline{S_o}$

The out-of-plane sinsusoidal stiffness matrix for long flat plate subjected to a basic uniform longitudinal compressive stress, is established using Ref.1. The system of edge forces and displacements is shown in Fig.2.2.

$$S_o = \begin{pmatrix} S_{FF} & S_{MF} & F_{FF} & F_{MF} \\ S_{MF} & S_{MM} & F_{MF} & F_{MM} \\ F_{FF} & F_{MF} & S_{FF} & S_{MF} \\ F_{MF} & F_{MM} & S_{MF} & S_{MM} \end{pmatrix} \qquad (1)$$

The influence coefficients are listed for three possibilities where $\phi < 1$, $\phi > 1$ and $\phi = 1$.

<u>Case (i) $\phi < 1$</u>

$$\left.\begin{aligned}
S_{MM} &= (D/b)(\sqrt{\phi}/Z)(\alpha \operatorname{Cos h}\alpha \operatorname{Sin h}\gamma - \gamma \operatorname{Cos h}\gamma \operatorname{Sin h}\alpha) \\
S_{MF} &= (D/b^2)\, w^2\, (1 - \nu - (\phi/Z) \sin h\alpha \ \sin h\gamma) \\
S_{FF} &= (D/b^3)\, (\sqrt{\phi}/Z)\alpha\gamma\, (\alpha \sin h\alpha \operatorname{Cos h}\gamma - \gamma \sin h\gamma \cos h\alpha) \\
F_{MM} &= (D/b)\, (\sqrt{\phi}/Z)\, (\gamma \sin h\alpha - \alpha \sin h\gamma) \\
F_{MF} &= -(D/b^2)\, (\sqrt{\phi}/Z)\alpha\gamma\, (\cos h\alpha - \cos h\gamma) \\
F_{FF} &= (D/b^3)\, (\sqrt{\phi}/Z)\, \alpha\gamma\, (\alpha \sin h\alpha - \gamma \sin h\gamma) \\
\text{where } Z &= \sin h\alpha \ \sin h\gamma + (\alpha\gamma/w^2)(1 - \cos h\alpha \cos h\gamma)
\end{aligned}\right\} \qquad (2)$$

and $w = \pi b/\lambda$ $\qquad K = \alpha b^2 t/\pi^2 D$

$\phi = \pi^2 K/w^2$

$$\left.\begin{aligned}
\alpha &= w(1 + \sqrt{\phi})^{\frac{1}{2}} \\
\gamma &= w(1 - \sqrt{\phi})^{\frac{1}{2}}
\end{aligned}\right\} \qquad (3)$$

<u>Case (ii) $\phi > 1$</u>

For this case it is necessary to replace γ, Sin h γ and Cos h γ wherever they appear in equations (3) by δ, sin δ and cos δ reppectively, where

$$\delta = w\,(\sqrt{\phi} - 1)^{\frac{1}{2}}, \qquad (4)$$

and to change the minus signs appearing in the expressions for S_{FF} and F_{FF} to plus signs.

Case (iii) $\varphi = 1$

The appropriate expressions for this case are obtained by taking the limit of equations (3) as $\varphi \longrightarrow 1$,

$$
\left.
\begin{aligned}
S_{mm} &= (D/b)\ (1/Z^{*})\ (\alpha \cos h(\alpha) - \sin h(\alpha)) \\
S_{mF} &= (D/b^{2})\ w^{2}\ (1 - \nu - (1/Z^{*}) \sin h(\alpha)) \\
S_{FF} &= F_{FF} = (D/b^{3})\ (1/Z^{*})\ ^{2} \sin h(\alpha) \\
F_{mm} &= (D/b)\ (1/Z^{*})\ (\sin h(\alpha) - \alpha) \\
F_{mF} &= -(D/b^{2})\ (\alpha/Z^{*})\ (\cos h(\alpha) - 1)
\end{aligned}
\right) \qquad (5)
$$

where $Z^{*} = \sin h(\alpha) + (\sqrt{2}/w)(1 - \cos h(\alpha))$,

and in this case, $\alpha = w\sqrt{2}$.

2.4.2 The out-of-plane stiffness matrix, S_1

The theory in Ref.1 is extended to establish the stiffness matrix for currugation flats.

The general loading and deflection system.

This is shown in the sketch below.

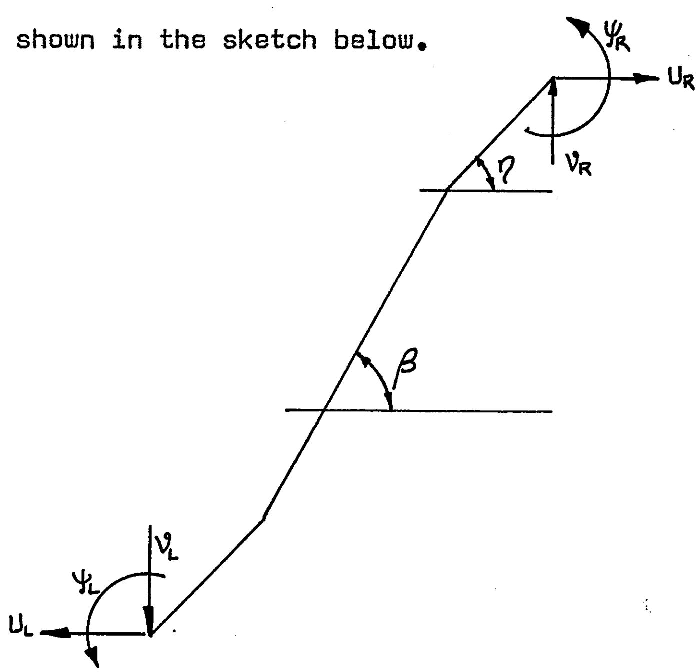

Due to high in-plane - stiffness of face plates,

$U_L = U_R = 0$ is assumed.

The general loading system is split into radially symmetric and radially anti-symmetric loading.

Radially symmetric.

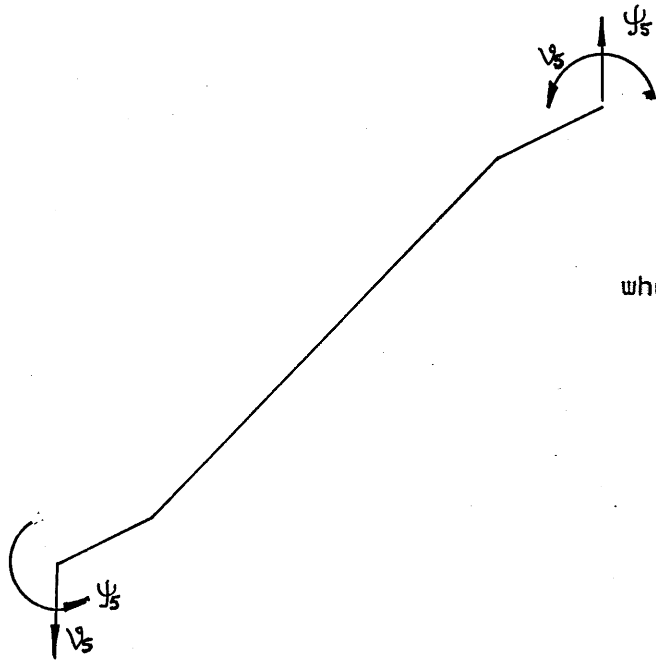

where

$$\left.\begin{aligned} \vartheta_S &= \tfrac{1}{2}(\vartheta_L + \vartheta_R) \\ \vartheta_S &= \tfrac{1}{2}(\psi_L + \psi_R) \end{aligned}\right) \quad (1)$$

Radially anti-symmetric.

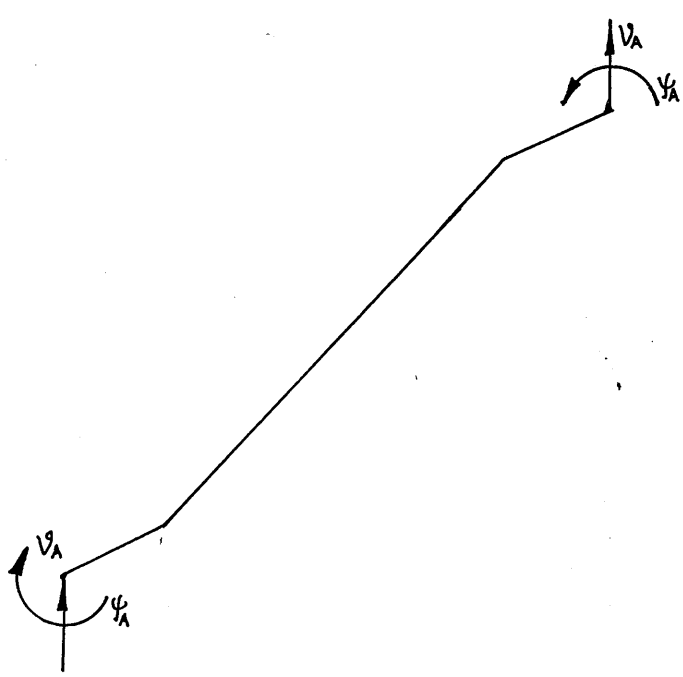

where

$$\left.\begin{aligned} \vartheta_A &= \tfrac{1}{2}(\vartheta_R - \vartheta_L) \\ \psi_A &= \tfrac{1}{2}(\psi_R - \psi_L) \end{aligned}\right) \quad (2)$$

Stiffness matrix for radially symmetric loading case.

Deflection system

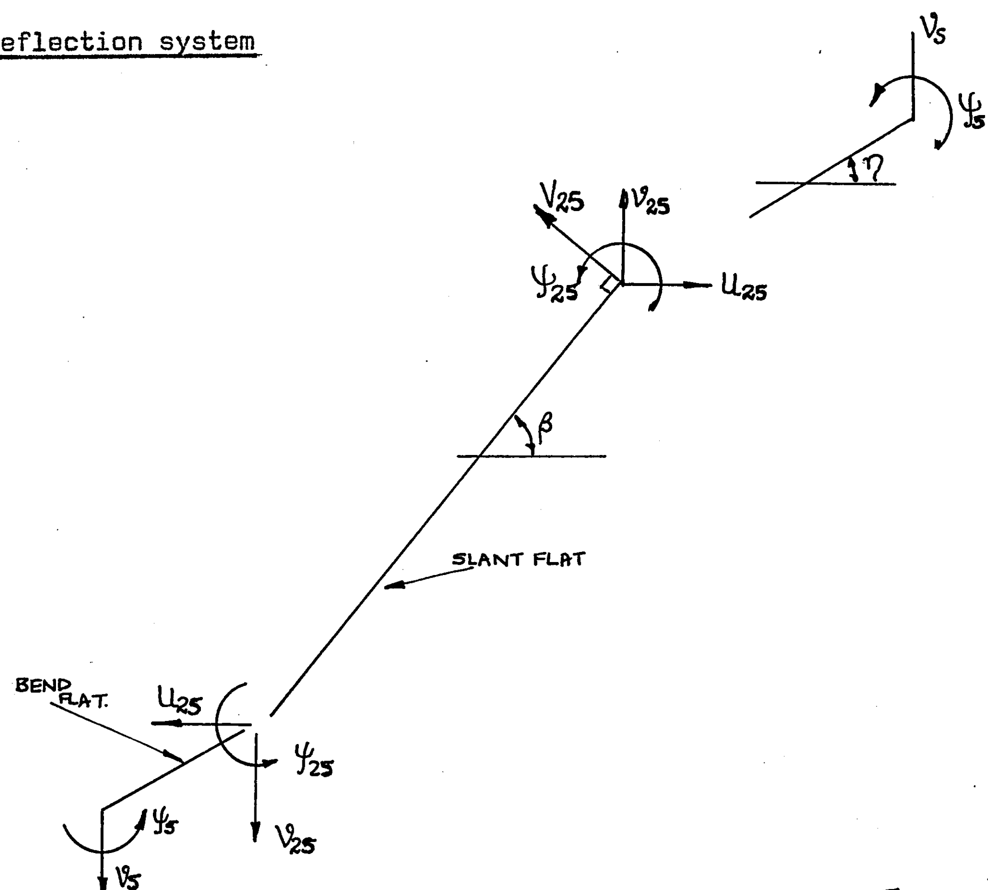

Loading system

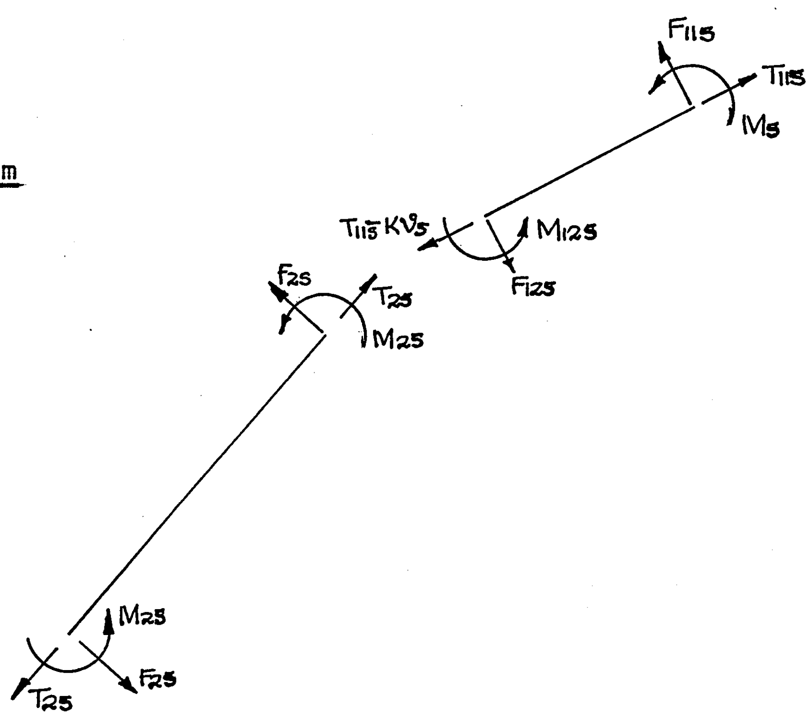

The loads on slant flat can be expressed in terms of stiffness coefficients as shown below.

$$\left.\begin{aligned} F_{25} &= (S_{SFF} + F_{SFF})\, V_{25} + (S_{SMF} + F_{SMF})\, \psi_{25} \\ M_{25} &= (S_{SMF} + F_{SMF})\, V_{25} + (S_{SMM} + F_{SMM})\, \psi_{25} \end{aligned}\right\} \quad (3)$$

where S denotes slant flat.

Due to high in-plane stiffness, (resolving parallel to bend flat).

$$V_{25} \operatorname{Sin}(\beta - \eta) + V_5 \operatorname{Sin} \eta = 0$$

$$\therefore V_{25} = - \frac{V_{15} \operatorname{Sin} \eta}{\operatorname{Sin}(\beta - \eta)} \quad (4)$$

The deflections can be expressed in notations used for the force system.

$$V_{115} = V_5 \operatorname{Cos} \eta \quad (5)$$

$$\begin{aligned} V_{125} &= - V_{25} \operatorname{Cos}(\beta - \eta) \\ &= V_5 \operatorname{Sin} \eta \operatorname{Cot}(\beta - \eta) \end{aligned} \quad (6)$$

Equations of equilibrium for the 'bend flat' can be expressed as:

$$\begin{pmatrix} F_{125} \\ M_{125} \\ F_{115} \\ M_5 \end{pmatrix} = \begin{pmatrix} S_{BFF} & S_{BMF} & F_{BFF} & F_{BMF} \\ S_{BMF} & S_{BMM} & F_{BMF} & F_{BMM} \\ F_{BFF} & F_{BMF} & S_{BFF} & S_{BMF} \\ F_{BMF} & F_{BMM} & S_{BMF} & S_{BMM} \end{pmatrix} \begin{pmatrix} V_{125} \\ \psi_{25} \\ V_{115} \\ \psi_5 \end{pmatrix} \quad (7)$$

Considering moment equilibrium at junction of slant and bend flats,

$$M_{25} + M_{125} = 0 \qquad (8)$$

Considering force equilibrium at junction of slant and bend flat,

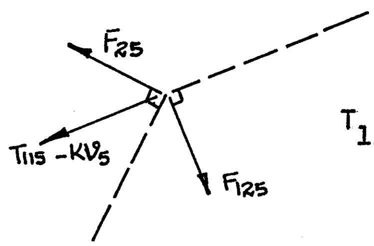

$$T_{115} = KV_5 + F_{125}\,\mathrm{Cot}(\beta - \eta) - F_{25}\,\mathrm{Cosec}(\beta - \eta) \qquad (9)$$

<u>Evaluation of K.</u>

$$w = V_5 \,\mathrm{Sin}\, \eta \;\mathrm{Sin}\left(\frac{\pi x}{\lambda}\right) \qquad (a)$$

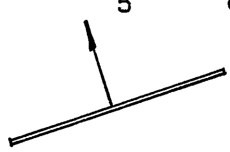

consider the equilibrium of an element

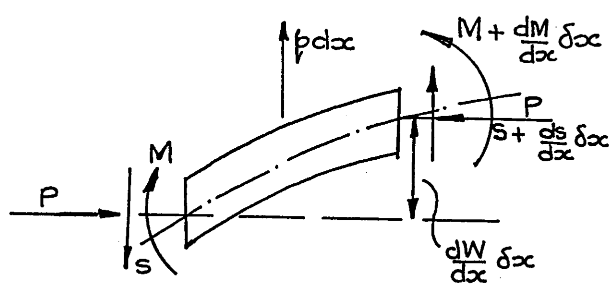

$$\text{where } p = KV_5 \,\mathrm{Sin}\, \frac{\pi x}{\lambda} \qquad (b)$$

For vertical equilibrium

$$p = -\frac{ds}{dx} \qquad (c)$$

For moment equilibrium

$$S = -\frac{dM}{dx} - P\frac{dW}{dx} \qquad (d)$$

From equations (c) and (d),

$$p = \frac{d^2 M}{dx^2} + P \frac{d^2 w}{dx^2}$$

$$= EI \frac{d^4 w}{dx^4} + P \frac{d^2 w}{dx^2} \qquad (e)$$

From equations (a) and (e),

$$p = EI \left(\frac{\pi^4}{\lambda^4} - P \frac{\pi^2}{EI \lambda^2} \right) v_5 \operatorname{Sin} \eta \operatorname{Sin} \frac{\pi x}{\lambda} \qquad (f)$$

From equations (b) and (f),

$$K = \frac{\pi^2}{\lambda^2} \left(EI \frac{\pi^2}{\lambda^2} - P \right) \operatorname{Sin} \eta \qquad (10)$$

Note that $I = \frac{tb^3}{12}$

and $P = tb\sigma$

where t = thickness of bend flat

b = width of bend flat

and σ = basic longitudinal compressive stress.

From equations (4), (5) and (6),

$$\left.\begin{aligned} \frac{v_{25}}{v_5} &= -\frac{\operatorname{Sin} \eta}{\operatorname{Sin}(\beta - \eta)} \\ \frac{v_{115}}{v_5} &= \operatorname{Cos} \eta \\ \frac{v_{125}}{v_5} &= \operatorname{Sin} \eta \operatorname{Cot}(\beta - \eta) \end{aligned}\right\} \qquad (11)$$

From equations (3), (7) and (8),

$$\psi_{25} = -\left(\frac{F_{BMM}\,\psi_5 + (S_{SMF}+F_{SMF})V_{25} + F_{BMF}\,V_{115} + S_{BMF}\,V_{125}}{S_{SMM} + F_{SMM} + S_{BMM}}\right) \qquad (12)$$

where B and S denote bend and slant flat respectively. Substituting equations (11) into equation (12) and comparing the coefficients with

$$\psi_{25} = A_{V5}\;V_5 \;+\; A_{\psi 5}\;\psi_5 \;,$$

we get,

$$A_{V5} = -\left(\frac{(S_{SMF} + F_{SMF})\left(-\dfrac{\sin\eta}{\sin(\beta-\eta)}\right) + F_{BMF}\cos\eta + S_{BMF}\sin\cot(\beta-\eta)}{S_{SMM} + F_{SMM} + S_{BMM}}\right)$$

(13)

$$A_{\psi 5} = -\left(\frac{F_{BMM}}{S_{SMM} + F_{SMM} + S_{BMM}}\right) \qquad (14)$$

From equations (7), (11), (13) and (14),

$$M_5 = A_{215}\,V_5 + A_{225}\;\psi_5 \qquad (15)$$

where $A_{215} = \left(S_{BMF}\cos\eta + F_{BMM}\,A_{V5} + F_{BMF}\sin\eta\;\cot(\beta-\eta)\right)$

$$A_{225} = \left(S_{BMM} + F_{BMM}\,A_{\psi 5}\right)$$

$$F_{115} = \left\{S_{BFF} \cos\eta + F_{BMF} A_{V5} + F_{BFF} \sin\eta \cot(\beta-\eta)\right\} \vartheta_5$$

$$+ \left\{S_{BMF} + F_{BMF} A_{\psi 5}\right\} \psi_5 \qquad (16)$$

$$F_{125} = \left\{F_{BFF} \cos\eta + S_{BMF} A_{V5} + S_{BFF} \sin\eta \cot(\beta-\eta)\right\} \vartheta_5$$

$$+ \left\{F_{BMF} + S_{BMF} A_{\psi 5}\right\} \psi_5 \qquad (17)$$

From equations (3), (11), (13) and (14),

$$F_{25} = \left\{(S_{SMF} + F_{SMF})A_{V5} + (S_{SFF} + F_{SFF}) \left(\frac{-\sin\eta}{\sin(\beta-\eta)}\right)\right\} \vartheta_5$$

$$+ \left\{(S_{SMF} + F_{SMF}) A_{\psi 5}\right\} \psi_5 \qquad (18)$$

Resolving the forces perpendicular to the face plate at junction of bend flat and bonded flat,

$$Y_5 = F_{115} \cos\eta + T_{115} \sin\eta \qquad (19)$$

From equations (9), (10), (16), (17), (18) and (19),

$$Y_5 = A_{115} \vartheta_5 + A_{125} \psi_5 \qquad (20)$$

where

$$A_{115} = \left\{(S_{BFF} \cos\eta + F_{BMF} A_{V5} + F_{BFF} \sin\eta \cot(\beta-\eta)\right\} \cos\eta$$

$$+ K \sin\eta + \left\{F_{BFF} \cos\eta + S_{BMF} A_{V5} + S_{BFF} \sin\eta \cot(\beta-\eta) \cot(\beta-\eta)\right\} \sin(\eta)$$

$$- \left\{(S_{SMF} + F_{SMF}) A_{V5} + (S_{SFF}+F_{SFF})\left(\frac{-\sin\eta}{\cot(\beta-\eta)}\right) \sin\eta \operatorname{cosec}(\beta-\eta)\right\}$$

$$A_{125} = \left\{ (S_{BMF} + F_{BMF}\, A\psi_5) \operatorname{Cos} \eta + \left\{ (F_{BMF} + S_{BMF} A\, \psi_5) \operatorname{Cot}(\beta - \eta) - (S_{SMF} + F_{SMF})\, A\,\psi_5 \operatorname{Cosec}(\beta - \eta) \right\} \operatorname{Sin} \eta \right\}$$

Equations (15) and (20) can be written as

$$\begin{pmatrix} Y_5 \\ \\ M_5 \end{pmatrix} = \begin{pmatrix} A_{115} & A_{125} \\ & \\ A_{215} & A_{225} \end{pmatrix} \begin{pmatrix} \vartheta_5 \\ \\ \psi_5 \end{pmatrix} \qquad (21)$$

noting that $A_{125} = A_{215}$

Stiffness matrix for radially antisymmetric loading case.

Deflection system.

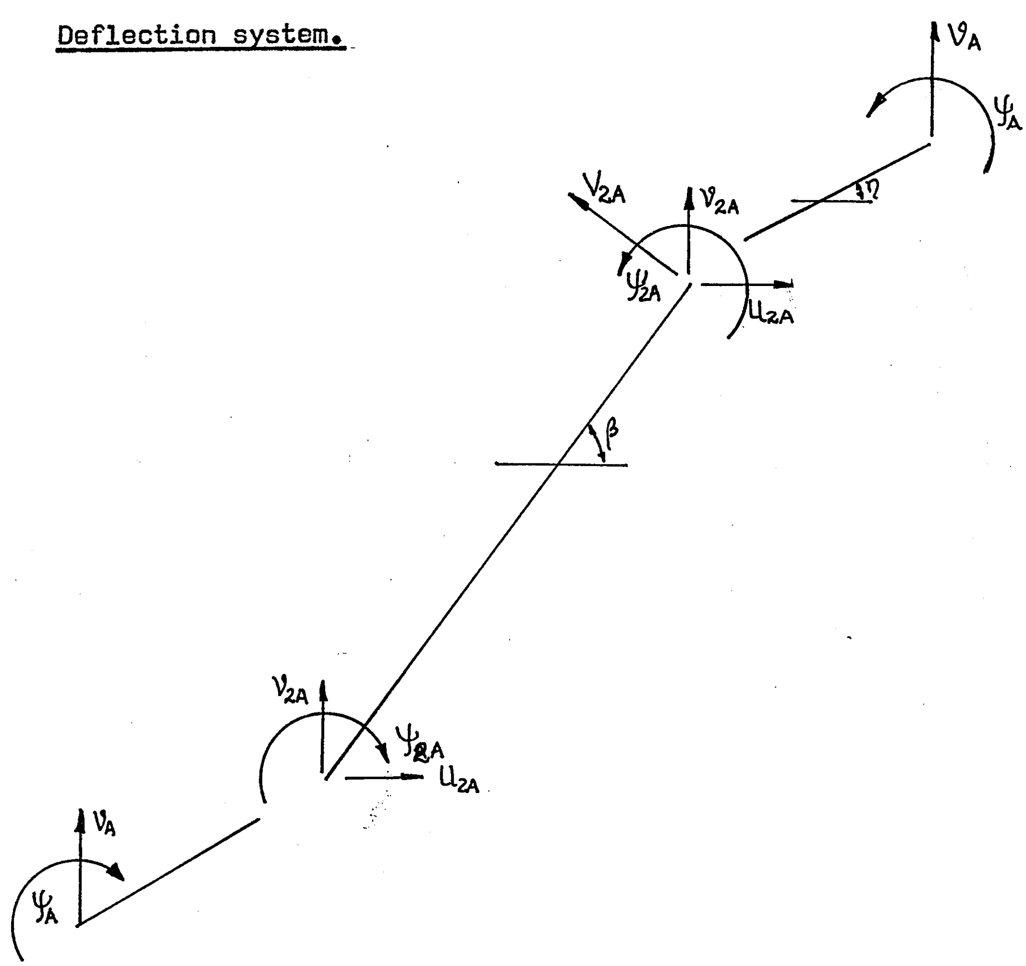

Loading system.

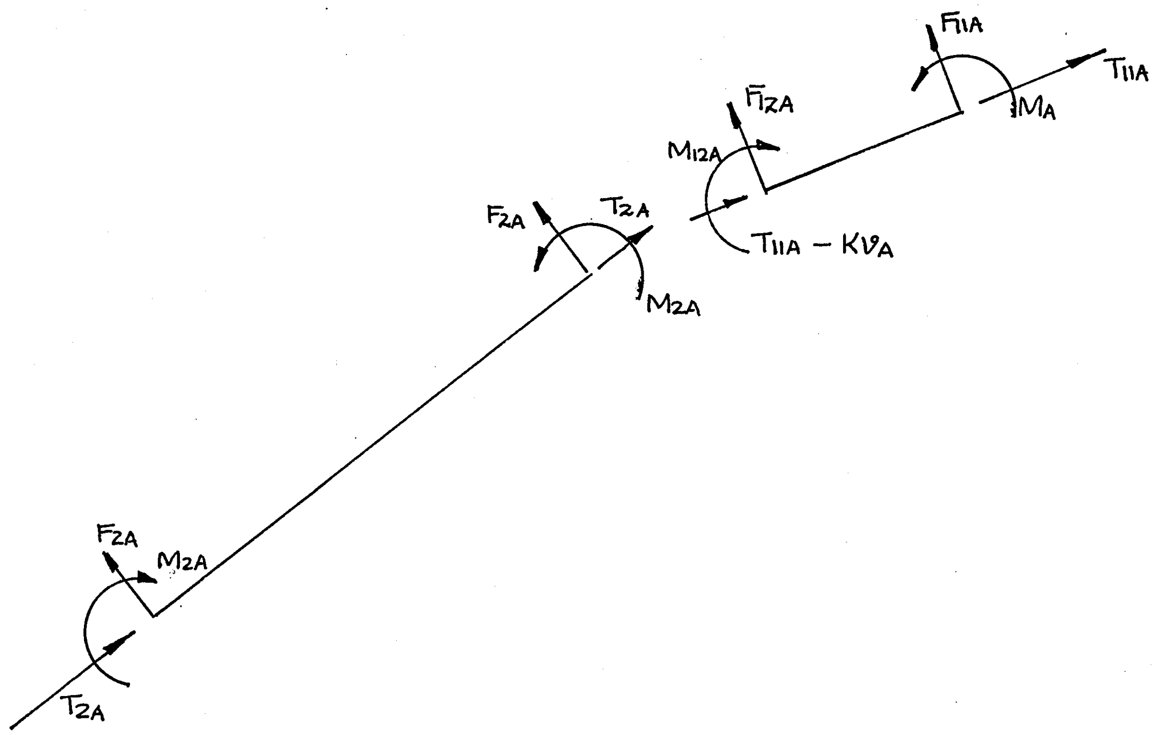

$$\left.\begin{aligned} F_{2A} &= (S_{SFF} - F_{SFF})\, V_{2A} + (S_{SMF} - F_{SMF})\, \psi_{2A} \\ M_{2A} &= (S_{SMF} - F_{SMF})\, V_{2A} + (S_{SMM} - F_{SMM})\, \psi_{2A} \end{aligned}\right) \qquad (22)$$

As for symmetric case,

$$\left.\begin{aligned} \frac{V_{2A}}{\vartheta_A} &= - \frac{\sin \eta}{\sin(\beta - \eta)} \\ \frac{\vartheta_{11A}}{\vartheta_A} &= \cos \eta \\ \frac{\vartheta_{12A}}{\vartheta_A} &= \sin \eta \ \cot(\beta - \eta) \end{aligned}\right) \qquad (23)$$

Equations of equilibrium for the bend flat can be expressed as:

$$\begin{pmatrix} F_{12A} \\ M_{12A} \\ F_{11A} \\ M_{A} \end{pmatrix} = \begin{pmatrix} S_{BFF} & S_{BMF} & -F_{BFF} & -F_{BMF} \\ S_{BMF} & S_{BMM} & -F_{BMF} & -F_{BMM} \\ -F_{BFF} & -F_{BMF} & S_{BFF} & S_{BMF} \\ -F_{BMF} & -F_{BMM} & S_{BMF} & S_{BMM} \end{pmatrix} \begin{pmatrix} \vartheta_{12A} \\ \psi_{2A} \\ \vartheta_{11A} \\ \psi_{A} \end{pmatrix} \qquad (24)$$

Considering moment equilibrium at junction of slant and bend flats.

$$M_{2A} + M_{12A} = 0 \qquad (25)$$

considering force equilibrium at the same junction,

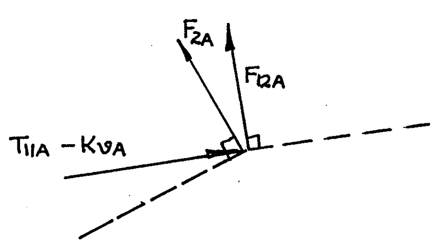

$$T_{11A} = KV_A + F_{12A}\,\mathrm{Cot}\,(\beta - \eta) + F_{2A}\,\mathrm{Cosec}\,(\beta - \eta) \qquad (26)$$

From equations (22), (23) and (24),

$$\psi_{2A} = A_{\vartheta A}\,\vartheta_A + A_{\psi A}\,\psi_A$$

where

$$A_{\vartheta A} = -\left(\frac{(S_{SMF} - F_{SMF})\left(\dfrac{-\mathrm{Sin}\,\eta}{\mathrm{Sin}(\beta - \eta)}\right) - F_{BMF}\,\mathrm{Cos}\,\eta + S_{BMF}\,\mathrm{Sin}\,\eta\,\mathrm{Cot}(\beta - \eta)}{S_{BMM} - F_{SMM} + S_{BMM}} \right) \qquad (27)$$

$$A_{\psi A} = \left(\frac{F_{BMM}}{S_{SMM} - F_{SMM} + S_{BMM}} \right) \qquad (28)$$

From equations (23), (24), (27) and (28),

$$M_A = A_{21A}\, \nu_A + A_{22A}\, \psi_A \tag{29}$$

where

$$A_{21A} = \left\{ S_{BMF} \cos\eta - F_{BMM} A_{VA} - F_{BMF} \sin\eta \cot(\beta - \eta) \right\}$$

$$A_{22A} = \left\{ S_{BMM} - F_{BMM} A_{\psi A} \right\}$$

$$F_{11A} = \left\{ S_{BFF} \cos\eta - F_{BMF} A_{VA} - F_{BFF} \sin\eta \cot(\beta - \eta) \right\} \nu_A$$

$$+ \left\{ S_{BMF} - F_{BMF} A_{\psi A} \right\} \psi_A \tag{30}$$

$$F_{12A} = \left\{ -F_{BFF} \cos\eta + S_{BMF} A_{VA} + S_{BFF} \sin\eta \cot(\beta - \eta) \right\} \nu_A$$

$$+ \left\{ - F_{BMF} + S_{BMF} A_{\psi A} \right\} \psi_A \tag{31}$$

From equations (22), (23), (27) and (28),

$$F_{2A} = \left\{ (S_{SMF} - F_{SMF}) A_{VA} + (S_{SFF} - F_{SFF}) \left(\frac{-\sin\eta}{\sin(\beta - \eta)} \right) \right\} \nu_A$$

$$+ \left\{ (S_{SMF} - F_{SMF}) A_{\psi A} \right\} \psi_A \tag{32}$$

As for symmetric case,

$$Y_A = F_{11A} \cos\eta + T_{11A} \sin\eta \tag{33}$$

From equations (10), (26), (30), (31), (32), and (33),

$$Y_A = A_{11A}\, \nu_A + A_{12A}\, \psi_A \tag{34}$$

where

$$A_{11A} = \left\{ \left\{ S_{BFF} \cos\eta - F_{BMF} A_{VA} - F_{BFF} \sin\eta \cot(\beta-\eta) \right\} \cos\eta \right.$$

$$+ K\sin\eta + \left\{ -F_{BFF} \cos\eta + S_{BMF} A_{VA} + S_{BFF} \sin\eta \cot(\beta-\eta) \right\} \frac{\cot(\beta-\eta)}{\sin\eta}$$

$$\left. + \left\{ (S_{SMF}-F_{SMF})A_{VA} + (S_{SFF}-F_{SFF}) \left(\frac{-\sin\eta}{\cot(\beta-\eta)} \right) \right\} \sin\eta \,\mathrm{Cosec}(\beta-\eta) \right\}$$

$$A_{12A} = \left\{ \left\{ S_{BMF} - F_{BMF} A_{\varphi A} \right\} \cos\eta + \left\{ (-F_{BMF} + S_{BMF} A_{\varphi A} \right\} \cot(\beta-\eta) \right.$$

$$\left. - (S_{SMF} - F_{SMF}) A_{\varphi A} \,\mathrm{Cosec}(\beta-\eta) \right\} \sin\eta$$

Equations (29) and (34),

$$\begin{pmatrix} Y_A \\ M_A \end{pmatrix} = \begin{pmatrix} A_{11A} & A_{12A} \\ A_{21A} & A_{22A} \end{pmatrix} \begin{pmatrix} \vartheta_A \\ \varphi_A \end{pmatrix} \qquad (35)$$

noting that $A_{12A} = A_{21A}$.

The out-of-plane stiffness matrix, S_1, for corrugation flats for a general loading and deflection system is obtained from equations (21) and (35).

$$\begin{pmatrix} Y_L \\ M_L \\ Y_R \\ M_R \end{pmatrix} = \tfrac{1}{2} \begin{pmatrix} (A_{115}+A_{11A}) & (A_{125}+A_{12A}) & (A_{115}-A_{11A}) & (A_{125}-A_{12A}) \\ (A_{125}+A_{12A}) & (A_{225}+A_{22A}) & (A_{125}-A_{12A}) & (A_{225}-A_{22A}) \\ (A_{115}+A_{11A}) & (A_{125}-A12A) & (A_{115}+A_{11A}) & (A_{125}+A_{12A}) \\ (A_{125}-A_{12A}) & (A_{225}-A_{22A}) & (A_{125}+A_{12A}) & (A_{225}+A_{22A}) \end{pmatrix} \begin{pmatrix} \vartheta_L \\ \varphi_L \\ \vartheta_R \\ \varphi_R \end{pmatrix}$$

2.4.3 Matrix analysis.

$R = A'S$ where R,S internal and external forces

$S = K\vartheta$ r,ϑ internal and external deflections

$\vartheta = Ar$

Therefore, final stiffness matrix is

$$A' \, k \, A$$

The condition for buckling is

$$/ A' \, k \, A / = 0$$

2.4.4 Buckling modes.

Initially four buckling modes are considered.

They are shown in Figs. 2.3, 2.4, 2.5 and 2.6.

The matrix A is of the form

$$\begin{pmatrix} A_1 \\ \hline A_2 \end{pmatrix}$$

A_1 being 16 x 8 matrix and is the same for all buckling modes.

A_2 being either an 8 x 8 or 16 x 8 matrix, and has to be established for each of the buckling mode.

The matrix k is of the form

$$\left(\begin{array}{c|c} k_1 & 0 \\ \hline o & k_2 \end{array}\right)$$

K_1 being a 16 x 16 matrix and is the same for all buckling modes.

K_2 being either an 8 x 8 or 16 x 16 matrix and has to be established for each of the buckling mode.

$$A' = \left(\begin{array}{c|c} A_1' & A_2' \end{array}\right)$$

$$KA = \begin{pmatrix} k_1 \; A_1 \\ k_2 \; A_2 \end{pmatrix}$$

$$A' \, k \, A = [A_1' \, k_1 \, A_1] + [A_2' \, k_2 \, A_2]$$

The matrices A_1, k_1, $A'_1 \, k_1 \, A_1$ are shown in Tables 2.2, 2.3 and 2.4.

The matrices A_2, k_2, $A'_2 \, k_2 \, A_2$ for each of the mode are given in Tables 2.5 to 2.15.

2.4.5 Sign convention used for matrices.

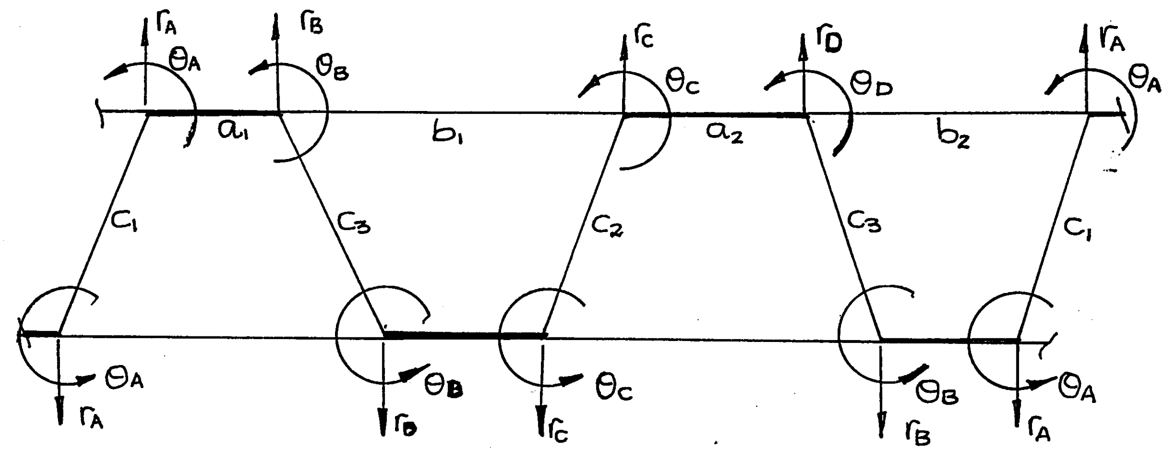

For panels of type 'a' and 'b' :

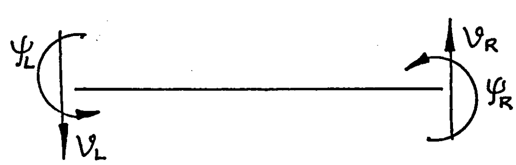

For panels of type 'c' :

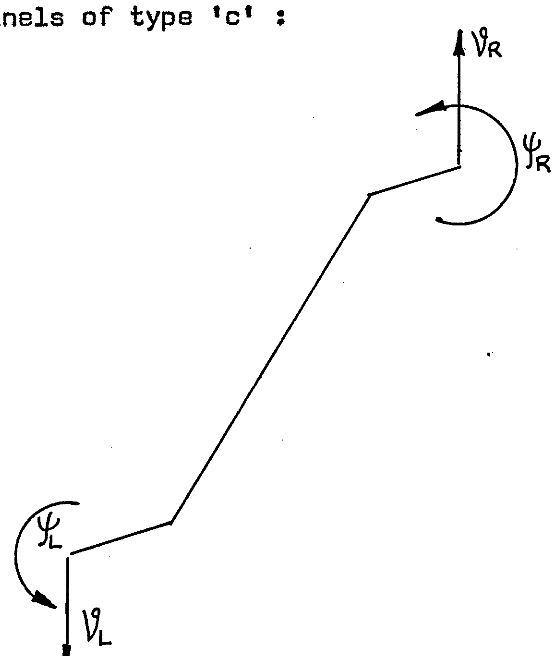

2.4.6 Deflections of points A,B, C and D on the panel. (See Figs. 2.2 to 2.6).

Subroutine F4DET evaluates the determinant using triangular decomposition.

The determinant is stored in A(64), and provision is made in REINT(I) to contain record of any row interchanges during the triangular decomposition, such that at the Ith step, Ith columns and the REINT(I)th rows were interchanged.

$$\left.\begin{aligned} A\underset{\sim}{r} &= 0 \\ \text{and} \quad A\underset{\sim}{r} &= LU\underset{\sim}{r} = 0 \end{aligned}\right) \qquad \text{(a)}$$

where L is lower triangular matrix

U is upper triangular matrix

$$L = \begin{bmatrix} L_{11} \\ L_{21} & L_{22} \\ L_{31} & L_{32} & L_{33} \\ L_{41} & L_{42} & L_{43} & L_{44} \\ L_{51} & L_{52} & L_{53} & L_{54} & L_{55} \\ L_{61} & L_{62} & L_{63} & L_{64} & L_{65} & L_{66} \\ L_{71} & L_{72} & L_{73} & L_{74} & L_{75} & L_{76} & L_{77} \\ L_{81} & L_{82} & L_{83} & L_{84} & L_{85} & L_{86} & L_{87} & L_{88} \end{bmatrix}$$

$$U = \begin{bmatrix} 1 & U_{12} & U_{13} & U_{14} & U_{15} & U_{16} & U_{17} & U_{18} \\ & 1 & U_{23} & U_{24} & U_{25} & U_{26} & U_{27} & U_{28} \\ & & 1 & U_{34} & U_{35} & U_{36} & U_{37} & U_{38} \\ & & & 1 & U_{45} & U_{46} & U_{47} & U_{48} \\ & & & & 1 & U_{56} & U_{57} & U_{58} \\ & & & & & 1 & U_{67} & U_{68} \\ & & & & & & 1 & U_{78} \\ & & & & & & & 1 \end{bmatrix}$$

r is a column matrix,

$$\begin{aligned} &= \{ r_1 \quad r_2 \quad r_3 \quad r_4 \quad r_5 \quad r_6 \quad r_7 \quad r_8 \} \\ \equiv &= \{ r_A \quad \theta_A \quad r_B \quad \theta_B \quad r_c \quad \theta_c \quad r_D \quad \theta_D \} \end{aligned}$$

$$L\,U\,r = LP = 0 \qquad \text{(b)}$$

where $P = Ur$

If $L_{88} = 0$;

$$\begin{aligned}
P_1 &= r_1 + U_{12}r_2 + U_{13}r_3 + U_{14}r_4 + U_{15}r_5 + U_{16}r_6 + U_{17}r_7 + U_{18}r_8 = 0 \\
P_2 &= r_2 + U_{23}r_3 + U_{24}r_4 + U_{25}r_5 + U_{26}r_6 + U_{27}r_7 + U_{28}r_8 = 0 \\
P_3 &= r_3 + U_{34}r_4 + U_{35}r_5 + U_{36}r_6 + U_{37}r_7 + U_{38}r_8 = 0 \\
P_4 &= r_4 + U_{45}r_5 + U_{46}r_6 + U_{47}r_7 + U_{48}r_8 = 0 \qquad \text{(C)} \\
P_5 &= r_5 + U_{56}r_6 + U_{57}r_7 + U_{58}r_8 = 0 \\
P_6 &= r_6 + U_{67}r_7 + U_{68}r_8 = 0 \\
P_7 &= r_7 + U_{78}r_8 = 0
\end{aligned}$$

From equations (c)

$$r_7/r_8 = \theta_7 = -U_{78}$$

$$r_6/r_8 = \theta_6 = -U_{67}\frac{r_7}{r_8} - U_{68}$$

$$r_5/r_8 = \theta_5 = -U_{56}\frac{r_6}{r_8} - U_{57}\frac{r_7}{r_8} - U_{58}$$

$$r_4/r_8 = \theta_4 = -U_{45}\frac{r_5}{r_8} - U_{46}\frac{r_6}{r_8} - U_{47}\frac{r_7}{r_8} - U_{48}$$

$$r_3/r_8 = \theta_3 = -U_{34}\frac{r_4}{r_8} - U_{35}\frac{r_5}{r_8} - U_{36}\frac{r_6}{r_8} - U_{37}\frac{r_7}{r_8} - U_{38}$$

$$r_2/r_8 = \theta_2 = -U_{23}\frac{r_3}{r_8} - U_{24}\frac{r_4}{r_8} - U_{25}\frac{r_5}{r_8} - U_{26}\frac{r_6}{r_8} - U_{27}\frac{r_7}{r_8} - U_{28}$$

$$r_1/r_8 = \theta_1 = -U_{12}\frac{r_2}{r_8} - U_{13}\frac{r_3}{r_8} - U_{14}\frac{r_4}{r_8} - U_{15}\frac{r_5}{r_8} - U_{16}\frac{r_6}{r_8} - U_{17}\frac{r_7}{r_8} - U_{18}$$

2.4.7 The computer program.

The computer program is developed to give the value of buckling stress by equating the determinant of total stiffness matrix for the panel to zero. A general flow chart for the master program is shown in Fig.2.7.

For a given value of half buckling wave length, λ, the longitudinal compressive stress, σ, is set to f_o, the buckling stress of simply supported panel of width equal to pitch. The the stress is increased by 0.5 f_o till the change of sign of total stiffness matrix determinant is achieved. The stress is varied by 1000's from nearer of the last two values to zero. When the change of sign of the determinant is achieved, the stress is varied in 100's from the last value of stress, to enclose the zero and the results are output. The value of λ is then changed and the computation repeated.

The Call of subroutines in XMODE series is governed by the input data.

Details of the computation logic and loops are given in Appendix 1.

The master program and the subroutine segments are shown on the following pages.

```
FORTRAN COMPILATION BY #XFAE MK 3C     DATE  15/08/69  TIME  21/33/54

      LIST(LP)
      SEND TO(ED,PROGRAM FILE.STORE)
      LIBRARY (SUBGROUPFSCE)
      PROGRAM(D10A)
      INPUT1=CR0
      OUTPUT2=LP0
      COMPRESS INTEGER AND LOGICAL
      TRACE
      END
```

```
      MASTER NG1
      DIMENSION F(8,8),B(8,8),C(8,8),DET(50),SIGMA(50),A(64),U(8,8),
     1THETA(8),REINT(8)
      COMMON/E/E/XMUE/XMUE/XLAMBDA/XLAMBDA/SIGMA/SIGMA/M/M/ZETA/ZETA
      COMMON/A11S/A11S/A12S/A12S/A22S/A22S/A11A/A11A/A12A/A12A/A22A/A22A
     1/B/B
  450 READ(1,402)T,TP,BB,BS,BJ,BP,ANGLE1,ANGLE2,E
  402 FORMAT(9F0.0)
      READ(1,451)FO,DELSIG,XLAMBDA,DEL,VAL
  451 FORMAT(5F0.0)
      READ(1,406)MODE
  406 FORMAT(I1)
      IF(T.EQ.0.0)GO TO 405
      TJ=T+TP
      XMUE=0.30
  103 WRITE(2,202)
  202 FORMAT(1H1///23X,5HSIGMA,12X,3HDET,13X,7HXLAMBDA,9X,4HZETA/)
  101 L,KX,N,MC,NC=0
      M=1
      NN=0
      N=N+1
   71 SIGMA(M)=FO
  100 K=0
      CALL WITTRICK(T,     BB,   SBMM,SBMF,SBFF,FBMM,FBMF,FBFF)
      CALL WITTRICK(T,     BS,    SSMM,SSMF,SSFF,FSMM,FSMF,FSFF)
      ETA=(ANGLE2*3.1416)/180.
      BETA=(ANGLE1*3.1416)/180.
      AVS=-((SSMF+FSMF)*SIN(ETA)/(-SIN(BETA-ETA))+FBMF*COS(ETA)+SBMF*SIN
```

```
     1(ETA)*COT(BETA-ETA))/(SSMM+FSMM+SBMM)
      TS1=(SBFF*COS( ETA)+FBMF*AVS+FBFF*SIN( ETA)*COT(BETA- ETA))*COS( E
     1TA)
      P=T*BB*SIGMA(M)
      XI=(T*BB**3.)/12.
      XKC=((E*XI*3.1416**2./XLAMBDA**2.-P)*3.1416**2.*SIN(ETA))/(XLAMBDA
     1**2.)
      TS2=XKC*SIN(ETA)
      TS3=(FBFF*COS( ETA)+SBMF*AVS+SBFF*SIN( ETA)*COT(BETA- ETA))*COT(BE
     1TA- ETA)*SIN( ETA)
      TS4=(((SSMF+FSMF)*AVS+(SSFF+FSFF)*SIN(ETA)/(-SIN(BETA-ETA)))*SIN(
     1ETA))/SIN(BETA- ETA)
      A11S=TS1+TS2+TS3-TS4
      A12S=SBMF*COS( ETA)+FBMM*AVS+FBMF*SIN( ETA)*COT(BETA- ETA)
      A21S=A12S
      APSIS=-FBMM/(SSMM+FSMM+SBMM)
      A22S=SBMM+FBMM*APSIS
      AVA=-((SSMF-FSMF)*SIN(ETA)/(-SIN(BETA-ETA))-FBMF*COS(ETA)+SBMF*SI
     1N( ETA)*COT(BETA- ETA))/(SSMM-FSMM+SBMM)
      TA1=(SBFF*COS( ETA)-FBMF*AVA-FBFF*SIN( ETA)*COT(BETA- ETA))*COS( E
     1TA)
      TA2=TS2
      TA3=(-FBFF*COS( ETA)+SBMF*AVA+SBFF*SIN( ETA)*COT(BETA- ETA))*COT(B
     1ETA- ETA)*SIN( ETA)
      TA4=(((SSMF+FSMF*AVA+SSFF-FSFF)*SIN(ETA)/(-SIN(BETA-ETA)))*SIN(ET
     1A))/SIN(BETA- ETA)
      A11A=TA1+TA2+TA3+TA4
      A12A=SBMF*COS( ETA)-FBMM*AVA-FBMF*SIN( ETA)*COT(BETA- ETA)
```

```
      A21A=A12A
      APSIA=FBMM/(SSMM-FSMM+SBMM)
      A22A=SBMM-FBMM*APSIA
      IF(MODE.EQ.1)GO TO 407
      IF(MODE.EQ.2)GO TO 408
      IF(MODE.EQ.3)GO TO 409
      IF(MODE.EQ.4)GO TO 410
  407 CALL XMODE1
      GO TO 411
  408 CALL XMODE2
      GO TO 411
  409 CALL XMODE3
      GO TO 411
  410 CALL XMODE4
  411 CONTINUE
      CALL WITTRICK(TJ,    BJ, SJMM,SJMF,SJFF,FJMM,FJMF,FJFF)
      CALL WITTRICK(TP,    BP, SPMM,SPMF,SPFF,FPMM,FPMF,FPFF)
      F(1,5),F(1,6),F(2,5),F(3,7),F(3,8),F(4,8),F(2,6),F(4,7)=0.0
      F(1,1),F(3,3),F(5,5),F(7,7)=SJFF+SPFF
      F(2,2),F(4,4),F(6,6),F(8,8)=SJMM+SPMM
      F(1,2),F(5,6)=-SJMF+SPMF
      F(1,3),F(5,7)=-FJFF
      F(1,4),F(5,8)=-FJMF
      F(1,7),F(3,5)=-FPFF
      F(1,8),F(4,5)=FPMF
      F(2,3),F(6,7)=FJMF
      F(2,4),F(6,8)=FJMM
      F(2,7),F(3,6)=-FPMF
```

```
      F(2,8),F(4,6)=FPMM
      F(3,4),F(7,8)=SJMF-SPMF
      DO 5 I=1,8
      DO 5 J=2,8
    5 F(J,I)=F(I,J)
      DO 8 I=1,8
      DO 8 J=1,8
      K=K+1
      C(I,J)=F(I,J)+B(I,J)
    8 A(K)=C(I,J)/1000.
      N=8
      NA=64
      CALL F4DET(A,N,NA,D,ID,REINT,IT)
      IF(NN)33,33,34
   33 DET(M)=D*2.**ID
      WRITE(2,201)SIGMA(M),DET(M),XLAMBDA,ZETA
  201 FORMAT(20X,E12.5,3E16.5)
      IF(KX)52,53,54
   52 M=M+1
      SIGMA(M)=SIGMA(M-1)+100.
      MC=MC+1
      KX=-1
      IF(MC-10)100,100,55
   54 M=M+1
      SIGMA(M)=SIGMA(M-1)-100.
      KX=1
      NC=NC+1
      IF(NC-10)100,100,55
```

```
 53 IF(L)56,57,58
 56 IF(DET(M))59,60,52
 59 M=M+1
    SIGMA(M)=SIGMA(M-1)-1000.
    L=-1
    GO TO 100
 57 IF(DET(M))61,60,64
 61 IF(ABS(DET(M-1))-ABS(DET(M)))62,62,59
 62 SIGMA(M)=SIGMA(M-1)
 80 M=M+1
    SIGMA(M)=SIGMA(M-1)+1000.
    L=1
    GO TO 100
 64 M=M+1
    SIGMA(M)=SIGMA(M-1)+DELSIG
    GO TO 100
 58 IF(DET(M))54,60,80
 60 WRITE(2,201)SIGMA(M),DET(M),XLAMBDA,ZETA
 55 M=M-1
    DO 50 I=1,20
    RAT=DET(M)/DET(M-1)
    IF(RAT)30,30,50
 50 M=M-1
 30 WRITE(2,400)
400 FORMAT(/23X, 7HXLAMBDA,7X,8HSIGMA(M),6X,6HDET(M),8X,8HDET(M 1),5X,
   110HSIGMA(M-1))
    WRITE(2,204)XLAMBDA,SIGMA(M),DET(M),DET(M-1),SIGMA(M-1)
204 FORMAT(/20X,5(2X,E12.5)/)
```

```
      IF(ABS(DET(M-1))-ABS(DET(M)))31,31,32
   31 SIGMA(49)=SIGMA(M-1)
      NN=1
      GO TO 100
   32 SIGMA(49)=SIGMA(M)
      NN=1
      GO TO 100
   34 THETA(8)=1.
      DO 74 IO=1,7
      I=8-IO
      THETA(I)=0.
      DO 74 J=I+1,8
   74 THETA(I)=THETA(I)-A(I+8*(J-1))*THETA(J)
      WRITE(2,401)
  401 FORMAT(20X,12HTHETA 1 TO 8/)
   75 WRITE(2,203)THETA
  203 FORMAT(18X,8(2X,F7.4))
      WRITE(2,404)
  404 FORMAT(/23X,1HT,6X,2HTJ,6X,2HTP,6X,2HBB,6X,2HBS,6X,2HBJ,6X,2HBP,
     18X,1HE,5X,4HMODE/)
      WRITE(2,403)T,TJ,TP,BB,BS,BJ,BP,E,MODE
  403 FORMAT(18X,7(2X,F6.3),2X,F10.0,2X,I1)
   35 XLAMBDA=XLAMBDA+DEL
      IF(XLAMBDA-VAL)103,103,450
  405 STOP
      END

END OF SEGMENT, LENGTH  1684, NAME  NG1
```

```
      SUBROUTINE WITTRICK (T,B,SMM,SMF,SFF,FMM,FMF,FFF)
      DIMENSION SIGMA(50)
      COMMON/E/E/XMUE/XMUE/XLAMBDA/XLAMBDA/SIGMA/SIGMA/M/M/ZETA/ZETA
      D=(E*T**3.)/(12.*(1.-XMUE**2.))
      XK=(SIGMA(M)*B*B*T)/(3.1416*3.1416*D)
      ZETA=XK*(XLAMBDA/B)**2.
      OMEGA=3.1416*B/XLAMBDA
      IF(ZETA-1.)1,2,3
    1 ALPHA=OMEGA*(1.+ZETA**.5)**.5
      GAMA=OMEGA*(1.-ZETA**.5)**.5
      Z=SINH(ALPHA)*SINH(GAMA)+(ALPHA*GAMA/OMEGA**2.)*(1.-COSH(ALPHA)*CO
     1SH(GAMA))
      R=ZETA**.5/Z
      SMM=D*R/B*(ALPHA*COSH(ALPHA)*SINH(GAMA)-GAMA*COSH(GAMA)*SINH(ALPH
     1A))
      SMF=D*OMEGA**2./B**2.*(1.-XMUE-ZETA*SINH(ALPHA)*SINH(GAMA)/Z)
      SFF=R*D*ALPHA*GAMA/B**3.*(ALPHA*SINH(ALPHA)*COSH(GAMA)-GAMA*SINH(G
     1AMA)*COSH(ALPHA))
      FMM=R*D/B*(GAMA*SINH(ALPHA)-ALPHA*SINH(GAMA))
      FMF=-R*ALPHA*GAMA*D/B**2.*(COSH(ALPHA)-COSH(GAMA))
      FFF=R*ALPHA*GAMA*D/B**3.*(ALPHA*SINH(ALPHA)-GAMA*SINH(GAMA))
      GO TO 4
    2 ALPHA=OMEGA*2.**.5
      ZSTAR=SINH(ALPHA)+(2.**.5*(1.-COSH(ALPHA)))/OMEGA
      R=1./ZSTAR
      SMM=R*D/B*(ALPHA*COSH(ALPHA)-SINH(ALPHA))
      SMF=(OMEGA/B)**2.*D*(1.-XMUE-R*SINH(ALPHA))
      SFF=R*D/B**3.*ALPHA**2.*SINH(ALPHA)
```

```
      FMM=R*D/B*(SINH(ALPHA)-ALPHA)
      FMF=-(ALPHA*D)/(ZSTAR*B*B)*(COSH(ALPHA)-1.)
      FFF=SFF
      GO TO 4
    3 DELTA=OMEGA*(ZETA**.5-1.)**.5
      ALPHA=OMEGA*(1.+ZETA**.5)**.5
      Z=SINH(ALPHA)*SIN(DELTA)+(ALPHA*DELTA*(1.-COSH(ALPHA)*COS(DELTA)))
     1/OMEGA**2.
      R=ZETA**.5/Z
      SMM=D*R/B*(ALPHA*COSH(ALPHA)*SIN(DELTA)-DELTA*COS(DELTA)*SINH(ALPH
     1A))
      SMF=D*OMEGA**2./B**2.*(1.-XMUE-ZETA*SINH(ALPHA)*SIN(DELTA)/Z)
      SFF=R*D*ALPHA*DELTA/B**3.*(ALPHA*SINH(ALPHA)*COS(DELTA)+DELTA*SIN(
     1DELTA)*COSH(ALPHA))
      FMM=R*D/B*(DELTA*SINH(ALPHA)-ALPHA*SIN(DELTA))
      FMF=-R*ALPHA*DELTA*D/B**2.*(COSH(ALPHA)-COS(DELTA))
      FFF=R*ALPHA*DELTA*D/B**3.*(ALPHA*SINH(ALPHA)+DELTA*SIN(DELTA))
    4 RETURN
      END

END OF SEGMENT, LENGTH   618, NAME  WITTRICK
```

```
      SUBROUTINE XMODE1
      DIMENSION B(8,8)
      COMMON/A11S/A11S/A12S/A12S/A22S/A22S/A11A/A11A/A12A/A12A/A22A/A22A
     1/B/B
      DO 7 I=1,8
      DO 7 J=1,8
    7 B(I,J)=0.
      B(5,5),B(1,1)=A11S
      B(6,5),B(5,6),B(1,2),B(2,1)=A12S
      B(6,6),B(2,2)=A22S
      B(3,3),B(7,7)=0.5*(A11S+A11A)
      B(4,4),B(8,8)=0.5*(A22S+A22A)
      B(3,4),B(4,3),B(7,8),B(8,7)=-0.5*(A12S+A12A)
      B(3,7),B(7,3)=0.5*(A11S-A11A)
      B(4,8),B(8,4)=0.5*(A22S-A22A)
      B(3,8),B(4,7),B(7,4),B(8,3)=-0.5*(A12S-A12A)
      RETURN
      END

END OF SEGMENT, LENGTH   262, NAME  XMODE1
```

```
      SUBROUTINE XMODE2
      DIMENSION B(8,8)
      COMMON/A11S/A11S/A12S/A12S/A22S/A22S/A11A/A11A/A12A/A12A/A22A/A22A
     1/B/B
      DO 7 I=1,8
      DO 7 J=1,8
    7 B(I,J)=0.0
      B(1,1),B(5,5)=(A11S+A11A)*.5
      B(2,2),B(6,6)=(A22S+A22A)*.5
      B(3,3),B(7,7)=A11S
      B(4,4),B(8,8)=A22S
      B(2,1),B(1,2),B(6,5),B(5,6)=(A12S+A12A)*.5
      B(5,1),B(1,5)=(A11S-A11A)*.5
      B(6,1),B(1,6),B(5,2),B(2,5)=(A12S-A12A)*.5
      B(2,6),B(6,2)=(A22S-A22A)*.5
      B(3,4),B(4,3),B(7,8),B(8,7)=-A12S
      RETURN
      END

  END OF SEGMENT, LENGTH   260, NAME  XMODE2
```

```
      SUBROUTINE XMODE3
      DIMENSION B(8,8)
      COMMON/A11S/A11S/A12S/A12S/A22S/A22S/A11A/A11A/A12A/A12A/A22A/A22A
     1/B/B
      DO 7 I=1,8
      DO 7 J=1,8
    7 B(I,J)=0.0
      B(1,1),B(3,3),B(5,5),B(7,7)=(A11S+A11A)
      B(2,2),B(4,4),B(6,6),B(8,8)=(A22S+A22A)
      B(1,3),B(1,7),B(3,5),B(5,7)=(A11S-A11A)*.5
      B(2,3),B(1,4),B(5,8),B(6,7)=(A12S-A12A)*.5
      B(2,8),B(2,4),B(4,6),B(6,8)=(A22S-A22A)*.5
      B(3,6),B(4,5),B(2,7),B(1,8)=(A12S-A12A)*(-0.5)
      DO 9 I=1,8
      DO 9 J=2,8
    9 B(J,I)=B(I,J)
      RETURN
      END

END OF SEGMENT, LENGTH   290, NAME  XMODE3
```

```
      SUBROUTINE XMODE4
      DIMENSION B(8,8)
      COMMON/A11S/A11S/A12S/A12S/A22S/A22S/A11A/A11A/A12A/A12A/A22A/A22A
     1/B/B
      DO 7 I=1,8
      DO 7 J=1,8
    7 B(I,J)=0.0
      B(1,1),B(3,3),B(5,5),B(7,7)=(A11S+A11A)
      B(2,2),B(4,4),B(6,6),B(8,8)=(A22S+A22A)
      B(1,3),B(1,7),B(3,5),B(5,7)=(A11S-A11A)*.5
      B(2,8),B(2,4),B(4,6),B(6,8)=(A22S-A22A)*.5
      B(1,8),B(2,7),B(3,6),B(4,5)=(A12S-A12A)*.5
      B(1,4),B(2,3),B(5,8),B(6,7)=-(A12S-A12A)*.5
      DO 9 I=1,8
      DO 9 J=2,8
    9 B(J,I)=B(I,J)
      RETURN
      END

END OF SEGMENT, LENGTH   288, NAME  XMODE4
```

Specimen No.	Buckling Stress (lb./in.^{2}) Mean Value	Equivalent Face Plate Width (in)		Equivalent Core Flat Width (in)		Actual Width (ins.)	
		b^x	b^{xx}	b^x	b^{xx}	Face Plate	Core
HP 21/22	38,900	1.06	1.40	0.83	1.09	1.17	0.81
HP 24	38,570	1.42	1.87	1.06	1.41	1.17	0.80
HP 37	30,800	2.12	2.80	1.19	1.57	1.64	1.11
HP 57	32,400	0.71	0.94	0.58	0.77	0.84	0.52
HP 59/60	47,800	0.95	1.25	0.74	0.97	0.84	0.51

b^x flat width assuming simply supported edges.

b^{xx} flat width assuming clamped edges.

Table. 2.1. Component Flat Edge Support Conditions.

		v_A	θ_A	v_B	θ_B	v_C	θ_C	v_D	θ_D
panel a_1	V_L	-1	0	0	0	0	0	0	0
	ψ_L	0	+1	0	0	0	0	0	0
	V_R	0	0	+1	0	0	0	0	0
	ψ_R	0	0	0	+1	0	0	0	0
panel a_2	V_L	0	0	0	0	-1	0	0	0
	ψ_L	0	0	0	0	0	+1	0	0
	V_R	0	0	0	0	0	0	+1	0
	ψ_R	0	0	0	0	0	0	0	+1
panel b_1	V_L	0	0	-1	0	0	0	0	0
	ψ_L	0	0	0	+1	0	0	0	0
	V_R	0	0	0	0	+1	0	0	0
	ψ_R	0	0	0	0	0	+1	0	0
panel b_2	V_L	0	0	0	0	0	0	-1	0
	ψ_L	0	0	0	0	0	0	0	+1
	V_R	+1	0	0	0	0	0	0	0
	ψ_R	0	+1	0	0	0	0	0	0

Table 2.2 Matrix A_1 (Common to all buckling modes)

$$\begin{bmatrix}
S_{JFF} & S_{JMF} & F_{JFF} & F_{JMF} & 0 & 0 & 0 & 0 & 0 & 0 & 0 & 0 & 0 & 0 & 0 & 0 \\
S_{JMF} & S_{JMM} & F_{JMF} & F_{JMM} & 0 & 0 & 0 & 0 & 0 & 0 & 0 & 0 & 0 & 0 & 0 & 0 \\
F_{JFF} & F_{JMF} & S_{JFF} & S_{JMF} & 0 & 0 & 0 & 0 & 0 & 0 & 0 & 0 & 0 & 0 & 0 & 0 \\
F_{JMF} & F_{JMM} & S_{JMF} & S_{JMM} & 0 & 0 & 0 & 0 & 0 & 0 & 0 & 0 & 0 & 0 & 0 & 0 \\
0 & 0 & 0 & 0 & S_{JFF} & S_{JMF} & F_{JFF} & F_{JMF} & 0 & 0 & 0 & 0 & 0 & 0 & 0 & 0 \\
0 & 0 & 0 & 0 & S_{JMF} & S_{JMM} & F_{JMF} & F_{JMM} & 0 & 0 & 0 & 0 & 0 & 0 & 0 & 0 \\
0 & 0 & 0 & 0 & F_{JFF} & F_{JMF} & S_{JFF} & S_{JMF} & 0 & 0 & 0 & 0 & 0 & 0 & 0 & 0 \\
0 & 0 & 0 & 0 & F_{JMF} & F_{JMM} & S_{JMF} & S_{JMM} & 0 & 0 & 0 & 0 & 0 & 0 & 0 & 0 \\
0 & 0 & 0 & 0 & 0 & 0 & 0 & 0 & S_{PFF} & S_{PMP} & F_{PFF} & F_{PMF} & 0 & 0 & 0 & 0 \\
0 & 0 & 0 & 0 & 0 & 0 & 0 & 0 & S_{PMF} & S_{PMM} & F_{PMF} & F_{PMM} & 0 & 0 & 0 & 0 \\
0 & 0 & 0 & 0 & 0 & 0 & 0 & 0 & F_{PFF} & F_{PMF} & S_{PFF} & S_{PMF} & 0 & 0 & 0 & 0 \\
0 & 0 & 0 & 0 & 0 & 0 & 0 & 0 & F_{PMF} & F_{PMM} & S_{PMF} & S_{PMM} & 0 & 0 & 0 & 0 \\
0 & 0 & 0 & 0 & 0 & 0 & 0 & 0 & 0 & 0 & 0 & 0 & S_{PFF} & S_{PMF} & F_{PFF} & F_{PMF} \\
0 & 0 & 0 & 0 & 0 & 0 & 0 & 0 & 0 & 0 & 0 & 0 & S_{PMF} & S_{PMM} & F_{PMF} & F_{PMM} \\
0 & 0 & 0 & 0 & 0 & 0 & 0 & 0 & 0 & 0 & 0 & 0 & F_{PFF} & F_{PMF} & S_{PFF} & S_{PMF} \\
0 & 0 & 0 & 0 & 0 & 0 & 0 & 0 & 0 & 0 & 0 & 0 & F_{PMF} & F_{PMM} & S_{PMF} & S_{PMM}
\end{bmatrix}$$

Table 2.3. Matrix K_1 (Common to all buckling modes).

Table 2.3. Matrix K_1 (Common to all buckling modes).

0	0	0	0	0	0	0	0	0	0	0	0	F_{PNF}	F_{PNN}	S_{PNF}	S_{PNN}
0	0	0	0	0	0	0	0	0	0	0	0	F_{PFF}	F_{PNF}	S_{PFF}	S_{PNF}
0	0	0	0	0	0	0	0	0	0	0	0	S_{PNF}	S_{PNN}	F_{PNF}	F_{PNN}
0	0	0	0	0	0	0	0	0	0	0	0	S_{PFF}	S_{PNF}	F_{PFF}	F_{PNF}
0	0	0	0	0	0	0	0	F_{PNF}	F_{PNN}	S_{PNF}	S_{PNN}	0	0	0	0
0	0	0	0	0	0	0	0	F_{PFF}	F_{PNF}	S_{PFF}	S_{PNF}	0	0	0	0
0	0	0	0	0	0	0	0	S_{PNF}	S_{PNN}	F_{PNF}	F_{PNN}	0	0	0	0
0	0	0	0	0	0	0	0	S_{PFF}	S_{PNF}	F_{PFF}	F_{PNF}	0	0	0	0
0	0	0	0	F_{JNF}	F_{JNN}	S_{JNF}	S_{JNN}	0	0	0	0	0	0	0	0
0	0	0	0	F_{JFF}	F_{JNF}	S_{JFF}	S_{JNF}	0	0	0	0	0	0	0	0
0	0	0	0	S_{JNF}	S_{JNN}	F_{JNF}	F_{JNN}	0	0	0	0	0	0	0	0
0	0	0	0	S_{JFF}	S_{JNF}	F_{JFF}	F_{JNF}	0	0	0	0	0	0	0	0
F_{JNF}	F_{JNN}	S_{JNF}	S_{JNN}	0	0	0	0	0	0	0	0	0	0	0	0
F_{JFF}	F_{JNF}	S_{JFF}	S_{JNF}	0	0	0	0	0	0	0	0	0	0	0	0
S_{JNF}	S_{JNN}	F_{JNF}	F_{JNN}	0	0	0	0	0	0	0	0	0	0	0	0
S_{JFF}	S_{JNF}	F_{JFF}	F_{JNF}	0	0	0	0	0	0	0	0	0	0	0	0

$$
\begin{bmatrix}
(S_{JFF} + S_{PFF}) & -(S_{JMF} - S_{PMF}) & -F_{JFF} & -F_{JMF} & 0 & 0 & -F_{PFF} & F_{PMF} \\
-(S_{JMF} - S_{PMF}) & (S_{JMM} + S_{PMM}) & F_{JMF} & F_{JMM} & 0 & 0 & -F_{PMF} & F_{PMM} \\
-F_{JFF} & F_{JMF} & (S_{JFF}+S_{PFF}) & (S_{JMF}+S_{PMF}) & -F_{PFF} & -F_{PMF} & 0 & 0 \\
-F_{JMF} & F_{JMM} & (S_{JMF}+S_{PMF}) & (S_{JMM}+S_{PMM}) & F_{PMF} & F_{PMM} & 0 & 0 \\
0 & 0 & -F_{PFF} & F_{PMF} & (S_{JFF}+S_{PFF}) & (S_{JMF}-S_{PMF}) & -F_{JFF} & -F_{JMF} \\
0 & 0 & -F_{PMF} & F_{PMM} & -(S_{JMF}-S_{PMF}) & (S_{JMM}+S_{PMM}) & F_{JMF} & F_{JMM} \\
-F_{PFF} & -F_{PMF} & 0 & 0 & -F_{JFF} & F_{JMF} & (S_{JFF}+S_{PFF}) & (S_{JMF}-S_{PMF}) \\
F_{PMF} & F_{PMM} & 0 & 0 & -F_{JMF} & F_{JMM} & (S_{JMF}-S_{PMF}) & (S_{JMM}+S_{PMM})
\end{bmatrix}
$$

Table 2.4 Matrix $A_1^{!}$ k_1 A_1 (Common to all buckling modes).

		r_A	θ_A	r_B	θ_B	r_C	θ_C	r_D	θ_D
panel c_1	V_R	+1	0	0	0	0	0	0	0
	Ψ_R	0	+1	0	0	0	0	0	0
panel c_2	V_R	0	0	0	0	+1	0	0	0
	Ψ_R	0	0	0	0	0	+1	0	0
	V_L	0	0	0	0	0	0	+1	0
panel c_3	Ψ_L	0	0	0	0	0	0	0	-1
	V_R	0	0	+1	0	0	0	0	0
	Ψ_R	0	0	0	-1	0	0	0	0

Table 2.5 Matrix A_2 for Mode 1.

$$\begin{bmatrix}
A_{115} & A_{125} & 0 & 0 & 0 & 0 & 0 & 0 \\
A_{125} & A_{225} & 0 & 0 & 0 & 0 & 0 & 0 \\
0 & 0 & A_{115} & A_{125} & 0 & 0 & 0 & 0 \\
0 & 0 & A_{125} & A_{225} & 0 & 0 & 0 & 0 \\
0 & 0 & 0 & 0 & \frac{1}{2}(A_{115}+A_{11A}) & \frac{1}{2}(A_{125}+A_{12A}) & \frac{1}{2}(A_{115}-A_{11A}) & \frac{1}{2}(A_{125}-A_{12A}) \\
0 & 0 & 0 & 0 & \frac{1}{2}(A_{125}+A_{12A}) & \frac{1}{2}(A_{225}+A_{22A}) & \frac{1}{2}(A_{125}-A_{12A}) & \frac{1}{2}(A_{225}-A_{22A}) \\
0 & 0 & 0 & 0 & \frac{1}{2}(A_{115}-A_{11A}) & \frac{1}{2}(A_{125}-A_{12A}) & \frac{1}{2}(A_{115}+A_{11A}) & \frac{1}{2}(A_{125}+A_{12A}) \\
0 & 0 & 0 & 0 & \frac{1}{2}(A_{125}-A_{12A}) & \frac{1}{2}(A_{225}-A_{22A}) & \frac{1}{2}(A_{125}+A_{12A}) & \frac{1}{2}(A_{225}+A_{22A})
\end{bmatrix}$$

Table 2.6. Matrix k_2 for Mode 1.

$$
\begin{bmatrix}
A_{115} & A_{125} & 0 & 0 & 0 & 0 & 0 & 0 \\
A_{125} & A_{225} & 0 & 0 & 0 & 0 & 0 & 0 \\
0 & 0 & \frac{1}{2}(A_{115}+A_{11A}) & -\frac{1}{2}(A_{125}+A_{12A}) & 0 & 0 & \frac{1}{2}(A_{115}-A_{11A}) & -\frac{1}{2}(A_{125}-A_{12A}) \\
0 & 0 & -\frac{1}{2}(A_{125}+A_{12A}) & \frac{1}{2}(A_{225}+A_{22A}) & 0 & 0 & -\frac{1}{2}(A_{125}-A_{12A}) & \frac{1}{2}(A_{225}-A_{22A}) \\
0 & 0 & 0 & 0 & A_{115} & A_{125} & 0 & 0 \\
0 & 0 & 0 & 0 & A_{125} & A_{225} & 0 & 0 \\
0 & 0 & \frac{1}{2}(A_{115}-A_{11A}) & -\frac{1}{2}(A_{125}-A_{12A}) & 0 & 0 & \frac{1}{2}(A_{115}+A_{11A}) & -\frac{1}{2}(A_{125}+A_{12A}) \\
0 & 0 & -\frac{1}{2}(A_{125}-A_{12A}) & \frac{1}{2}(A_{225}-A_{22A}) & 0 & 0 & -\frac{1}{2}(A_{125}+A_{12A}) & \frac{1}{2}(A_{225}+A_{22A})
\end{bmatrix}
$$

Table 2.7. Matrix A_2' K_2 A_2 for Mode 1.

$$
\begin{array}{ll}
 & \begin{array}{cccccccc} r_A & \theta_A & r_B & \theta_B & r_C & \theta_C & r_D & \theta_D \end{array} \\
\begin{array}{cc}
 & V_L \\
 & \Psi_L \\
\text{panel } c_1 & V_R \\
 & \Psi_R \\
\hline
\text{panel } & V_R \\
c_3 & \Psi_R \\
\hline
\text{panel } & V_R \\
c_4 & \Psi_R
\end{array}
&
\left[\begin{array}{cccccccc}
0 & 0 & 0 & 0 & +1 & 0 & 0 & 0 \\
0 & 0 & 0 & 0 & 0 & +1 & 0 & 0 \\
+1 & 0 & 0 & 0 & 0 & 0 & 0 & 0 \\
0 & +1 & 0 & 0 & 0 & 0 & 0 & 0 \\
0 & 0 & +1 & 0 & 0 & 0 & 0 & 0 \\
0 & 0 & 0 & -1 & 0 & 0 & 0 & 0 \\
0 & 0 & 0 & 0 & 0 & 0 & +1 & 0 \\
0 & 0 & 0 & 0 & 0 & 0 & 0 & -1
\end{array}\right]
\end{array}
$$

Table 2.8 Matrix A_2 for Mode 2.

$$\begin{bmatrix}
\frac{1}{2}(A_{115}+A_{11A}) & \frac{1}{2}(A_{125}+A_{12A}) & \frac{1}{2}(A_{115}-A_{11A}) & \frac{1}{2}(A_{125}-A_{12A}) & 0 & 0 & 0 & 0 \\
\frac{1}{2}(A_{125}+A_{12A}) & \frac{1}{2}(A_{225}+A_{22A}) & \frac{1}{2}(A_{125}-A_{12A}) & \frac{1}{2}(A_{225}-A_{22A}) & 0 & 0 & 0 & 0 \\
\frac{1}{2}(A_{115}-A_{11A}) & \frac{1}{2}(A_{125}-A_{12A}) & \frac{1}{2}(A_{115}+A_{11A}) & \frac{1}{2}(A_{125}+A_{12A}) & 0 & 0 & 0 & 0 \\
\frac{1}{2}(A_{125}-A_{12A}) & \frac{1}{2}(A_{225}-A_{22A}) & \frac{1}{2}(A_{125}+A_{12A}) & \frac{1}{2}(A_{225}+A_{22A}) & 0 & 0 & 0 & 0 \\
0 & 0 & 0 & 0 & A_{115} & A_{125} & 0 & 0 \\
0 & 0 & 0 & 0 & A_{125} & A_{225} & 0 & 0 \\
0 & 0 & 0 & 0 & 0 & 0 & A_{115} & A_{125} \\
0 & 0 & 0 & 0 & 0 & 0 & A_{125} & A_{225}
\end{bmatrix}$$

Table 2.9. Matrix k_2 for Mode 2.

$$\begin{bmatrix}
\frac{1}{2}(A_{115}+A_{11A}) & \frac{1}{2}(A_{125}+A_{12A}) & 0 & 0 & \frac{1}{2}(A_{115}+A_{11A}) & \frac{1}{2}(A_{125}-A_{12A}) & 0 & 0 \\
\frac{1}{2}(A_{125}+A_{12A}) & \frac{1}{2}(A_{225}+A_{22A}) & 0 & 0 & \frac{1}{2}(A_{125}-A_{12A}) & \frac{1}{2}(A_{225}-A_{22A}) & 0 & 0 \\
0 & 0 & A_{115} & -A_{125} & 0 & 0 & 0 & 0 \\
0 & 0 & -A_{125} & A_{225} & 0 & 0 & 0 & 0 \\
\frac{1}{2}(A_{115}-A_{11A}) & \frac{1}{2}(A_{125}-A_{12A}) & 0 & 0 & \frac{1}{2}(A_{115}+A_{11A}) & \frac{1}{2}(A_{125}+A_{12A}) & 0 & 0 \\
\frac{1}{2}(A_{125}-A_{12A}) & \frac{1}{2}(A_{225}-A_{22A}) & 0 & 0 & \frac{1}{2}(A_{125}+A_{12A}) & \frac{1}{2}(A_{225}+A_{22A}) & 0 & 0 \\
0 & 0 & 0 & 0 & 0 & 0 & A_{115} & -A_{125} \\
0 & 0 & 0 & 0 & 0 & 0 & -A_{125} & A_{225}
\end{bmatrix}$$

Table 2.10. Matrix A_2' k_2 A_2 for Mode 2.

		r_A	θ_A	r_B	θ_B	r_C	θ_C	r_D	θ_D
panel c_1	V_L	0	0	+1	0	0	0	0	0
	ψ_L	0	0	0	+1	0	0	0	0
	V_R	+1	0	0	0	0	0	0	0
	ψ_R	0	+1	0	0	0	0	0	0
panel c_2	V_L	0	0	0	0	+1	0	0	0
	ψ_L	0	0	0	0	0	-1	0	0
	V_R	0	0	+1	0	0	0	0	0
	ψ_R	0	0	0	-1	0	0	0	0
panel c_3	V_L	0	0	0	0	0	0	+1	0
	ψ_L	0	0	0	0	0	0	0	+1
	V_R	0	0	0	0	+1	0	0	0
	ψ_R	0	0	0	0	0	+1	0	0
panel c_4	V_L	+1	0	0	0	0	0	0	0
	ψ_L	0	-1	0	0	0	0	0	0
	V_R	0	0	0	0	0	0	+1	0
	ψ_R	0	0	0	0	0	0	0	-1

Table 2.11 Matrix A_2 for Mode 3.

$$
\begin{bmatrix}
\multicolumn{2}{c}{K_{c1}} & 0 & 0 & 0 & 0 & 0 & 0 \\
\multicolumn{2}{c}{(4 \times 4)} & 0 & 0 & 0 & 0 & 0 & 0 \\
0 & 0 & \multicolumn{2}{c}{K_{c2}} & 0 & 0 & 0 & 0 \\
0 & 0 & \multicolumn{2}{c}{(4 \times 4)} & 0 & 0 & 0 & 0 \\
0 & 0 & 0 & 0 & \multicolumn{2}{c}{K_{c3}} & 0 & 0 \\
0 & 0 & 0 & 0 & \multicolumn{2}{c}{(4 \times 4)} & 0 & 0 \\
0 & 0 & 0 & 0 & 0 & 0 & \multicolumn{2}{c}{K_{c4}} \\
0 & 0 & 0 & 0 & 0 & 0 & \multicolumn{2}{c}{(4 \times 4)}
\end{bmatrix}
$$

where, K_{c1}, K_{c2}, K_{c3} and K_{c4}

$$
= \frac{1}{2}\begin{bmatrix}
(A_{115} + A_{11A}) & (A_{125} + A_{12A}) & (A_{115} - A_{11A}) & (A_{125} - A_{12A}) \\
(A_{125} + A_{12A}) & (A_{225} + A_{22A}) & (A_{125} - A_{12A}) & (A_{225} - A_{22A}) \\
(A_{115} - A_{11A}) & (A_{125} - A_{12A}) & (A_{115} + A_{11A}) & (A_{125} + A_{12A}) \\
(A_{125} - A_{12A}) & (A_{225} - A_{22A}) & (A_{125} + A_{12A}) & (A_{225} + A_{22A})
\end{bmatrix}
$$

Table 2.12. Matrix k_2 for Mode 3 and Mode 4.

$$\begin{bmatrix}
(A_{11S}+A_{11A}) & 0 & \frac{1}{2}(A_{11S}-A_{11A}) & \frac{1}{2}(A_{12S}-A_{12A}) & 0 & 0 & \frac{1}{2}(A_{11S}-A_{11A}) & -\frac{1}{2}(A_{12S}-A_{12A}) \\
0 & (A_{22S}+A_{22A}) & \frac{1}{2}(A_{12S}-A_{12A}) & \frac{1}{2}(A_{22S}-A_{22A}) & 0 & 0 & -\frac{1}{2}(A_{12S}-A_{12A}) & \frac{1}{2}(A_{22S}-A_{22a}) \\
\frac{1}{2}(A_{11S}-A_{11A}) & \frac{1}{2}(A_{12S}-A_{12A}) & (A_{11S}+A_{11A}) & 0 & \frac{1}{2}(A_{11S}-A_{11A}) & -\frac{1}{2}(A_{12S}-A_{12A}) & 0 & 0 \\
\frac{1}{2}(A_{12S}-A_{12A}) & \frac{1}{2}(A_{22S}-A_{22A}) & 0 & (A_{22S}+A_{22A}) & -\frac{1}{2}(A_{12S}-A_{12A}) & \frac{1}{2}(A_{22S}-A_{22A}) & 0 & 0 \\
0 & 0 & \frac{1}{2}(A_{11S}-A_{11A}) & -\frac{1}{2}(A_{12S}-A_{12A}) & (A_{11S}+A_{11A}) & 0 & \frac{1}{2}(A_{11S}-A_{11A}) & \frac{1}{2}(A_{12S}-A_{12A}) \\
0 & 0 & -\frac{1}{2}(A_{12S}-A_{12A}) & \frac{1}{2}(A_{22S}-A_{22A}) & 0 & (A_{22S}+A_{22A}) & \frac{1}{2}(A_{12S}-A_{12A}) & \frac{1}{2}(A_{22S}-A_{22A}) \\
\frac{1}{2}(A_{11S}-A_{11A}) & -\frac{1}{2}(A_{12S}-A_{12A}) & 0 & 0 & \frac{1}{2}(A_{11S}-A_{11A}) & \frac{1}{2}(A_{12S}-A_{12A}) & (A_{11S}+A_{11A}) & 0 \\
-\frac{1}{2}(A_{12S}-A_{12A}) & \frac{1}{2}(A_{22S}-A_{22A}) & 0 & 0 & \frac{1}{2}(A_{12S}-A_{12A}) & \frac{1}{2}(A_{22S}-A_{22A}) & 0 & (A_{22S}+A_{22A})
\end{bmatrix}$$

Table 2.13. Matrix A_2' k_2 A_2 for Mode 3.

		r_A	θ_A	r_B	θ_B	r_C	θ_C	r_D	θ_D
panel c_1	V_L	0	0	0	0	0	0	+1	0
	ψ_L	0	0	0	0	0	0	0	+1
	V_R	+1	0	0	0	0	0	0	0
	ψ_R	0	+1	0	0	0	0	0	0
panel c_2	V_L	+1	0	0	0	0	0	0	0
	ψ_L	0	-1	0	0	0	0	0	0
	V_R	0	0	+1	0	0	0	0	0
	ψ_R	0	0	0	-1	0	0	0	0
panel c_3	V_L	0	0	+1	0	0	0	0	0
	ψ_L	0	0	0	+1	0	0	0	0
	V_R	0	0	0	0	+1	0	0	0
	ψ_R	0	0	0	0	0	+1	0	0
panel c_4	V_L	0	0	0	0	+1	0	0	0
	ψ_L	0	0	0	0	0	-1	0	0
	V_R	0	0	0	0	0	0	+1	0
	ψ_R	0	0	0	0	0	0	0	-1

Table 2.14 Matrix A_2 for Mode 4.

$$
\begin{bmatrix}
(A_{115}+A_{11A}) & 0 & \frac{1}{2}(A_{115}-A_{11A}) & -\frac{1}{2}(A_{125}-A_{12A}) & 0 & 0 & \frac{1}{2}(A_{115}-A_{11A}) & \frac{1}{2}(A_{125}-A_{12A}) \\
0 & (A_{225}+A_{22A}) & -\frac{1}{2}(A_{125}-A_{12A}) & \frac{1}{2}(A_{225}-A_{22A}) & 0 & 0 & \frac{1}{2}(A_{125}-A_{12A}) & \frac{1}{2}(A_{225}-A_{22A}) \\
\frac{1}{2}(A_{115}-A_{11A}) & -\frac{1}{2}(A_{125}-A_{12A}) & (A_{115}+A_{11A}) & 0 & \frac{1}{2}(A_{115}-A_{11A}) & \frac{1}{2}(A_{125}-A_{12A}) & 0 & 0 \\
-\frac{1}{2}(A_{125}-A_{12A}) & \frac{1}{2}(A_{225}-A_{22A}) & 0 & (A_{225}+A_{22A}) & \frac{1}{2}(A_{125}-A_{12A}) & \frac{1}{2}(A_{225}-A_{22A}) & 0 & 0 \\
0 & 0 & \frac{1}{2}(A_{115}-A_{11A}) & \frac{1}{2}(A_{125}-A_{12A}) & (A_{115}+A_{11A}) & 0 & \frac{1}{2}(A_{115}-A_{11A}) & -\frac{1}{2}(A_{125}-A_{12A}) \\
0 & 0 & \frac{1}{2}(A_{125}-A_{12A}) & \frac{1}{2}(A_{225}-A_{22A}) & 0 & (A_{225}+A_{22A}) & -\frac{1}{2}(A_{125}-A_{12A}) & \frac{1}{2}(A_{225}-A_{22A}) \\
\frac{1}{2}(A_{115}-A_{11A}) & \frac{1}{2}(A_{125}-A_{12A}) & 0 & 0 & \frac{1}{2}(A_{115}-A_{11A}) & -\frac{1}{2}(A_{125}-A_{12A}) & (A_{115}+A_{11A}) & 0 \\
\frac{1}{2}(A_{125}-A12A) & \frac{1}{2}(A_{225}-A_{22A}) & 0 & 0 & -\frac{1}{2}(A_{125}-A_{12A}) & \frac{1}{2}(A_{225}+A_{22A}) & 0 & (A_{225}+A_{22A})
\end{bmatrix}
$$

Table 2.15. Matrix A_2' k_2 A_2 for Mode 4.

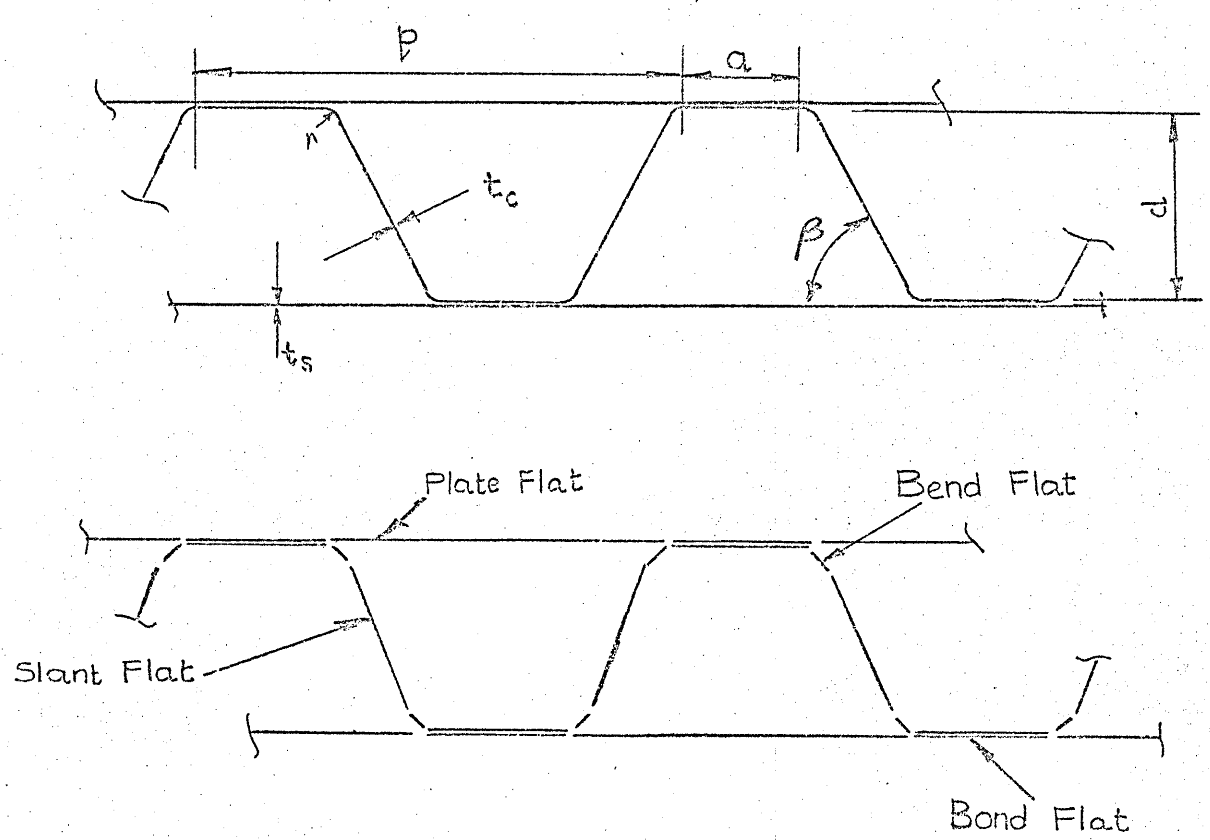

Fig. 2.1 Spliting of the Panel into Component Flats

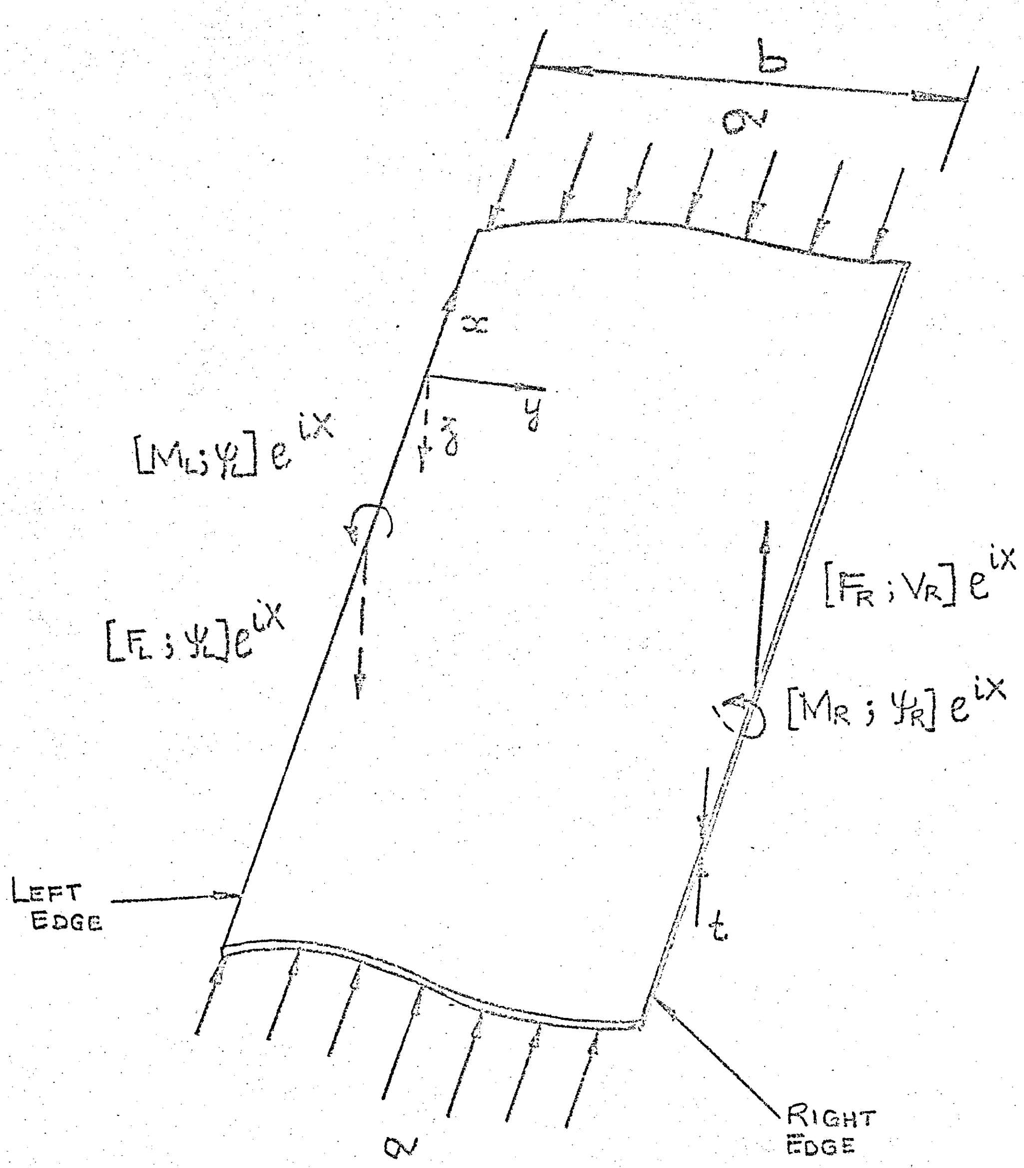

Fig. 2.2 The System of Forces and Displacements.

Fig. 2.3 Buckling Mode 1.

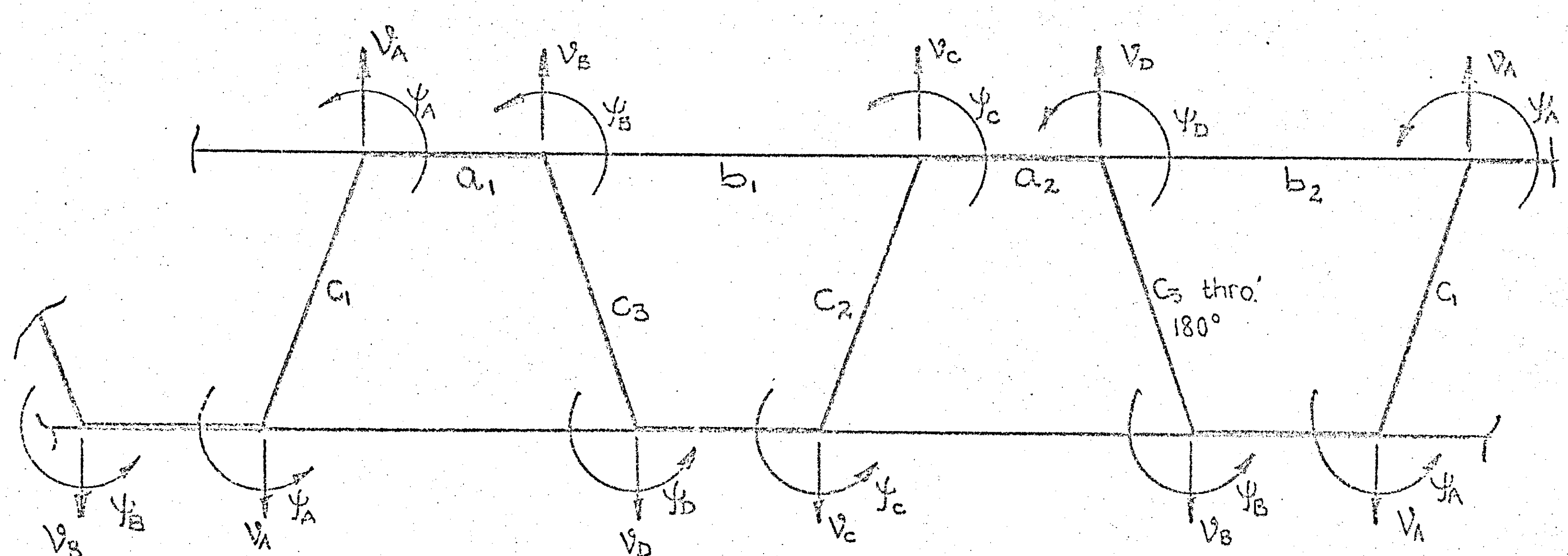

Fig. 2.4 Buckling Mode 2.

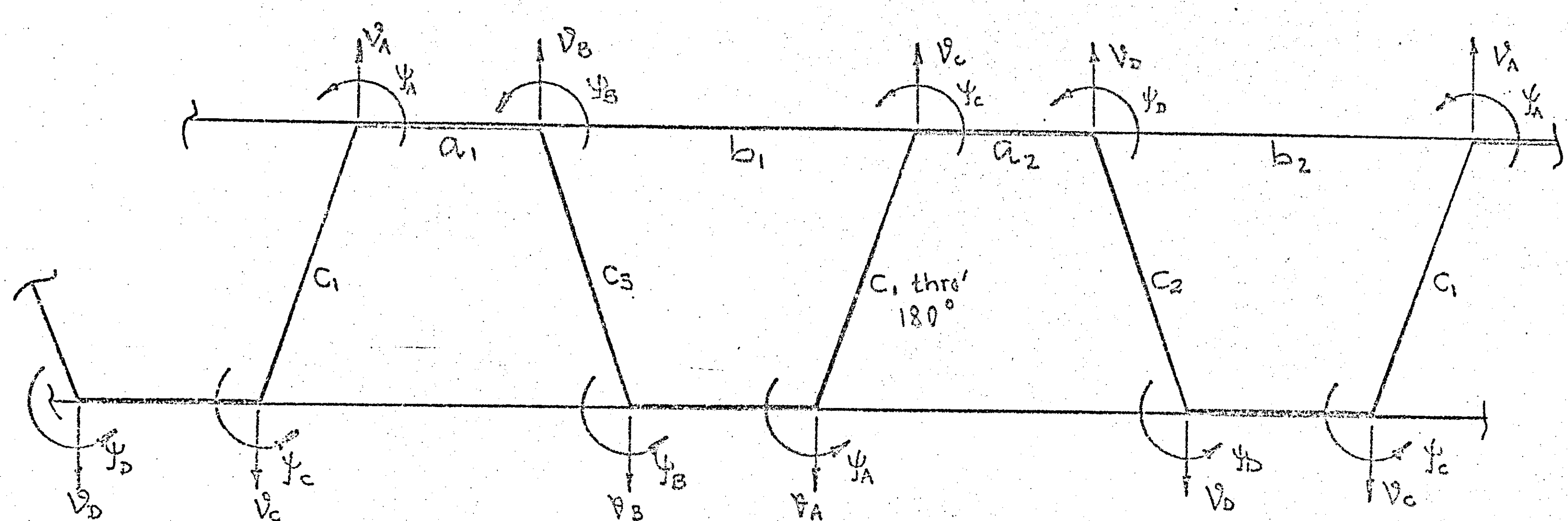

FIG. 2.5 Buckling Mode 3

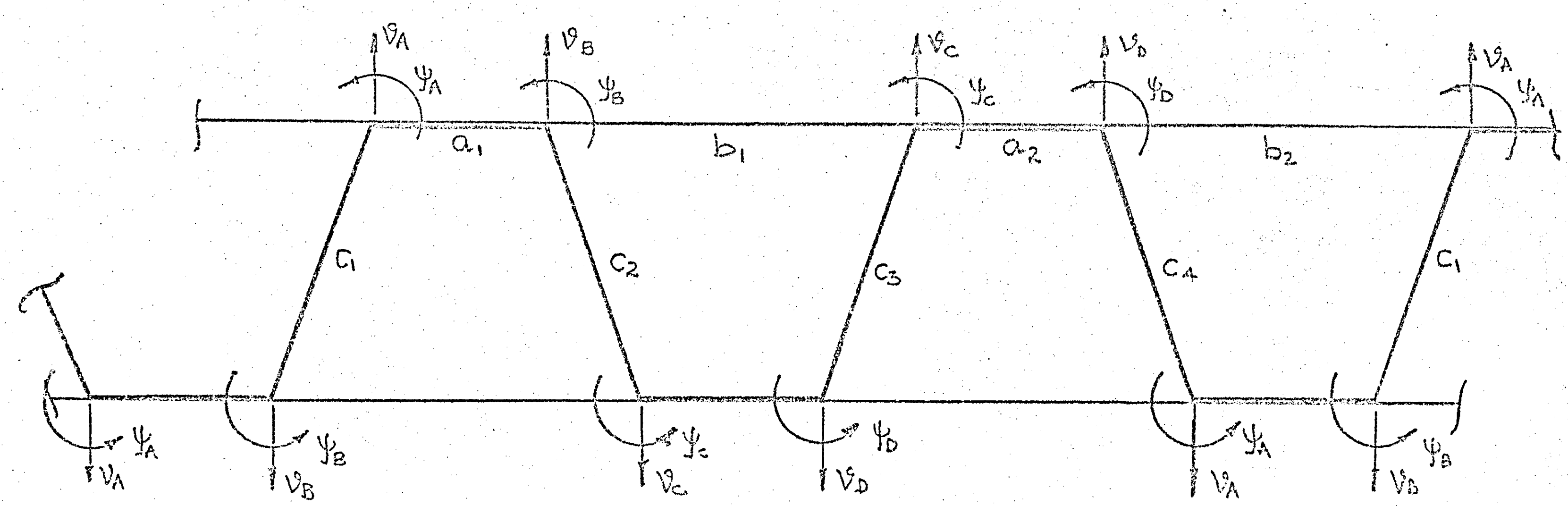

FIG. 2.6 Buckling Mode 4

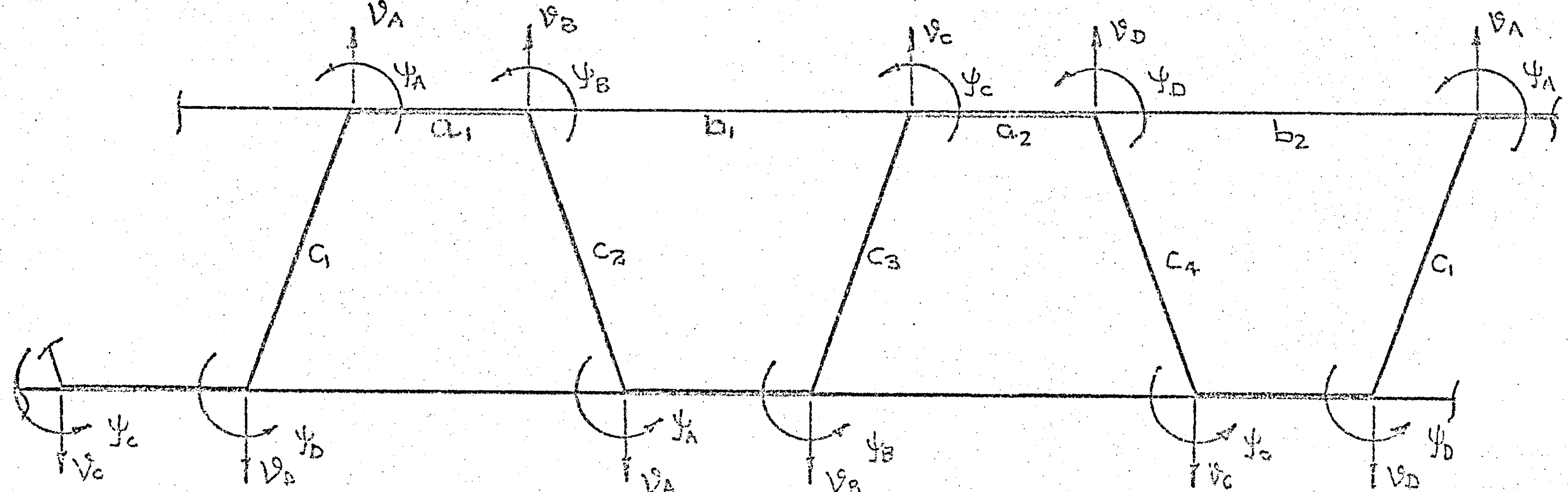

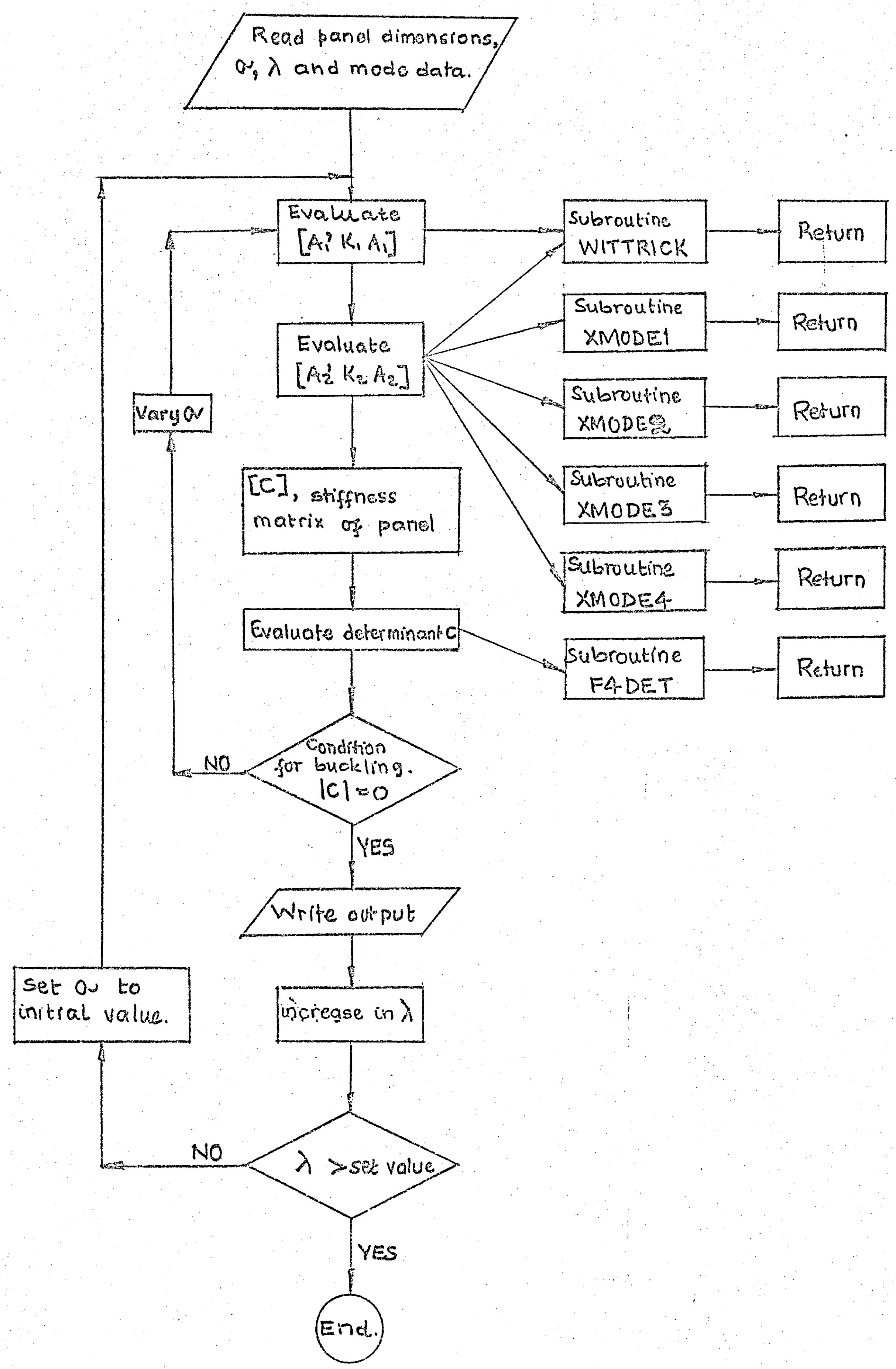

Fig. 2.7 General Flow-chart For the Program.

SECTION 3.

EXPERIMENTAL PROGRAMME

3. EXPERIMENTAL PROGRAMME

3.1 Review of Previous Work

Several configurations of bonded corrugated core sandwich panels have been tested by Handley Page Test Department. The results are presented in Report No. 8834. (see Ref.2). Though the information about buckling stresses and failure stresses have been tabulated in the report, the actual buckling mode shapes have not been recorded.

Table 3.1 shows the series of panel configurations tested by Handley Page Ltd. The overall panel dimensions and notations used in Table 3.1 are explained in Figure 3.1. Each specimen was six inches long with a core four pitch wide. Outer face-plates spanned three pitches and inner face-plates four pitches.

The values of buckling and failure stresses are tabulated in Table 3.2.

3.2 Design of Specimens

It was decided to have the corrugated core folded in the Aircraft Design departmental workshop and contract-out for the bonding of face-plates to the core.

3.2.1 Design considerations

The experimental programme was established by taking into consideration several factors.

a. The specimen configuration had to cover the range tested by Handley Page Ltd.

b. For realistic comparison with the H.P. test specimens, the specimens had to be made from aluminium alloy in DTD 687 specification.

c. Increase in overall size of the panels to enable easier recording of the panel buckling mode shapes.

d. A range of bend radius of the corrugation to determine the effect of bend radius on the buckling mode shape and on buckling stresses.

e. Limit the overall dimensions and the skin thicknesses used so that the specimens could be tested on the available 150 ton Denison Test Machine.

3.2.2 Specimen configurations

Taking into consideration the factors listed above, the specimen configurations chosen for the test programme are shown in Table 3.3.

Four basic core configurations are employed. Three specimens for each configuration were made. This was done so that first panel of each configuration could be tested to obtain buckling stress trends, attempting to avoid failure. The second and third panels to be tested to measure buckle form on at least one, and on both where indicated by the stress trends. Having three specimens for each configuration also allows for bond failure or similar mishap without upsetting the test program seriously.

The overall dimensions of the specimens are 4 pitch wide and 12 ins. long. The only exception being specimen no.1 which is 4 pitch wide and six inches long. The ends of the specimens are milled flat and parallel. Before testing, skin and core thicknesses and other dimensions are measured at several points. Individual dimensions are not recorded but mean values are quoted in Table 3.4.

Cross-sectional areas were determined by multiplying measured thicknesses by nominal developed widths. The developed widths of cores were computed from the expression:

$$b_c = 2 \left\{ (d - t_c) - (2r + t_c)(1 - \mathrm{Cos}\beta) \right\} \mathrm{Cosec}\beta$$

$$+ 2\left\{ a + \frac{\beta\pi}{180} (2r + t_c) \right\} \quad \text{per pitch}$$

Cross-sectional areas are tabulated in Table 3.4.

3.3 Deflection Measurements

Initially, taking into consideration the application of heat and pressure during bonding of face-plates to core, it was decided to mount the strain gauges externally. Fig.3.2 shows the proposed strain gauging of the panel. For further measurements of buckling deflections, lateral and axial traverses with dial gauges were proposed.

Due to several production difficulties (see para.3.4) it was decided to revise the 'gauging' of the specimen.

3.3.1 Deflection measurement by strain gauges

At the time of testing panel 5B/1, the availability of the remainder of the specimens was not known. For this reason, it was decided to 'gauge' the panel 5B/1 extensively. (see Plate 3.1).

The locations of strain gauges are shown in Fig. 3.3 'Solartron Compact Logger' and 'Addo Printer' were used to record the strain gauge readings.

3.3.2 Deflection measurement by contractometers

Initially, three 'contractometers' comprising dial gauges attached to the specimen through linkages (2:1 lever ratio) measuring on 10 in. gauge lengths were used. (see Fig.3.4).

Later in the test programme, four 'contractometers' were used. (see Fig.3.5).

3.3.3 Observation of buckling deflections

Buckle shapes were observed by studying the reflections of an 'illuminated grid' on the polished face-plates and the exposed slant flats of the core.

3.4 Production Difficulties

For this test programme it is necessary to have tight control on the various parameter of the core, especially, the core bend radius, r, and the attachment width, a.

As the cores were folded in a folding press, the desired tight control was not possible, and production of 'identical' cores was even more difficult. Further, the aluminium alloy used for the core is in DTD 687 specification, which is not particularly suitable for tight bend radius.

For the bonding of the face-plates to the core, Bonded Structures Division, CIBA Ltd., imposed a maximum limit of .020 ins. on the core depth variation for producing a reasonably satisfactory bond. The three panels in 5B configuration (see Table 3.3) were bonded by Ciba Ltd., and delivered for inspection. Out of the three panels, only one did not show broken bond lines.

It was therefore, decided to check the remaining 36 cores for depth variation. This revealed that only 10 cores satisfied the 0.020 ins. limit. The panels using these cores are indicated in Table 3.3.

3.5 Test Procedure

The specimens were tested in the 150 ton Denison compressive machine.

The position of each specimen between the plattens was adjusted and in some cases packing strips used to ensure even loading of the specimen.

Deflections were measured at approximately ton loading increments for panels in '5' series and at approximately 1 ton loading increments for panels in '2' series; extending close to the buckling load.

3.6 Determination of Buckling Loads

Face-plate or core slant-flat buckling load is taken as the load at which a change in slope of the load/deflection graph occurs.

Load-deflection plots for the specimens are given in Appendix 2.

Specimen No.	p (ins.)	d (ins.)	β (deg.)	a (ins.)	r (ins.)	Number tested	t_c (SWG)	t (SWG)
21 +	1.65	0.75	63°	0.32	0.16	3	22	20
22 ++	1.65	0.75	63	0.32	0.16	3	22	20
24	1.65	0.75	63	0.32	0.16	3	20	18
37	2.20	1.00	61	0.40	0.10	3	20	16
39	2.20	1.00	61	0.40	0.10	0 X	16	13
57	1.10	0.50	67	0.26	0.08	1	26	24
59 +	1.10	0.50	67	0.26	0.08	3	22	20
60 ++	1.10	0.50	67	0.26	0.08	3	22	20

\+ Redux bonded by Handley Page Ltd.

++ Redux bonded by A.R. Ltd.

X Curing fault.

Table 3.1. Handley Page Test Specimen Configurations.

Specimen No.		Buckling Stress (lb./in.^{2})		Failing Stress (lb./in.^{2})	
		Test Value	Mean Value	Test Value	Mean Value
	a	38,900		50,700	
21	b	37,800		50,100	
(H.P.Ltd)	c	40,400	38,900	47,400	48,530
	a	38,800		50,300	
22	b	40,900		47,500	
(A.R.Ltd)	c	36,600		45,200	
	a	39,900		57,600	
24	b	40,200	38,570	61,500	59,200
	c	38,600		58,500	
	a	30,500		52,300	
37	b	30,500	30,800	55,800	54,330
	c	31,400		54,900	
57	a	32,400	32,400	40,600	40,600
	a	44,600		59,900	
59	b	43,000		66,900	
(H.P.Ltd)	c	43,000	47,800	61,900	64,480
	a	50,700		66,500	
60	b	53,300		73,300	
(A.R.Ltd)	c	52,200		61,100	

Table 3.2 Handley Page Test Results.

Specimen No.	p (ins.)	d (ins.)	(deg.)	a (ins.)	r (ins.)	t_c (SWG)	t (SWG)	N++
1 +	2.2	1.0		0.4	0.156	18	16	0
2A	4.4	2.0	59	0.8	0.175	18	18	1
2B	4.4	2.0	60	0.7	0.300	18	18	1
2C	4.4	2.2	66	0.7	0.400	18	18	2
3A	4.4	2.0	59	0.8	0.175	18	16	0
3B	4.4	2.0	60	0.7	0.300	18	16	0
3C	4.4	2.2	66	0.7	0.400	18	16	0
4A	4.4	2.0	59	0.8	0.175	18	14	1
4B	4.4	2.0	60	0.7	0.300	18	14	1
4C	4.4	2.2	66	0.7	0.400	18	14	2
5A	4.4	2.0	59	0.8	0.175	18	12	1
5B	4.4	2.0	60	0.7	0.300	18	12	1
5C	4.4	2.2	66	0.7	0.400	18	12	1

\+ Core used in Specimen No.1 is a standard corrugation.

All specimens except specimen No.1, are four pitch wide and 12 ins. long.

Specimen No.1 is four pitch wide and 6 ins. long.

++ N is the number of panels that could be produced. (See Section 3, para. 3.4).

Table 3.3. Panel Configurations for the Test Programme.

Panel No.	a (ins)	d (ins)	p (ins)	r (ins)	Wo (ins)	Wi (ins)	t_c (ins)	t_s (ins)	h (ins)	Cross-sectional area ($in.^2$)
5B/1	.7	2	4.25	.3	14.0	17.85	.049	.104	11.98	4.593
5B/2	.7	2	4.2	.3	9.85	13.03	.049	.104	11.80	3.337
5B/3	.7	2	4.2	.3	13.98	17.94	.049	.104	11.90	4.595
2A/1	.8	2	4.2	.175	13.65	17.64	.048	.048	11.90	2.747
2B/1	.8	2	4.2	.3	13.65	17.60	.048	.048	11.93	2.780
2C/1	.8	2	4.2	.4	14.28	18.00	.049	.048	11.96	2.865
2C/2	.8	2	4.3	.4	14.30	17.80	.049	.048	11.92	2.855

Table 3.4 Measured specimen **Dimensions**. (Mean Values)

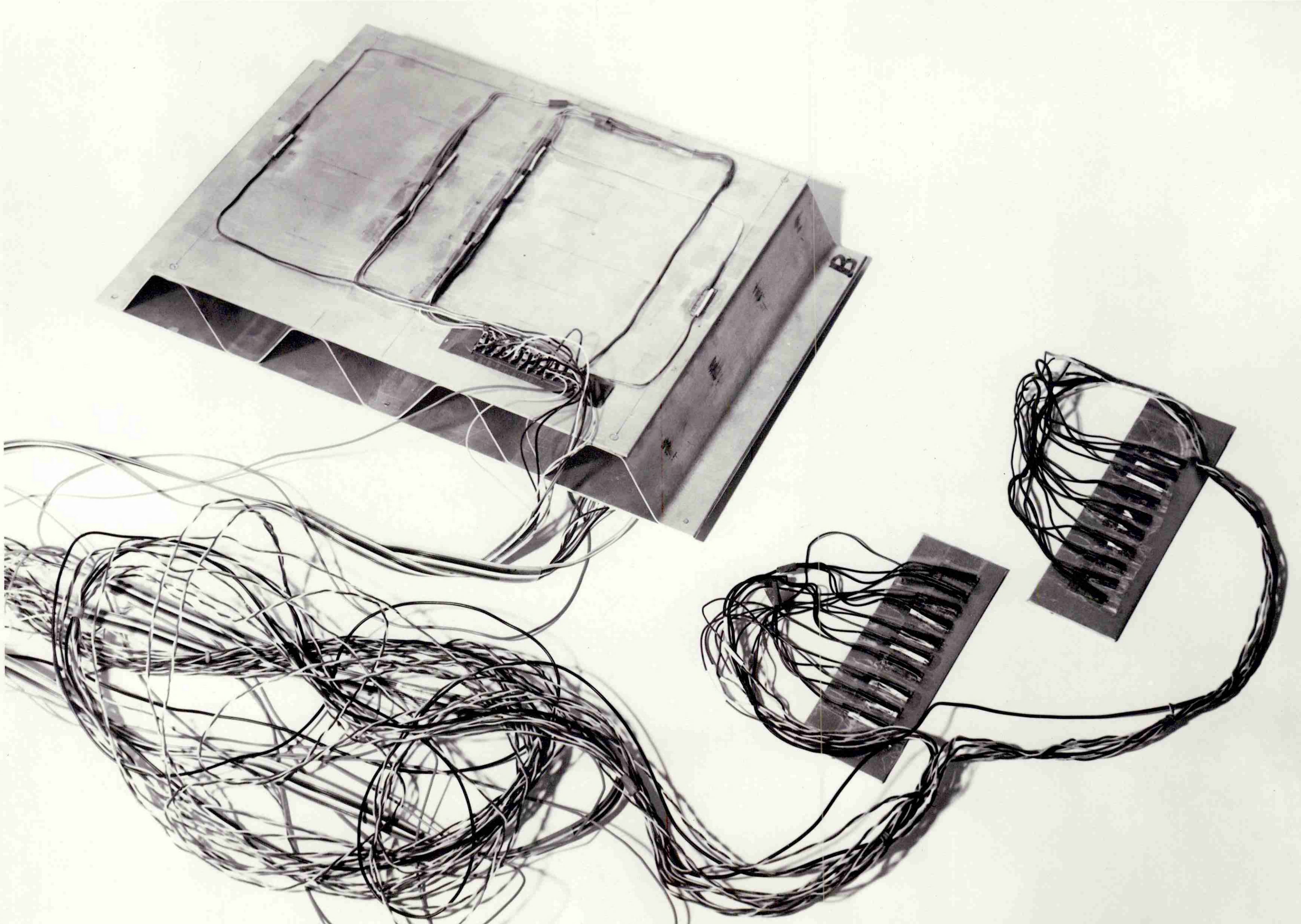

Plate 3·1 Strain Gauging of Panel 5B/1.

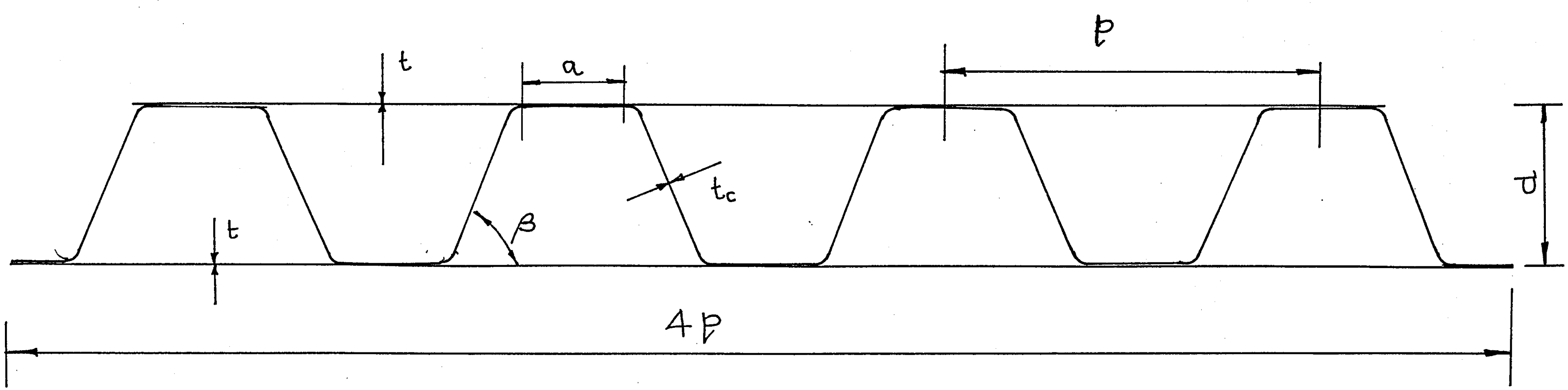

Length of Panel = 6 ins.

Fig. 3.1 Handley Page Test Specimens.

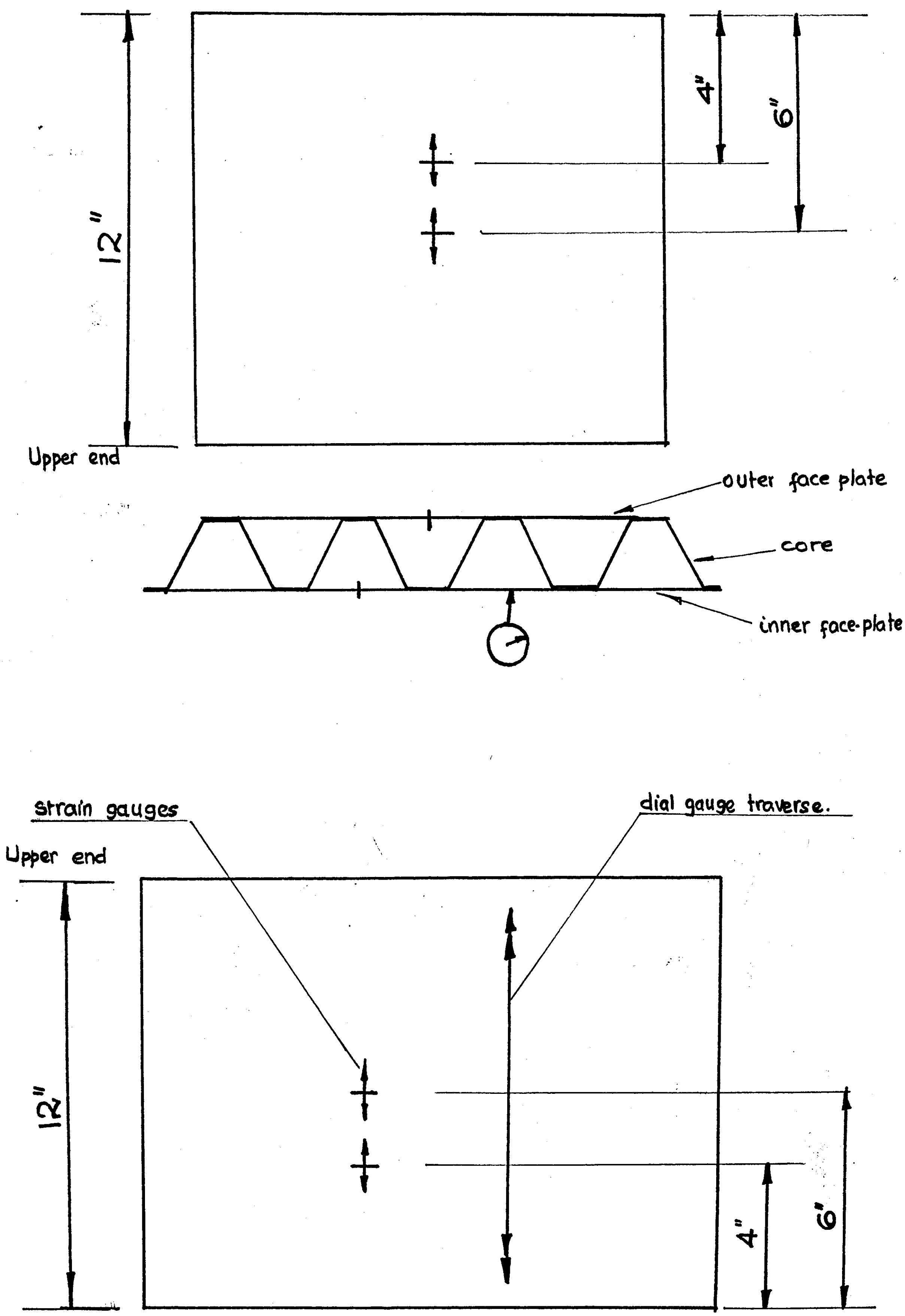

Fig. 3.2 Proposed Method of Deflection Measurement.

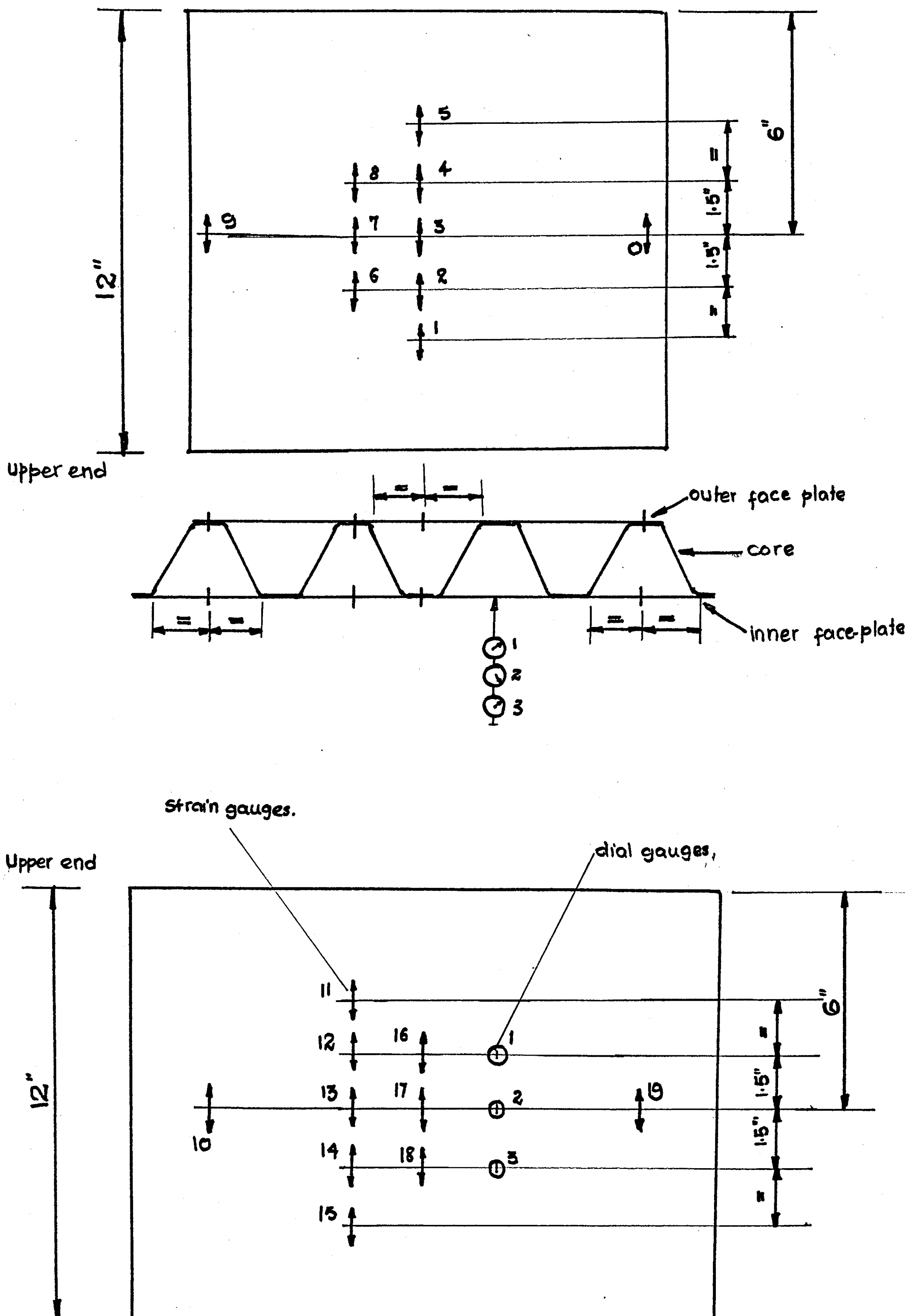

Fig. 3.3 Deflection Measurement Gauges for Panel 5B/1.

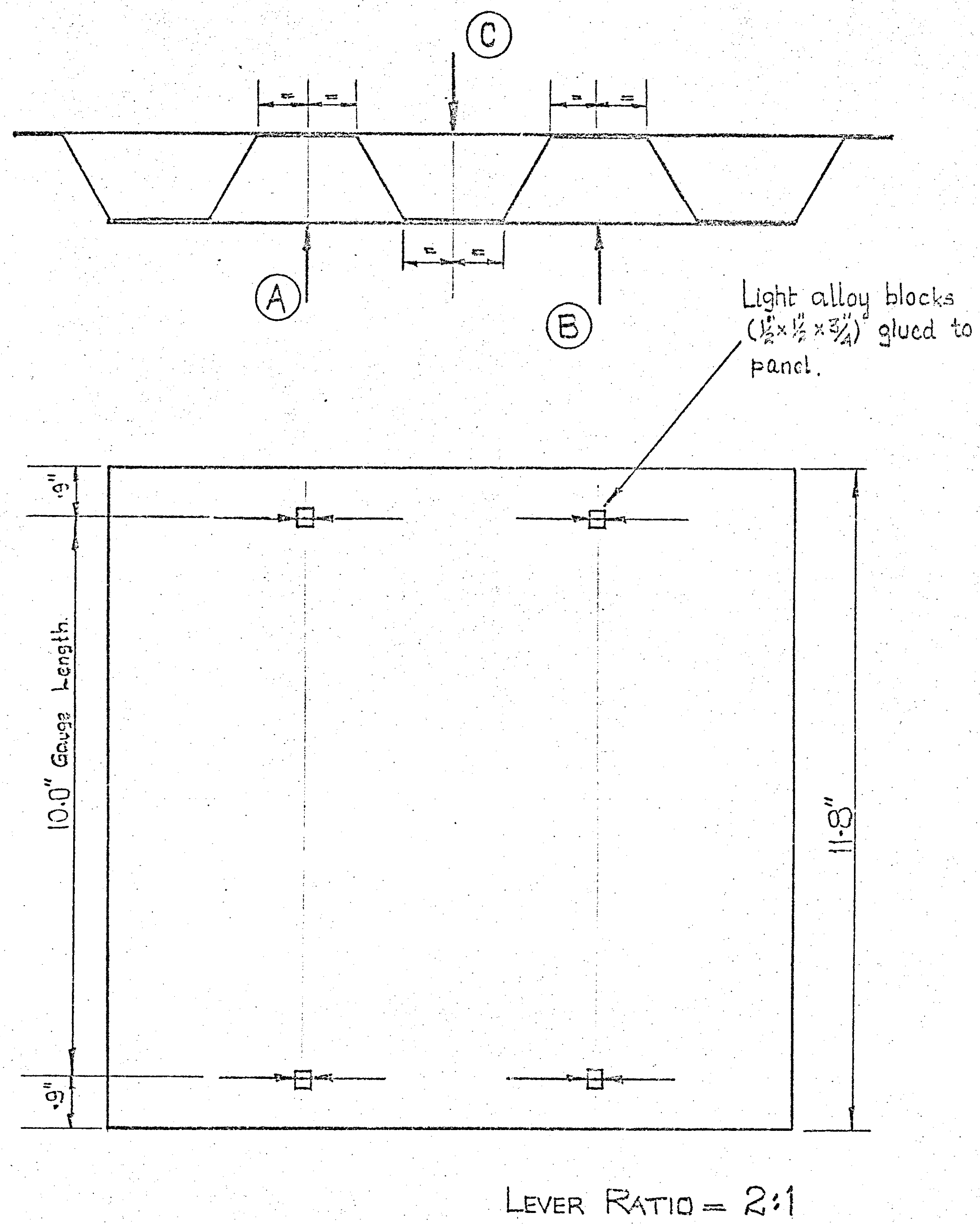

FIG. 3·4 Contractometer Positions for Panel 5B/2.

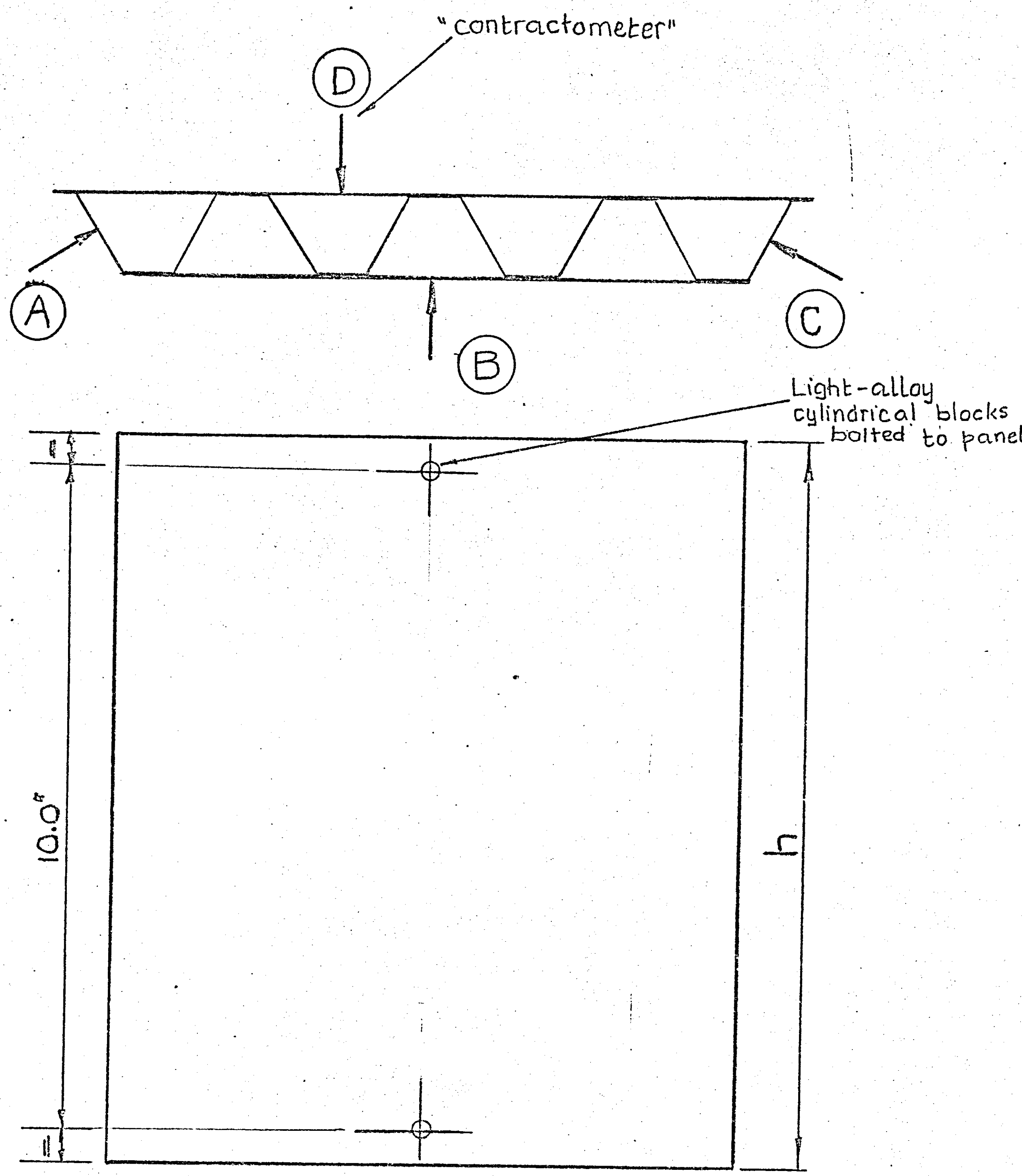

Lever Ratio = 2:1

Fig. 3·5 General Contractometer Layout.

SECTION 4.

RESULTS

4. RESULTS

4.1 Results from the Computer Program (D10A)

The computer program has been run with specimen configuration data to calculate buckling stress, and deflections and rotations at attachment points (See Figs.2.3 - 2.6) for the range of Handley Page specimens (Table 3.1) and the test program specimens (Table 3.3).

The program has also been run to study the effect of variation of several parameters.

The results from the program are tabulated and graphically represented (where applicable) at the end of this section.

4.1.1 Buckling stresses and buckling wave-lengths

The computer program results for Handley Page specimens and the test program specimens are tabulated in Tables 4.1 and 4.2 respectively. They are plotted in Figs. 4.1 to 4.4.

In Table 4.3, minimum buckling stresses for Handley Page specimens are compared with the theoretical values predicted by Ref.4 and Ref.5 and the test values from Ref.2.

4.1.2 Buckling modes

For the four buckling modes considered (see section 2) the buckling stresses are tabulated in Table 4.5 and plotted in Fig. 4.5.

Results indicate that buckling modes 1 and 2 and 3 and 4 are identical from the point of view of buckling stresses.

4.1.3 Effect of variation of the basic parameters

The titles are self explanatory. The values of buckling stresses are tabulated and plotted.

Effect of variation of Young's Modulus: Table 4.7; Fig.4.7

Effect of variation of 'bond-flat' width:Table 4.8; Fig.4.8

Effect of variation of 'skin-bond-core'
thickness: Table 4.9; Fig.4.9

Effect of variation of 'bend-flat'width: Table 4.10; Fig.4.10

4.1.4 Buckling deflections

For reasons outlined in Appendix 5, the deflections at lower buckling wave-lengths cannot be relied upon.

A general case of buckling deflections for the buckling mode considered is shown in Fig.4.6.

4.2 Test Programme Results

The buckling load of the panel is taken as the load at which a change in the slope of the 'load-strain' graph occurs.

Initial irregularities are difficult to assess. This method is, therefore, somewhat subjective in application.

Experimental records are presented in Appendix 4. The load-deflection graphs and the values of buckling stresses for the face-plates and the core for each of the specimen are derived in Appendix 2.

4.2.1 Mean buckling stresses

For comparison with theoretically predicted values it is necessary to quote an average buckling stress for each of the panels.

For this purpose, it is assumed that the average buckling stress for the panel is the stress at which both the core and the face-plates have buckled.

In cases where the core has buckled before the face-plates, the mean of the inner and outer face-plate buckling stress value is given. (See Table 4.4).

Where more than one of the same specimen configuration were tested, the average buckling stress value is quoted. (Panels 5B and 2C).

4.2.2 Buckling wave-lengths

Rough measurements were made for the buckling wave-lengths.

Panels in 5B configuration

Core slant-face buckle pattern for panel 5B/1 is illustrated by Fig.4.11. Average buckling wave-length, $2 \times \lambda$, for the core slant-face was 3 ins. Average face-plate buckle wave-length was 4.3 ins.

Similar buckling wave-lengths were exhibited by panels 5B/2 (See Plates 4.2 and 4.3) and 5B/3.

Failed panel 5B/2 is illustrated by Plate 4.4.

Panels in series 2

Average buckle wave-lengths were:

Inner face-plate: 4.2 ins.

Outer face-plate: 4.5 ins.

Core slant-face: 4.1 ins.

λ (ins.)	Buckling Stress, σ (lb/in^2)				
	HP 21/22	HP 24	HP 37	HP 57	HP 59/60
0.50		150,700	97,500	34,800	89,900
0.75	45,500	78,400	86,600	28,800	71,800
1.00	39,900	67,200	72,000	28,300	69,800
1.25	37,900	63,200	61,400	30,300	74,800
1.50	37,900	63,200	58,600	34,000	84,200
1.75	39,500	66,000	59,700	39,200	112,700
2.00	42,300	70,800	63,300	45,500	131,000
2.25	46,000	77,200	68,700	53,000	151,800

Table 4.1 : Buckling Stresses for Handley Page Specimens (using the computer program)
($E = 9.3 \times 10^6$ lb/in^2)

λ (ins.)	Buckling Stresses, $\sigma \times 10^{-3}$ (lb/in^2)								
	5A	5B	5C	4A	4B	4C	2A	2B	2C
1.25	32.9	31.6	30.0	32.8	31.6	29.9			
1.50	32.7	31.1	25.3	32.6	31.0	25.3			
1.75	34.7	32.6	25.6	30.8	30.5	25.5	11.3	11.2	11.3
2.00	38.2	35.6	27.0	26.1	25.8	26.8	10.1	9.9	10.1
2.25	42.8	39.6	29.3	23.3	23.0	24.2	9.4	9.2	9.4
2.50	35.0	35.4	32.3	21.7	21.2	22.3	9.1	8.8	9.0
2.75	32.4	32.1	35.7	20.6	20.0	21.0	9.0	8.5	8.9
3.00	30.8	30.2	34.2	20.1	19.2	20.2	9.1	8.5	8.8
3.25	29.9	28.9	31.3	19.8	18.7	19.6	9.3	8.6	8.9
3.50	29.5	28.2	30.0	19.9	18.5	19.3	9.6	8.7	9.1
3.75	29.4	27.8	29.2	20.1	18.4	19.2	10.0	9.0	9.3
4.00	29.5	27.6	28.8	20.5	18.5	19.2	10.5	9.3	9.6
4.25	29.9	27.6	28.8	21.1	18.7	19.4			
4.50	30.5	27.9	28.9	21.8	19.1	19.6			

Table 4.2 : Buckling Stresses for the Test Programme Specimens.

(Using the Computer Program D10A.)

Specimen No.	Buckling Stress Value, σ, (lb./in.^{2})			
	Test value (Ref. 2)	Wittrick (Ref. 4)	Data Sheet Value (Ref. 5)	Program D10A Value (Fig. 4.1)
21/22	38900	41000	44460 at λ=.8"	37600 at λ= 1.3"
24	38570	70500	76800 .9"	62800 1.3"
37	30800	48500	58580 .8"	58400 1.55"
57	32400	*	32630 .6"	28000 0.9"
59/60	47800	*	87260 .6"	69800 1.0"

* Values not available

(Theoretical values calculated using E= 9.3 x 10^6 lb/in^2)

Table 4.3 : Comparision of Buckling Stresses for Handley Page Specimens.

Specimen No.	Buckling Stress Value, σ (lb./in.^{2})		
	Test value (Section 4)	Data Sheet value (Ref. 5.)	Program D10A value (Figs.:4.2/3/4/7)
1	*	98700 at λ =1.0"	55500 at λ =1.6"
5A	*	**	29400 3.75"
5B	32500	**	27600 4.10"
5C	*	**	25200 1.60"
4A	*	**	17800 3.25"
4B	*	**	17200 3.75"
4C	*	**	16400 3.75"
2A	11200	**	9000 2.75"
2B	10450	**	8470 2.90"
2C	11250	**	8800 3.00"

* Not available for testing

** Outside the range of Data Sheets.

(Theoretical values calculated using E= 9.7×10^6 lb/in^2)

Table 4.4 : Comparison of Buckling Stresses for the Test Programme Specimens.

λ	Buckling Stress, σ (lb/in^2)			
(ins.)	Mode 1	Mode 2	Mode 3	Mode 4
1.0	68,500	68,500	74,700	74,700
1.2	60,100	60,100	70,000	70,000
1.4	56,500	56,500	71,500	71,500
1.6	55,500	55,500	75,900	75,900
1.8	56,400	56,400	82,900	82,900
2.0	58,500	58,500	91,900	91,900
2.2	61,600	61,600	102,700	102,700
2.4	65,600	65,600	115,000	115,000

Table 4.5 : Buckling Stress for Specimen 1, under Buckling Modes 1 to 4.

λ (ins.)	Buckling Stress, σ (lb/in^2)	
	$E = 9.7 \times 10^6$ lb/in^2	$E = 9.3 \times 10^6$ lb/in^2
1.0	68,500	65,700
1.2	60,100	57,700
1.4	56,500	54,100
1.6	55,500	53,300
1.8	56,400	54,100
2.0	58,500	56,100
2.2	61,600	59,100
2.4	65,600	62,900

Table 4.7 : Effect of Variation of Young's Modulus E.

(Mode 1)

λ (ins)	Buckling Stress, σ (lb/in^2)			
	a = 0.2 ins	a = 0.3 ins	a = 0.4 ins	a = 0.5 ins
1.00	68,100	68,300	68,500	68,600
1.25	58,600	58,700	58,900	59,100
1.50	55,600	55,500	55,700	56,000
1.75	56,100	55,800	56,100	56,500
2.00	58,800	58,200	58,500	59,200
2.25	63,000	62,100	62,600	63,500
2.50	68,500	67,200	67,800	69,100

Table 4.8 : Effect of Variation of Bond-Flat Width.

λ (ins.)	Buckling Stress, σ (lb/in^2)				
	t = .048 in	t = .064 in	t = .104 in	t = .112 in	t = .128 in
1.00	62,700	63,500	67,600	68,500	70,300
1.25	51,900	52,800	57,700	58,900	61,400
1.50	48,100	49,100	54,300	55,700	58,700
1.75	48,100	49,100	54,500	56,100	59,400
2.00	50,400	51,300	56,900	58,500	62,200
2.25	54,300	55,300	60,900	62,600	66,400
2.50	59,600	60,500	66,100	67,800	71,800

Table 4.9 : Effect of Variation of Skin-Bond-Core Thickness.

λ (ins)	Buckling Stress, σ (lb/in^2)				
	b = .10 in	b = .15 in	b = .20 in	b = .25 in	b = .30 in
1.0	69,000	68,300	68,600	69,100	69,600
1.2	61,800	60,200	60,200	60,700	61,400
1.4	59,700	56,900	56,500	56,800	57,500
1.6	60,600	56,400	55,500	55,500	56,100
1.8	63,600	57,800	56,300	56,000	56,300
2.0	68,200	60,500	58,300	57,600	57,600
2.2	74,100	64,300	61,300	60,200	59,900
2.4	81,100	69,000	65,100	63,600	62,900

Table 4.10 : Effect of Variation of 'Bend-Flat' Width.

(Mode 1)

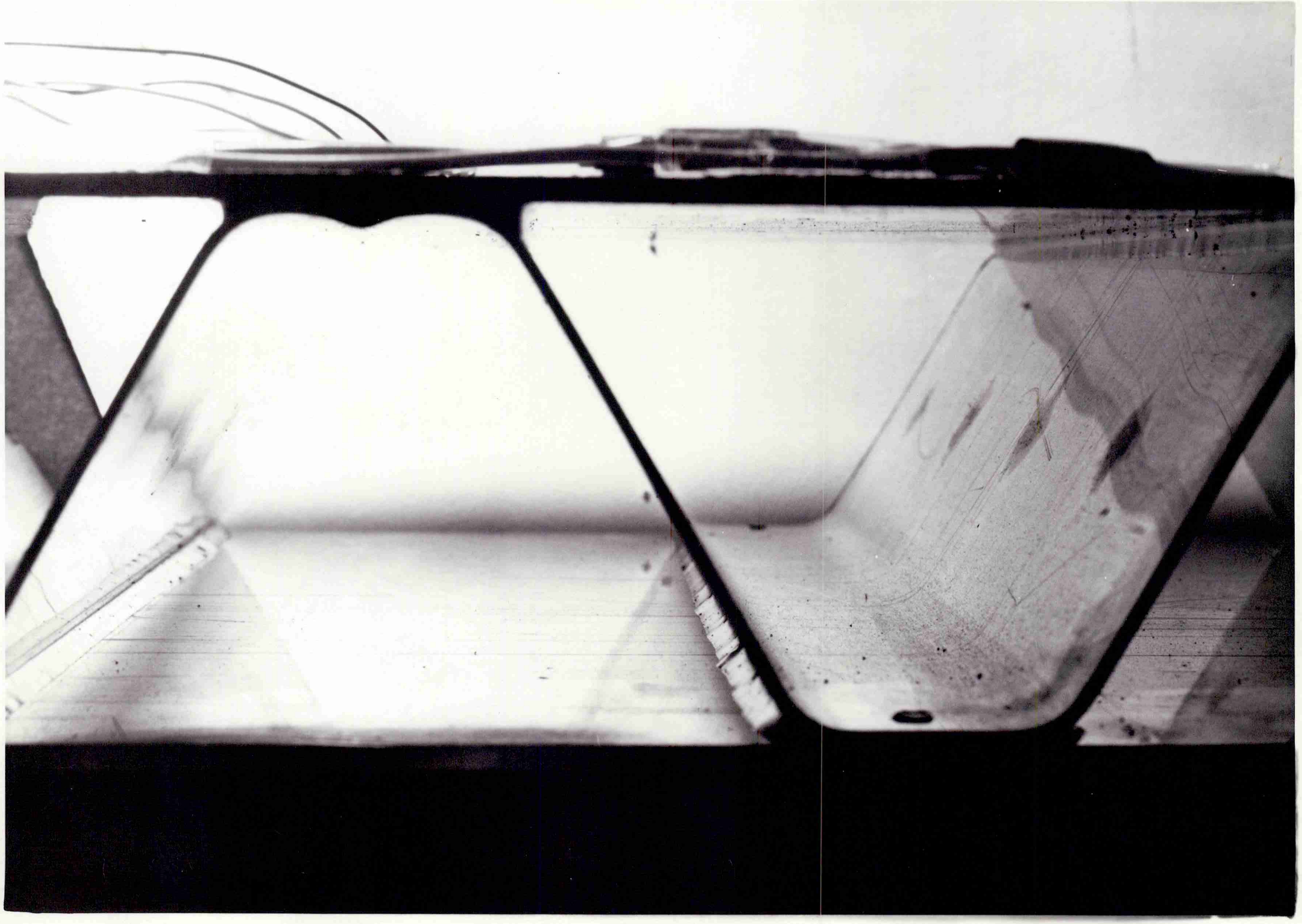

Plate 4.1 Core Slant-face Buckle Pattern (Panel 5B/1)

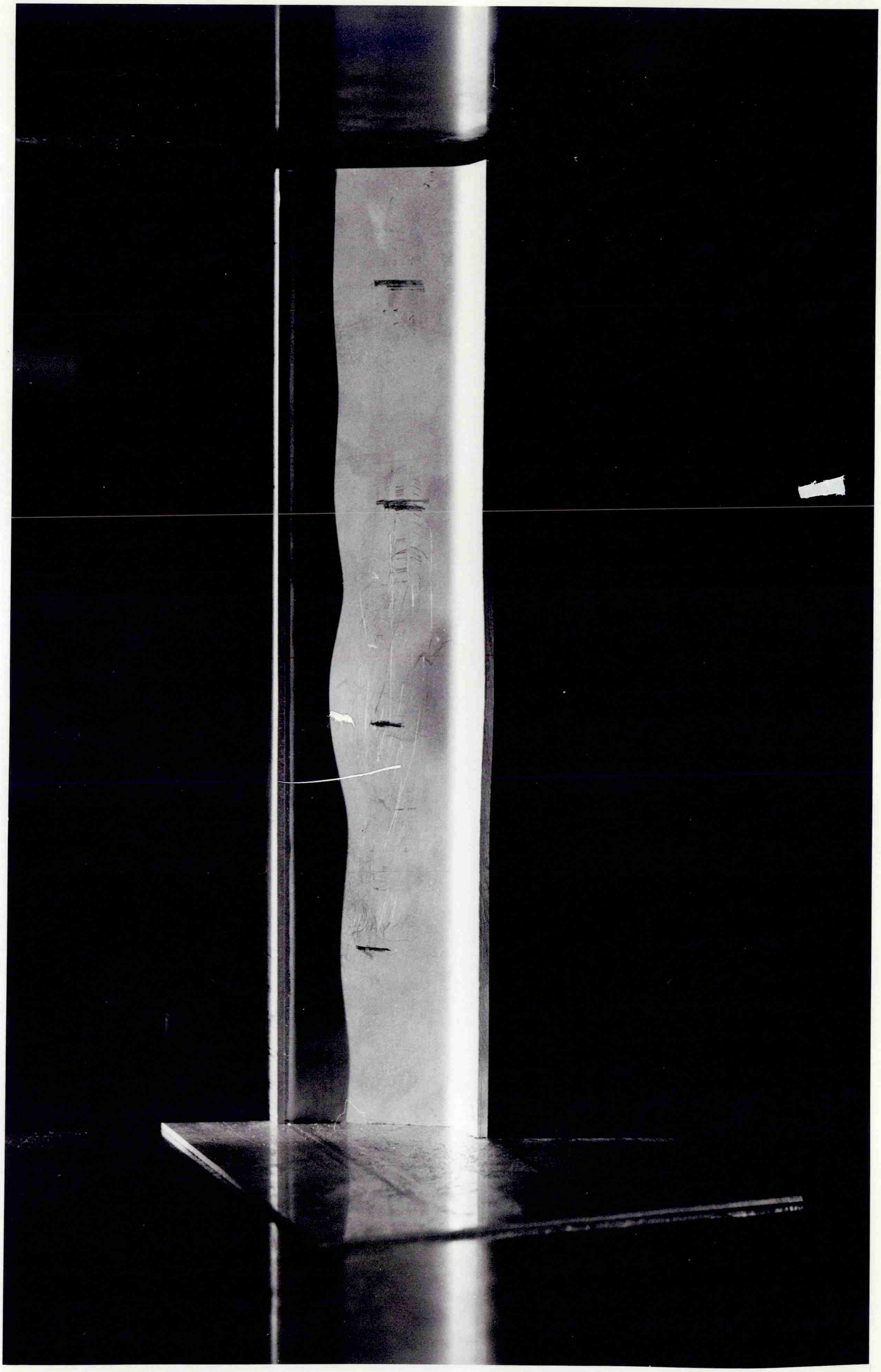

Plate 4.2 Core Slant-face Buckle Pattern (Panel 5B/2)

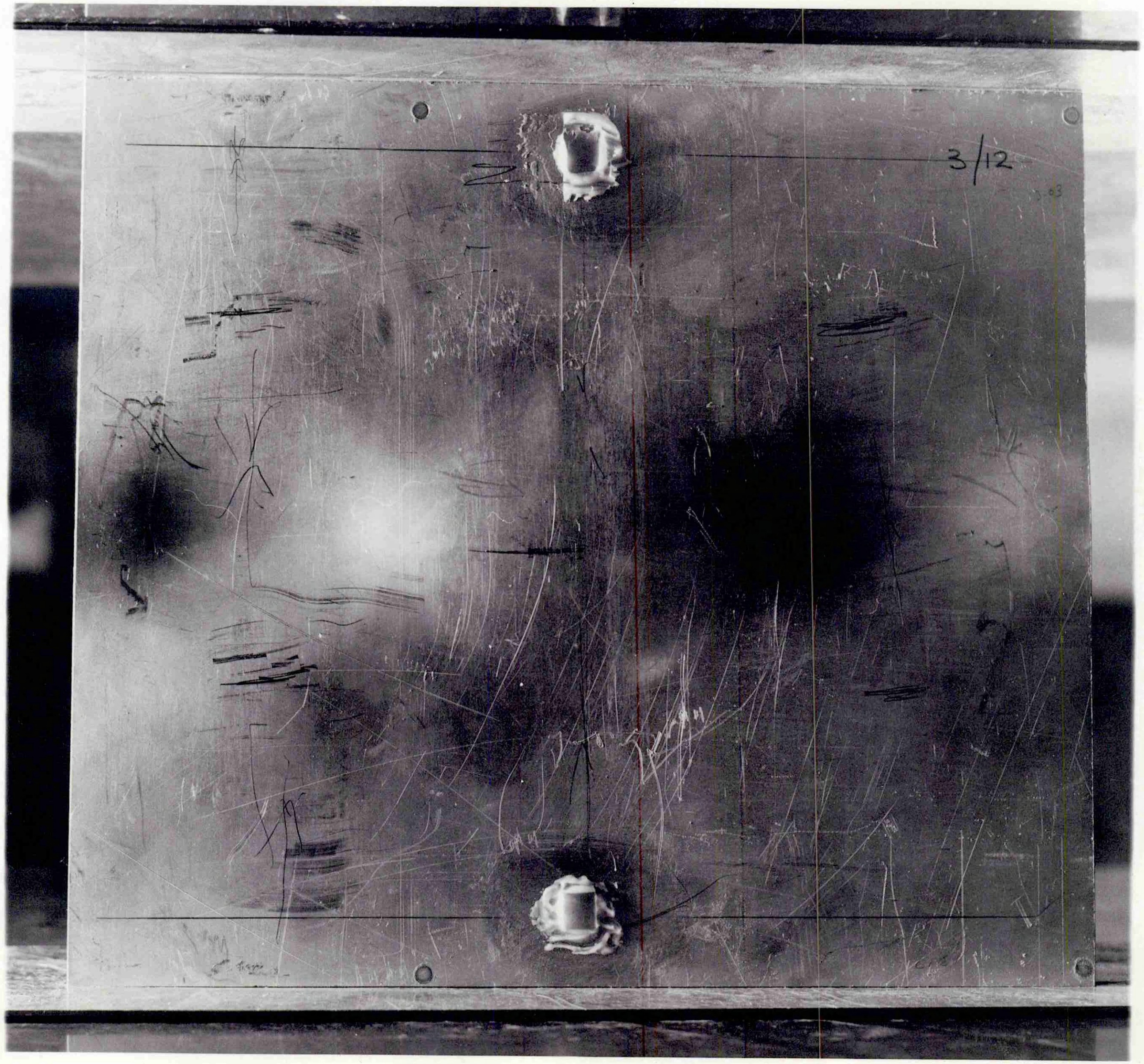

Plate 4.3 Face Plate Buckle Pattern (Panel 5B/2)

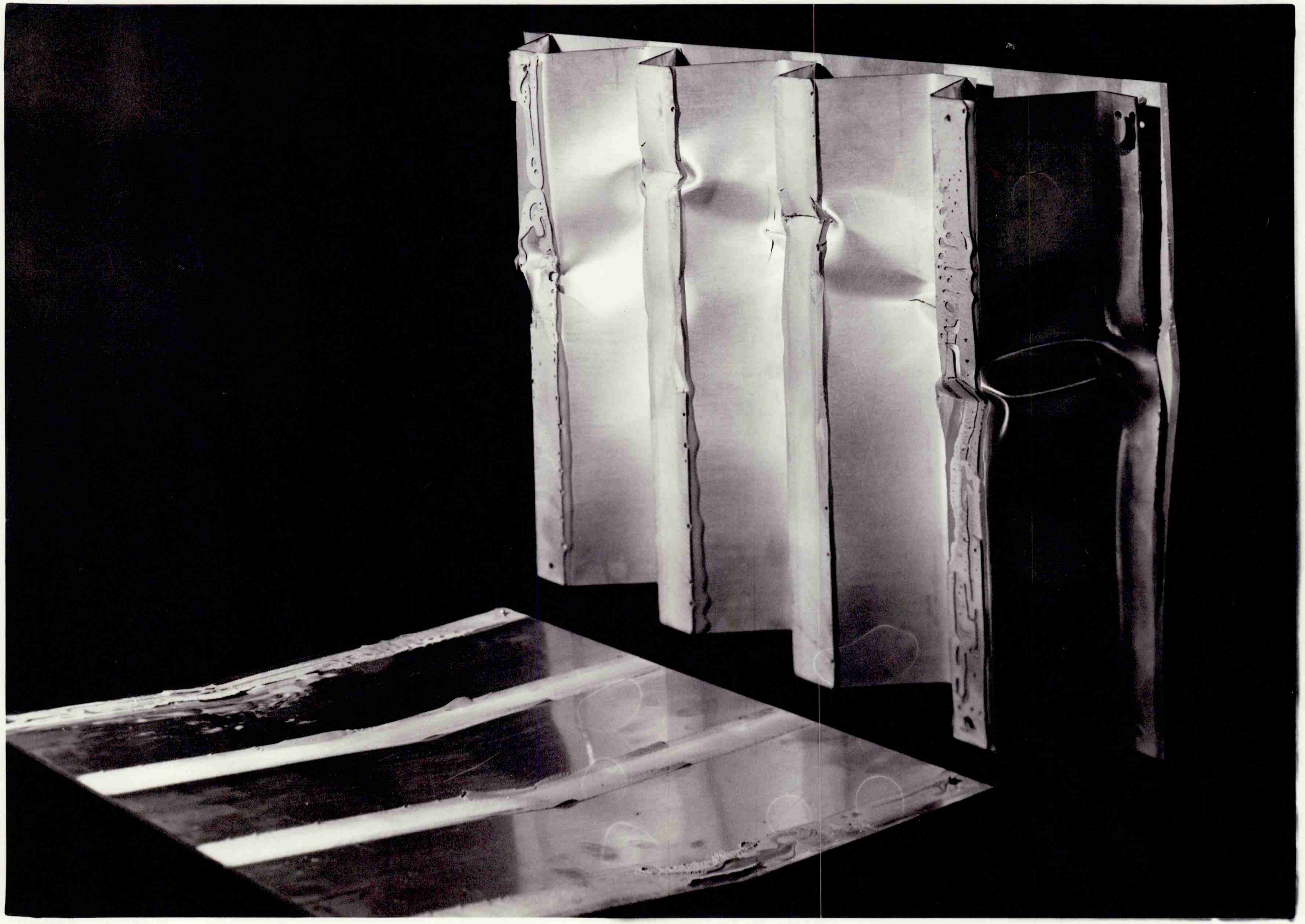

Plate 4.4 Panel 5B/3 at Failure

FIG. 4·1 Buckling Stresses for Handley Page Specimens.

(Using the Computer Program D10A)

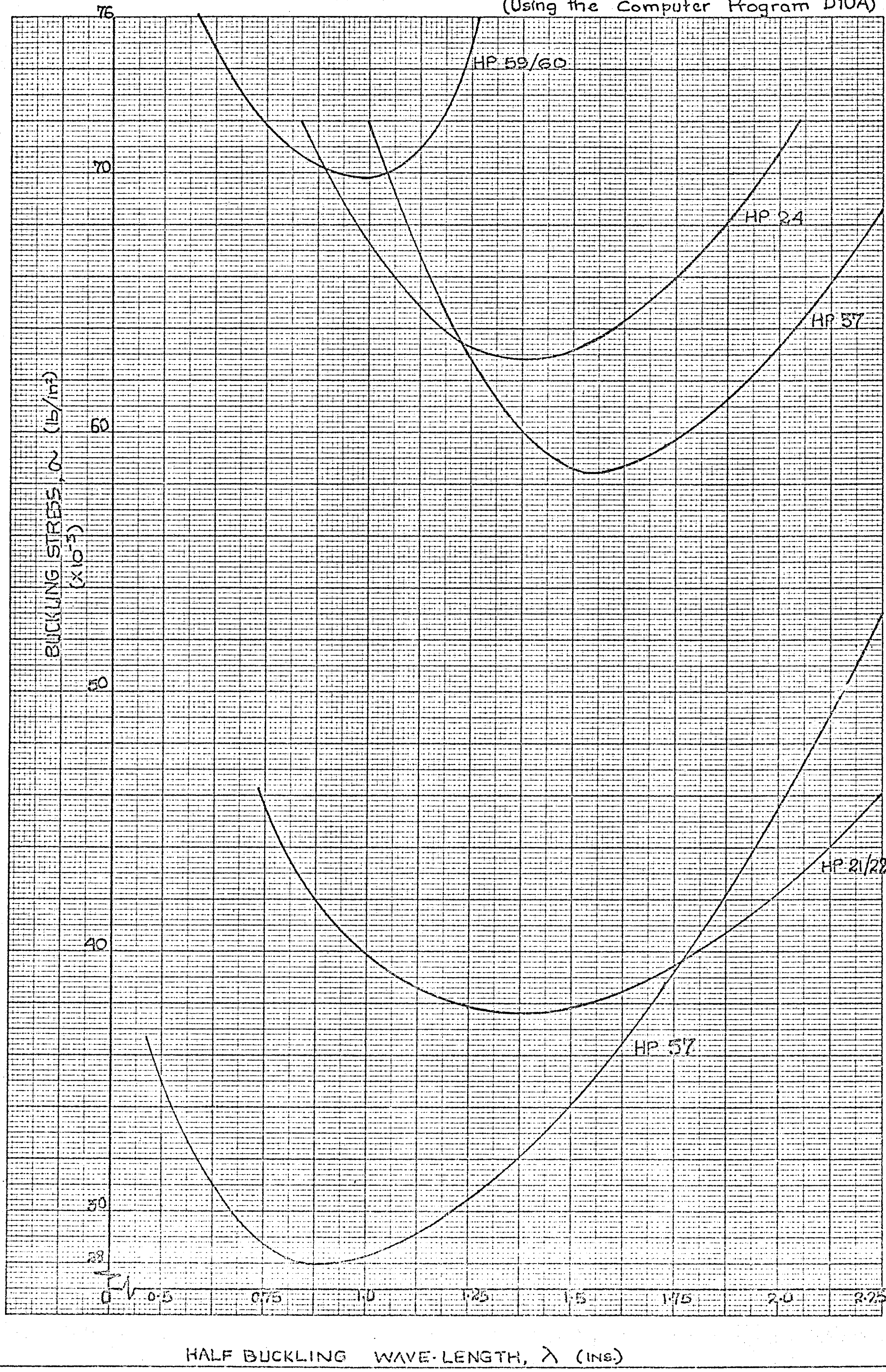

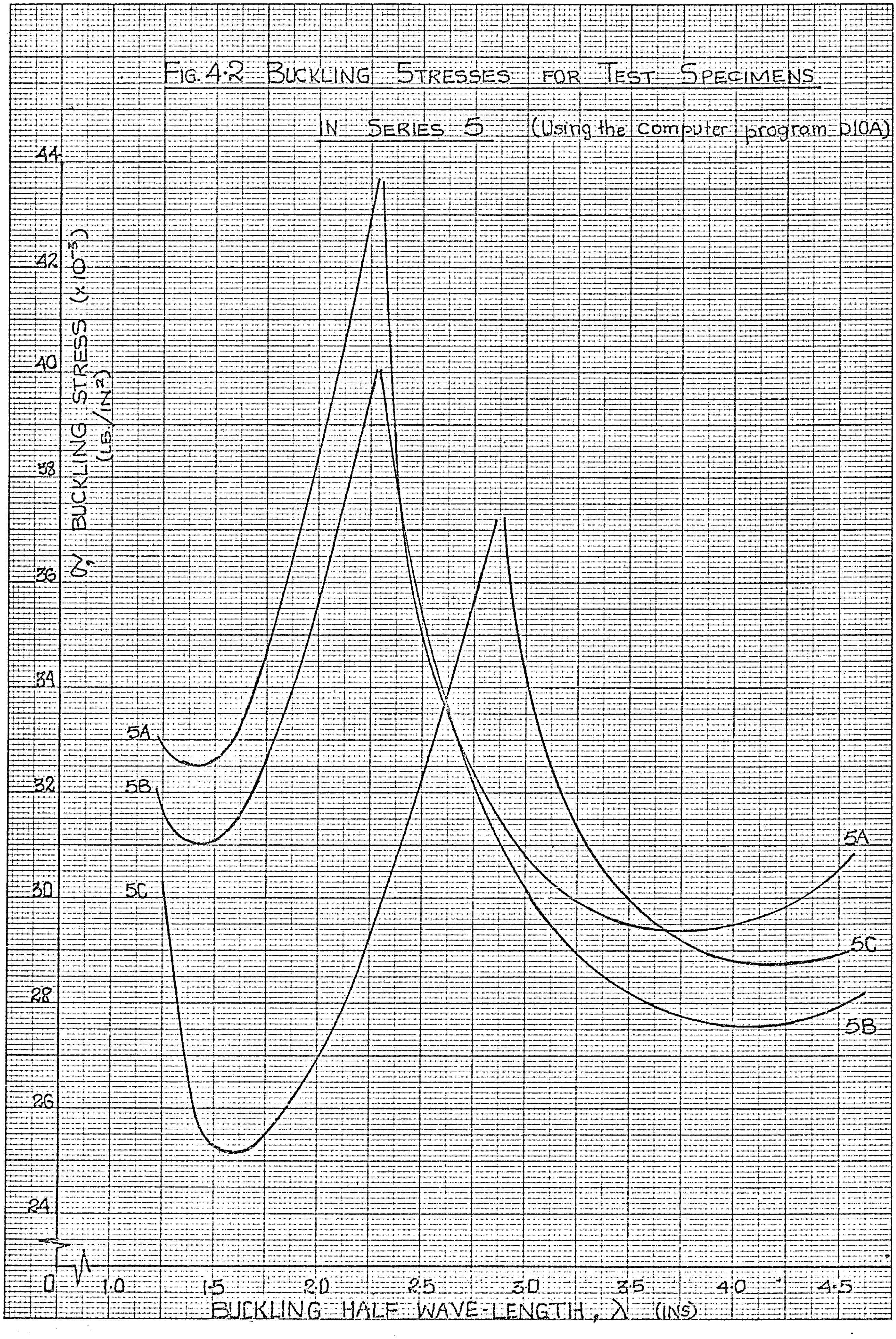

FIG. 4.2 BUCKLING STRESSES FOR TEST SPECIMENS IN SERIES 5 (Using the computer program D10A)

FIG. 4·3 BUCKLING STRESSES FOR TEST SPECIMENS IN SERIES 4 (Using the computer program D10A)

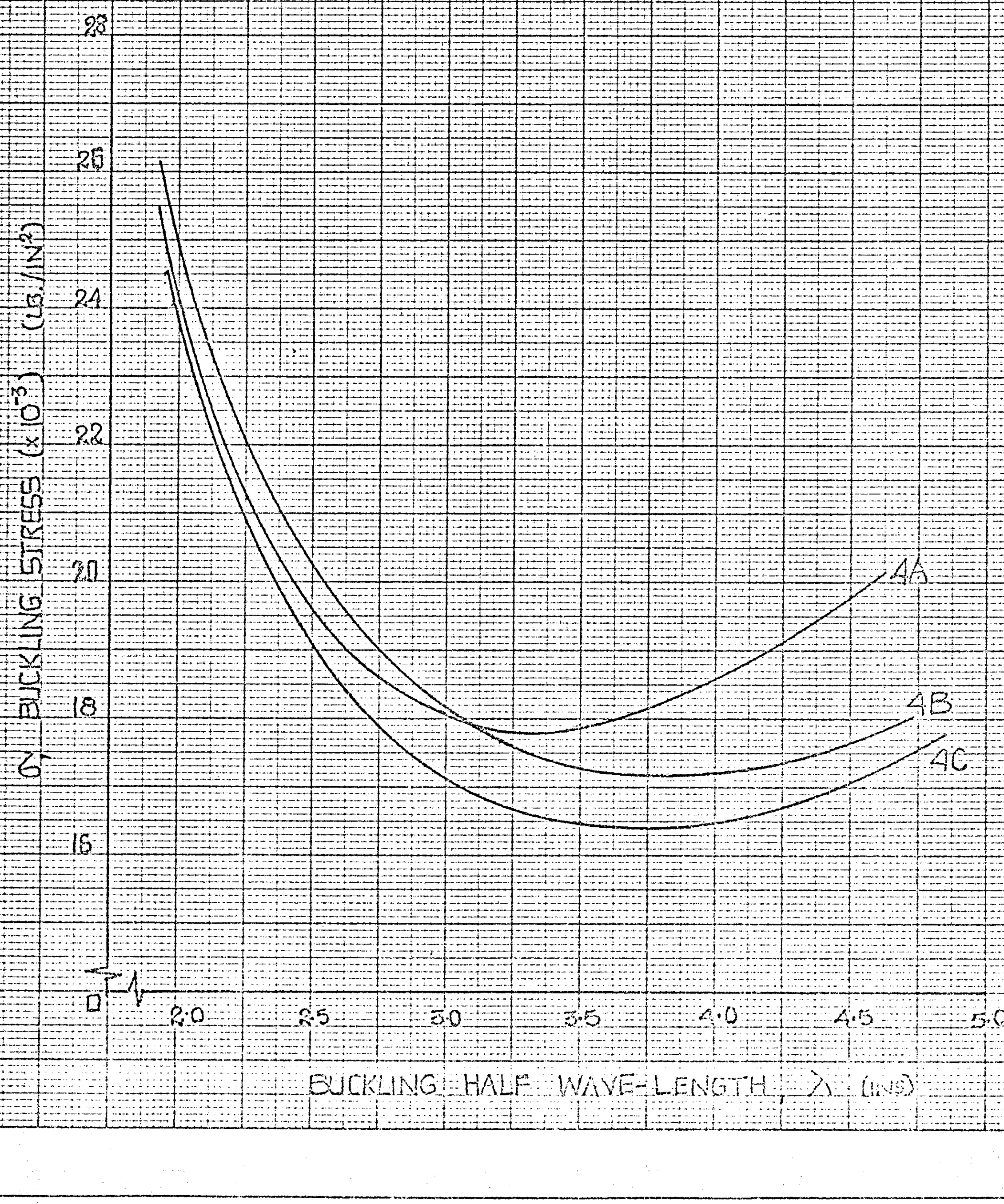

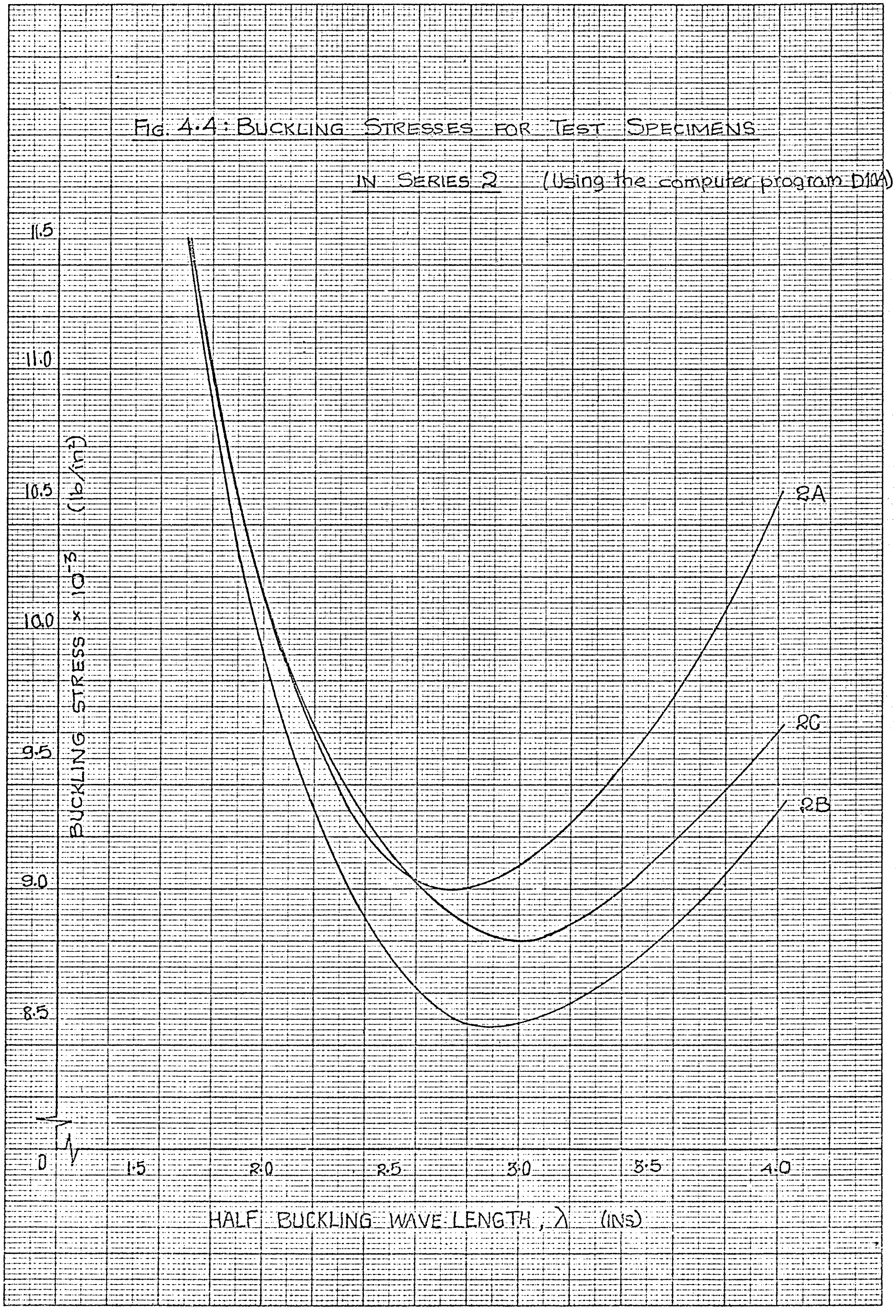
FIG. 4.4: BUCKLING STRESSES FOR TEST SPECIMENS
IN SERIES 2 (Using the computer program D10A)
11.5
11.0
10.5
10.0
9.5
9.0
8.5
0
BUCKLING STRESS × 10⁻³ (lb/in²)
1.5
2.0
2.5
3.0
3.5
4.0
2A
2C
2B
HALF BUCKLING WAVE LENGTH, λ (INS)

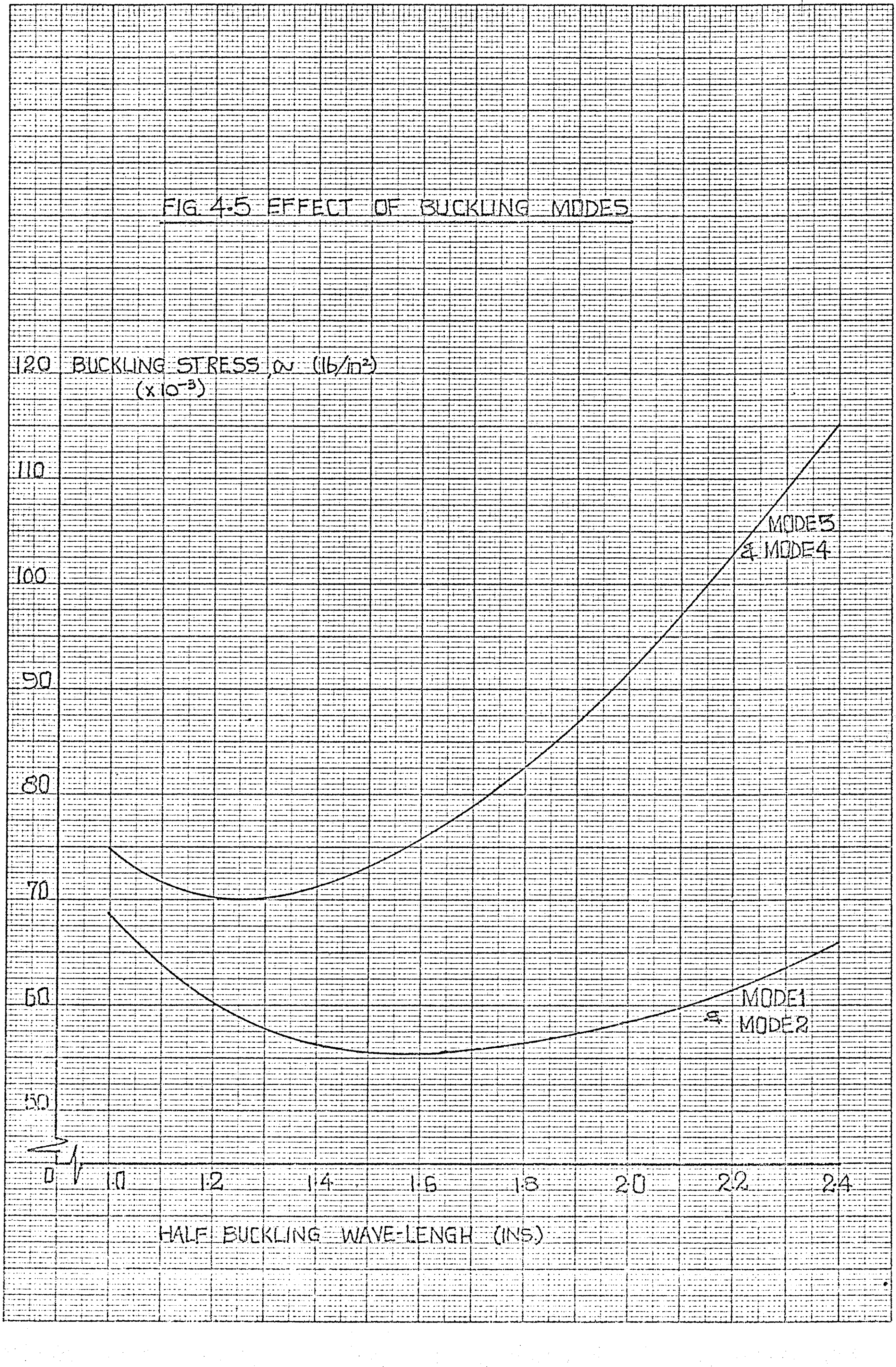
FIG 4.5 EFFECT OF BUCKLING MODES
120 BUCKLING STRESS, σ (lb/in²) (x10⁻³)
110
100
90
80
70
60
50
0
1.0
1.2
1.4
1.6
1.8
2.0
2.2
2.4
MODE5 & MODE4
MODE1 & MODE2
HALF BUCKLING WAVE-LENGH (INS.)

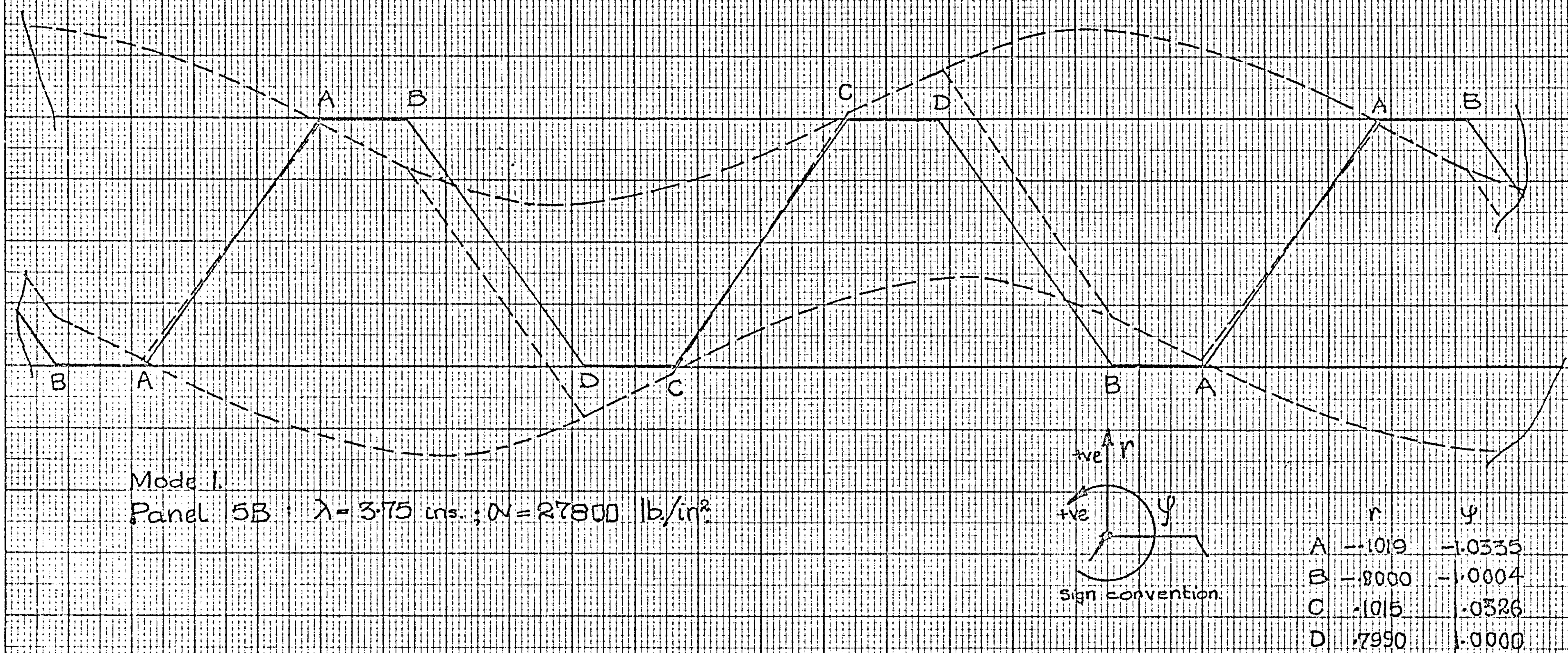

FIG. 4·6 : THEORETICAL BUCKLING DEFLECTIONS.

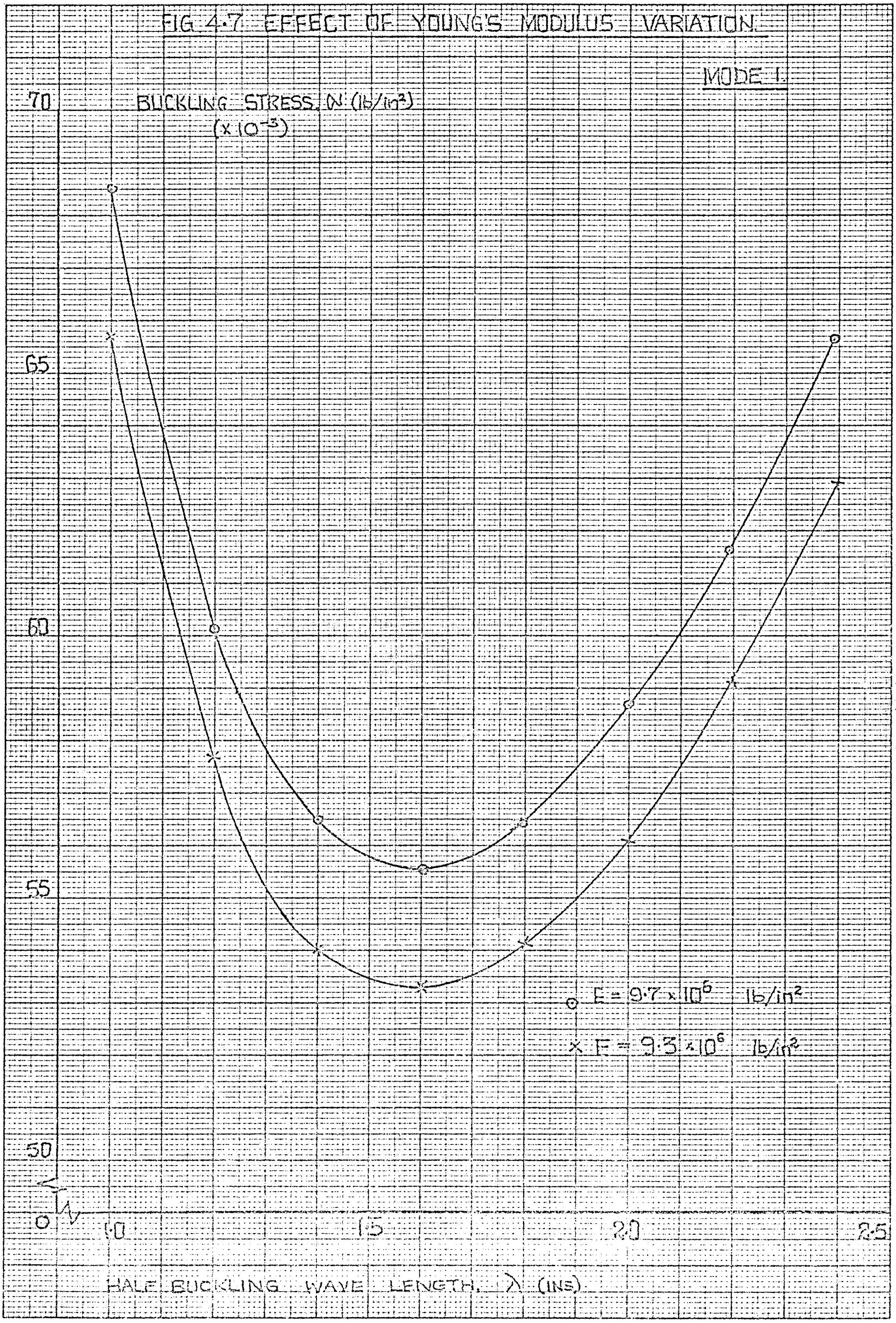
FIG 4·7 EFFECT OF YOUNG'S MODULUS VARIATION
MODE I.
BUCKLING STRESS, σ (lb/in²) (x 10⁻³)
70
65
60
55
50
0
1·0
1·5
2·0
2·5
⊙ E = 9·7 x 10⁶ lb/in²
x E = 9·3 x 10⁶ lb/in²
HALF BUCKLING WAVE LENGTH, λ (INS)

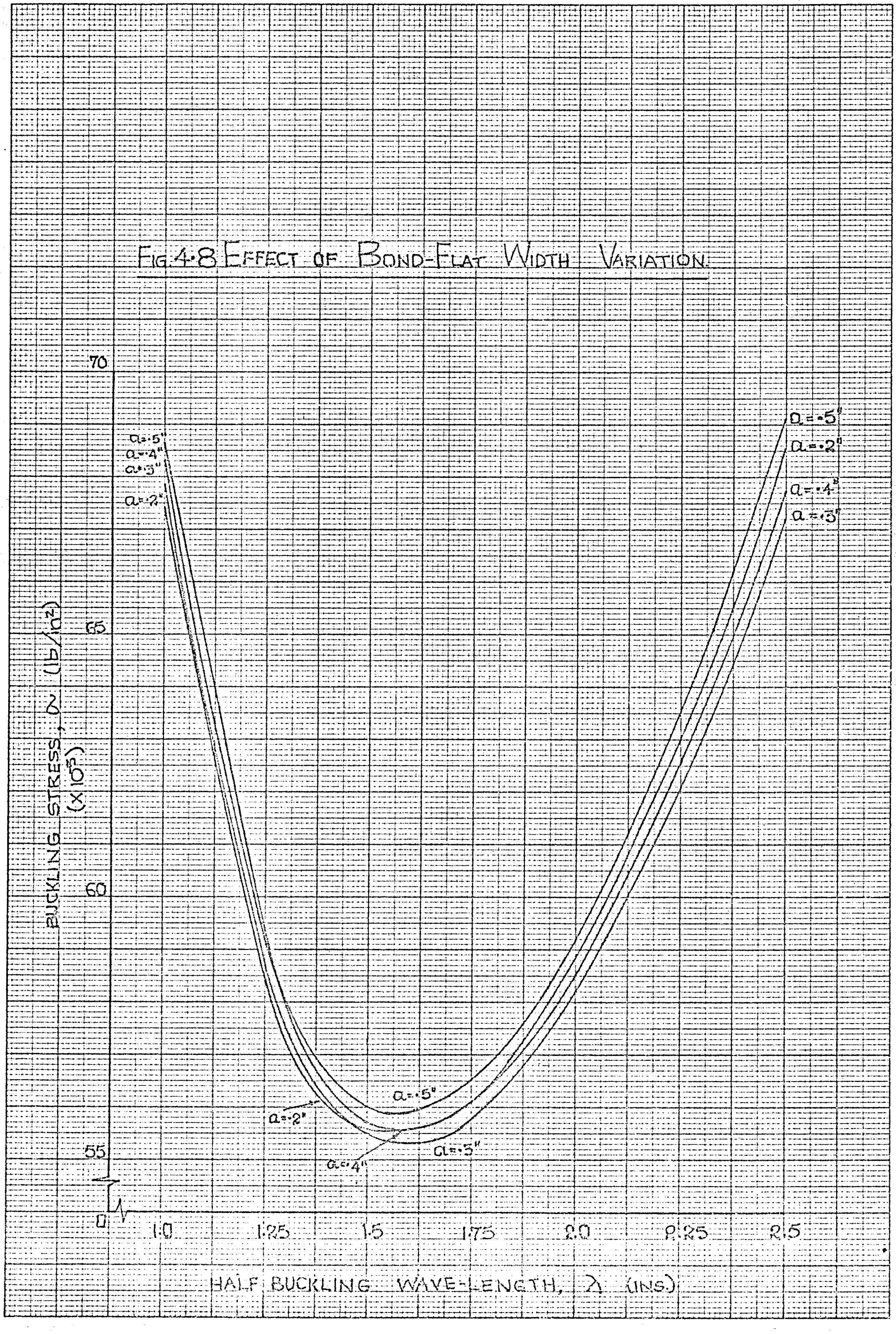

FIG 4.8 EFFECT OF BOND-FLAT WIDTH VARIATION

FIG 4·9 Effect of 'Skin-Bond-Core' Thickness Variation

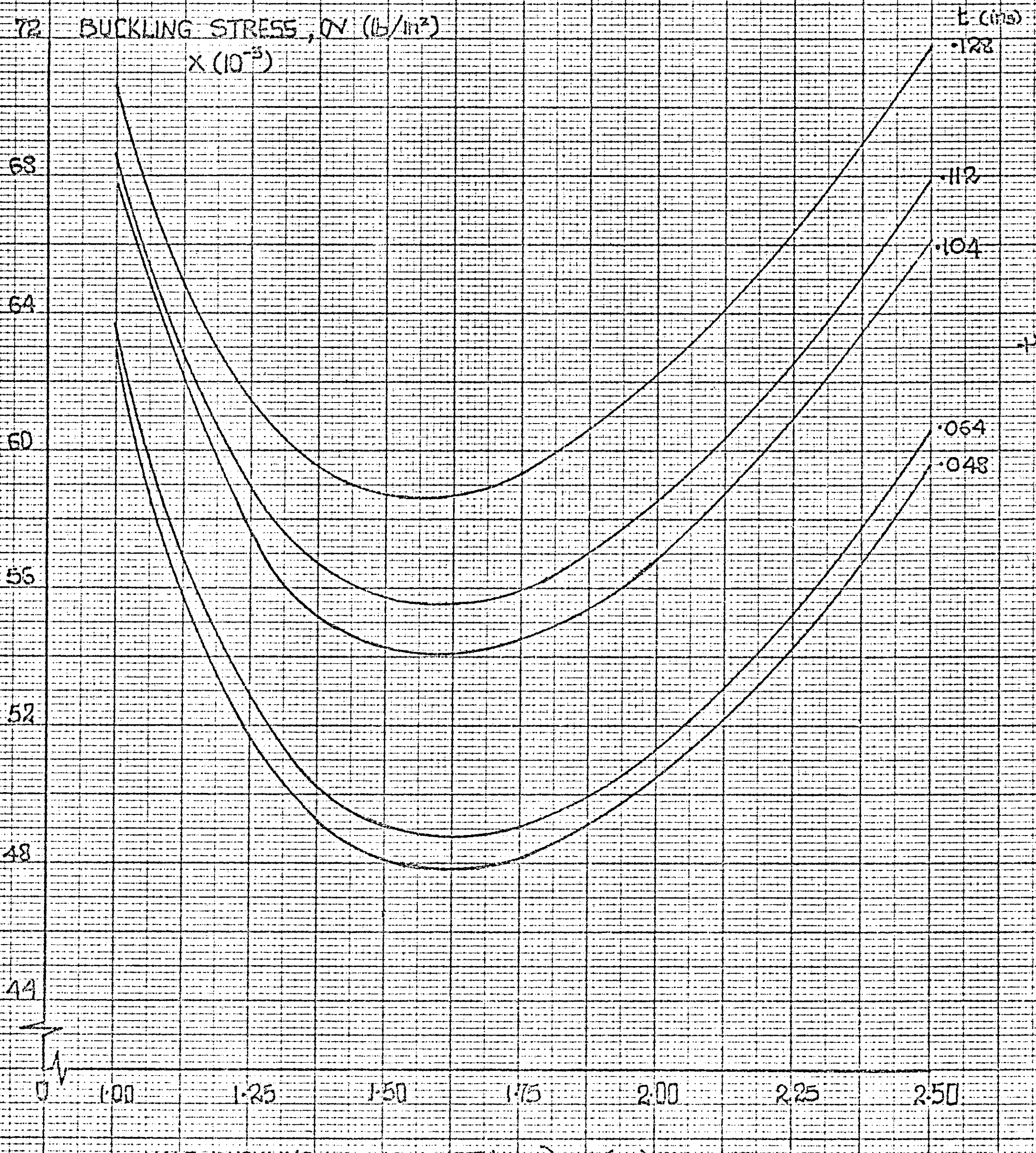

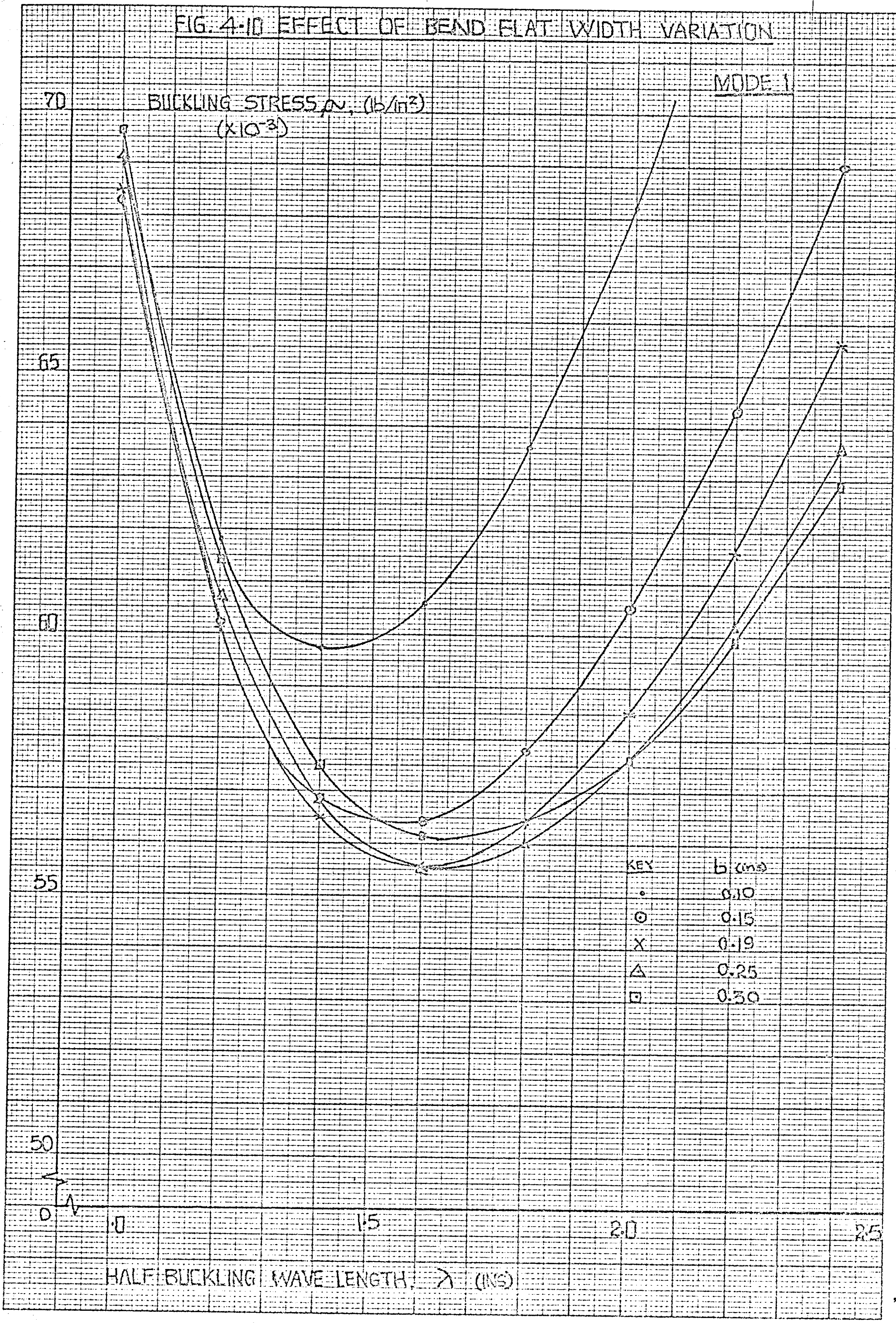
FIG. 4·10 EFFECT OF BEND FLAT WIDTH VARIATION
MODE 1
BUCKLING STRESS, p, (lb/in²) (x10⁻³)
70
65
60
55
50
0
1·0
1·5
2·0
2·5
HALF BUCKLING WAVE LENGTH, λ (INS)
KEY
b (ins)
0.10
0.15
0.19
0.25
0.30

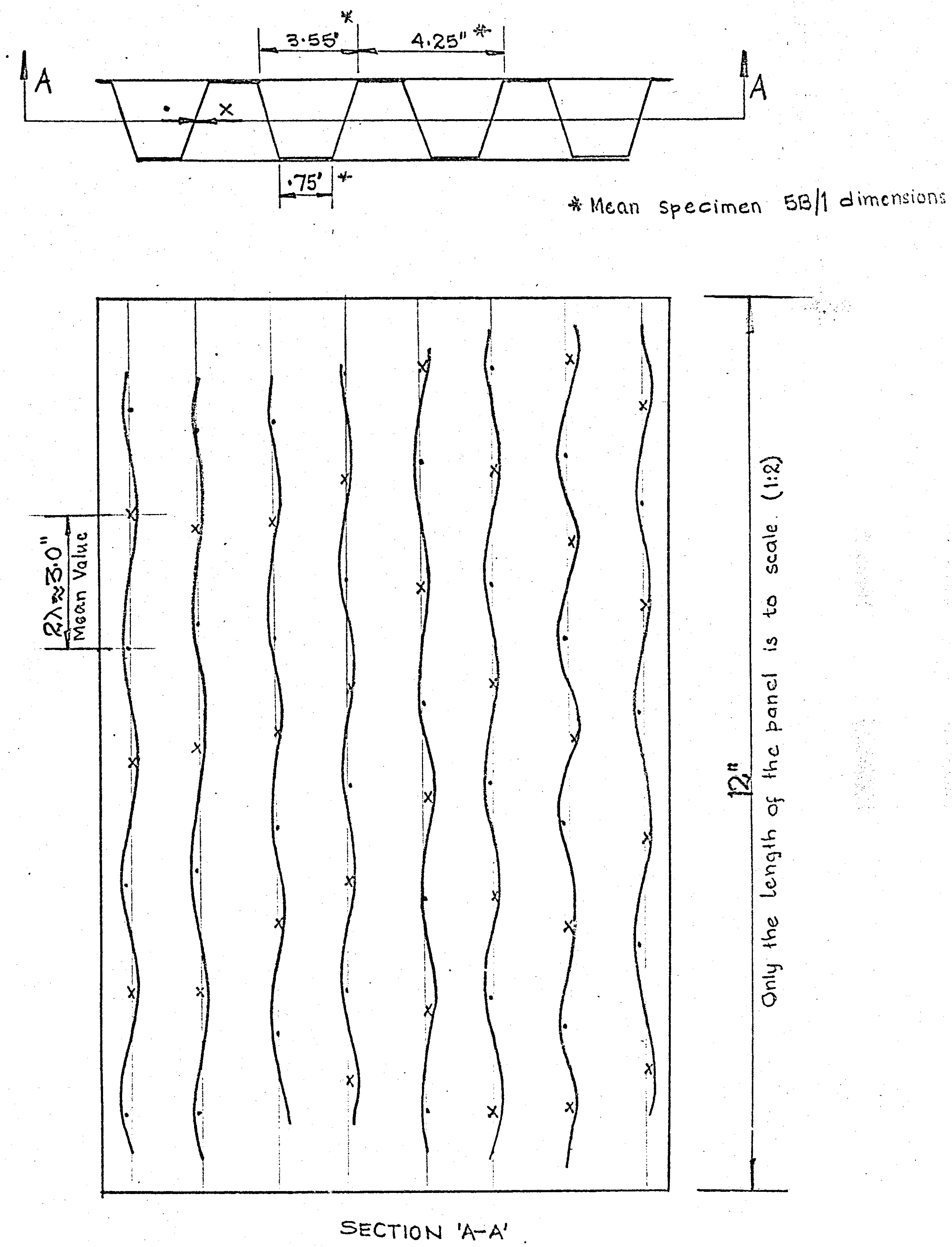

FIG. 4·11: Core Slant-Face Buckle Pattern (Panel 5B/1)

SECTION 5

DISCUSSION

5. DISCUSSION

5.1 The Computer Program, D10A

5.1.1 Buckling Stresses

The program is adequate in predicting the buckling stress of a corrugated-core sandwich panel under compression with certain reservations regarding the stress increments. The stress increments have to be kept small when working in the region of low buckling wave-lengths because of the apparently sudden changes in the buckling deflections at the attachment points.(See Appendix 5).

5.1.2 Buckling deflections

For the buckling mode 1, which is considered in detail in this thesis, the values of deflections at attachment points computed for the specimens at low buckling wave-lengths cannot be relied upon. (See Appendix 5).

For buckling modes at higher wave-lengths, the deflections of attachment points are symmetric. (See Fig.4.6). This suggests a buckling mode which is repeated at every corrugation pitch.

5.1.3 Variation of specimen parameters

From Fig.4.8, variation of core and face-plate attachment width does not seem to have any significant effect on the critical buckling stress.

When the'skin-bond-core' thickness is increased, the program gives a higher buckling stress at the same value of buckling wave-length. (See Fig.4.9).

Fig.4.10 shows the effect of variation of bend flat width on the minimum buckling stress. It can be seen that when the bend flat width is very small (this corresponds to perfect connection between the core and the face-plate as assumed in the theory used for developing the Data Sheets), a high value of buckling stress is predicted.

Increase in bend flat width over a critical value has very small effect on the value of the buckling stress. This critical value of bend flat width, below which a high buckling stress is predicted cannot be established without further detailed investigation. (See section 7).

5.2 The Test Programme

5.2.1 Inadequacy of the test programme

As explained in Section 3, para 3.4, only a third of the panels which were envisaged for the test programme could be produced.

Further difficulties were encountered as only seven of the specimens were delivered in time for testing. Of the seven that were available, three had unsatisfactory adhesive joint between the face-plates and the core.

As the delivery of the last four of the seven specimens that were tested was delayed, other methods of determining buckling loads and measuring the actual buckling wave-lengths and amplitudes could not be attempted. (See recommendations made in Section 7).

5.2.2 Determination of buckling loads

Buckling load is taken as the load at which a change in the slope of the load/deflection graph occurs.

As initial irregularities are difficult to assess, this method is somewhat subjective in application.

Further difficulties are encountered because in many cases the change in slope is very small as can be seen in Figs.A2.4 - A2.16. Confusion with non-linear occurences in the stress-strain relationship of the material is difficult to avoid.

Recommendations are made in Section 7 for trying two other methods of determining the buckling loads.

5.3 Theoretical and Test Results

5.3.1 Handley Page Specimens

Comparison of buckling stresses is made in Table 4.3.

It can be seen that, in general, the program D10A predicts a lower buckling stress than that predicted by Wittrick and the Data Sheets.

The test buckling stresses of specimens HP37 and HP 59/60 are much lower than that predicted by the program D10A, Wittrick and the Data Sheets. It seems probable that bond failure or some similar effect occured in these specimens.

5.3.2 The test programme specimens

The buckling stresses for the test programme specimens are compared in Table 4.4.

Accuracy of the determination of the buckling stresses (see para. 5.2.2) is difficult to assess.

Further, the method outlined in Section 4 for obtaining the average test buckling stress for the panel is questionable.

Fluctuations, if any, in the test values for the specimens of the same configuration cannot be assessed as, in general, only one of each of the specimen configuration was tested.

The buckling stresses predicted by the program D10A are approximately 15% lower than the test value.

Unfortunately, the Data Sheets (ref.5) could not be used for predicting the buckling stresses for the specimens tested as they were outside the range of the data sheets.

Buckling stress for only one of the specimens in the test series could be predicted by the data sheets. The value predicted is almost 40% higher than that predicted by the D10A. The data sheets predict a buckling wave-length of 1.0 in. compared with 1.6 in. predicted by the D10A; the former corresponding to core slant-flat buckling and the latter to face-plate buckling.

It is felt that the theory on which the data sheets are based would give higher buckling stresses for the specimens tested than that given by the program D10A. This is because the data sheet theory assumes no lateral movement of the attachment points. The theory from which the program D10A is developed makes provision for lateral movement. (See Fig.4.6).

From Fig.4.2, it seems that as the bend radius of the core increases, the value of buckling stress decreases. The minimum buckling stress occuring at a higher wave-length, corresponding to the face-plate buckling. Above a 'certain' value of bend radius, the buckling mode changes, and the critical buckling stress occurs at a lower wave-length, corresponding to core slant flat buckling.

This behaviour is exhibited by panels in series 5, which have high face-plate-to-core thickness ratio. Panels in series 4 and series 2 (see Figs.4.3 and 4.4 respectively) do not exhibit this behaviour.

This behaviour cannot be generalised for panels with high face-plate-to-core thickness ratios without further investigation. (See Section 7).

SECTION 6

CONCLUSIONS

6. CONCLUSIONS

6.1 Theoretical Analysis

6.1.1 The program D10A is adequate in predicting the buckling stress of a corrugated-core sandwich panel under compression with certain reservations regarding the stress increment.

6.1.2 The buckling modes 1 and 2 and modes 3 and 4 are identical from the point of view of buckling stresses.

6.1.3 The computed values of deflections at attachment points for the specimens at low buckling wave-lengths are not reliable.

6.1.4 Variation of core-face-plate attachment width does not have any significant effect on the buckling stress.

6.1.5 Increase in the 'face-plate-bond-core' thickness gives a higher value of buckling stress at the same value of buckling wave-length.

6.1.6 When the core bend radius is increased over a critical value, a reduction in critical buckling stress and a change in buckling mode is expected; this behaviour is exhibited only by panels with high face-plate-to-core thickness ratio.

6.2 Experimental Analysis

6.2.1 The method used for determining the panel buckling loads is somewhat subjective in application. Reliability and accuracy of this method are difficult to assess.

6.2.2 Due to the inadequate experimental work, it is not possible to draw any conclusions on the effect of core bend radii on the critical buckling stress.

6.3 Comparison of Results

6.3.1 In common with references 4 and 5, the program D10A predicts values of buckling stresses for the Handley Page specimens HP 37 and HP 59/60 which are much greater than the test values. It is probable that bond failure or some similar effect occured in these specimens. Presence of an entirely different buckling mode cannot be over-looked.

6.3.2 For the specimens tested, the test values of buckling stresses are approximately 15% higher than those predicted by the D10A.

6.3.3 These discrepancies are not large when dimensional and material property variations are considered and indicate that the computer results are giving the correct trend, and are conservative.

6.3.4 The computer program D10A allows lateral movement of the attachment points and therefore, is expected to predict a lower buckling stress than ref.5.

SECTION 7

RECOMMENDATIONS FOR FURTHER INVESTIGATIONS.

7. RECOMMENDATIONS FOR FURTHER INVESTIGATION

7.1 Theoretical Investigation

7.1.1 Examine the elements of the overall stiffness determinant at buckling stress associated with a low buckling wave-length in order to explain the apparently sudden changes in the buckling deflections at the attachment points.

7.1.2 Extend the above investigation to cover a wide range of buckling wave-lengths in order to determine the value of wave-length at which the transition occurs from 'sudden' to 'well-behaved' change of the attachment point deflections. (See Appendix 5).

7.1.3 Examine the Wittrick 'incluence coefficients' for each of the component flat of the panel to determine their relative contribution towards buckling.

7.1.4 Modify the program D10A to compute deflections at the intersections of the core bend-flat and the slant-flat. This would enable to present a complete buckling deflection pattern of the core.

7.1.5 With small increments in buckling wave-length, examine the buckling deflections to establish the effect of the bend-flat-width variation on the minimum buckling stress. (See Fig.4.2).

7.2 Experimental Investigation

7.2.1 Specimen Configurations

a. The specimen configurations originally envisaged for the test programme of this study should be covered. (See Table 3.3).

b. Vary the core thickness in the test programme specimens keeping other parameters constant to study the effect of face-plate-to-core thickness ratio on the buckling mode.

c. Cover a wider range of core bend radii to investigate in detail the behaviour exhibited by panels in series 5. (See Fig.4.2).

7.2.2 Material to be used for the specimens

The original test programme specimens were made from aluminium alloy in DTD 687 specification for reasons outlined in Section 3, para. 3.2.1. For future work, the specimens should be made out of an aluminium alloy (for example, L72) which possesses better forming properties.

The problem of manufacturing tolerances (See Section 3, para.3.4) would be further alleviated by using a break press.

7.2.3 Handley Page test specimens

Repeat the tests on the Handley Page specimens HP 37 and HP 59/60 (See Table 3.1) to confirm or otherwise, the test values given in Ref.2.

7.2.4 Determination of buckling loads

The method used for determining the buckling load is somewhat subjective application.

To determine the relative reliability and the accuracy of the above method, the following two methods are recommended.

a. The Southwell Plot; in which amplitude prior to buckling is plotted against amplitude divided by load. The slope of this graph gives the buckling load.

b. The second method is based upon the relationship given in the National Advisory Committee for Aeronautics, Technical Note number 752.

$$a^2 = \frac{4\lambda^2}{\pi^2}(e - e_b)$$

where, a and λ are post buckling amplitude and wavelength, e is panel strain and e_b is its value at buckling. a^2 is plotted against e giving a straight line whose intercept on the e axis gives e_b, from which the buckling load can be determined.

As both the methods depend upon measurements of face-plate wave amplitude, they might not be suitable for panels with thick face-plates which give small buckling amplitudes.

REFERENCES

REFERENCES

1. A unified approach to the initial buckling of stiffened panels in compression - W. H. Wittrick - The Aeronautical Quarterly Vol. XIX, August 1968.

2. Strength and stiffness tests on corrugated core sandwich - Handley Page Test Department Report No. 8B34.

3. Computation of initial buckling stress for sheet-stiffener combinations - H. L. Cox - The Royal Aeronautical Society Journal, September 1954.

4. The local instability of corrugated core sandwich panels - Engineering Sciences Data Unit Report No. 5337, May 1969.

5. The Royal Aeronautical Society Data Sheets, Structures, Volume 2, Series 02.01.28.

NOTATIONS.

NOTATIONS

Those notations which are frequently used in the text are defined here; others are defined locally.

σ	= basic longitudinal compressive stress in plate
E	= Young's modulus
ν	= Poisson's ratio
b	= width of flat
t	= thickness of flat
D	= $Et^3/12(1-\nu^2)$, flexural rigidity of plate
K	= $\sigma b^2 t/\pi^2 D$
ϵ	= σ/E
λ	half wavelength of applied edge forces
x, y	longitudinal and widthwise co-ordinates
z	normal co-ordinate
X, Y	= $\pi x/\lambda$, $\pi y/\lambda$ respectively
w	displacement of middle surface in Z direction
ω	= $\pi b/\lambda$
ϕ	= $\pi^2 K/\omega^2$
α	= $\omega(1 + \sqrt{\phi})^{\frac{1}{2}}$
γ	= $\omega(1 - \sqrt{\phi})^{\frac{1}{2}}$
δ	= $\omega(\sqrt{\phi} - 1)^{\frac{1}{2}}$
m_L, m_R	amplitudes of sinusoidal edge moments
Y_L, Y_R	amplitudes of sinusoidal out-of-plane edge shear forces
ψ_L, ψ_R	amplitudes of sinusoidal edge rotations
w_1, w_2	amplitudes of sinusoidal out-of-plane edge displacements
S_{mm}, S_{mF}, S_{FF} ; F_{mm}, F_{mF}, F_{FF}	influence coefficients; elements of out-of-plane stiffness matrix
d	= depth of core (ins.)
a	= bond width (ins.)
β	inclination of core slant flat to horizontal (degrees)
p	core pitch (ins.)

Suffices

c	core
s	core slant flat
b	core bend flat
j	joint flat
p	face-plate flat

APPENDIX 1.

DEVELOPMENT OF THE COMPUTER PROGRAM (D10A)

APPENDIX 1

DEVELOPMENT OF THE COMPUTER PROGRAM (D10A)

1.0 Introduction

The purpose and the basic programming cycle of the program have been outlined in Section 2, para. 2.4.5.

1.1 Notations Used

(For the Master Program and the Subroutine segments)
(Eqn. nos. refer to Section 2, para 2.4).

F(I,J)	Matrix $A_1' K_1 A_1$
B(I,J)	Matrix $A_2' K_2 A_2$
C(I,J)	Matrix $(A_1' K_1 A_1 + A_2' K_2 A_2)$
A(K)	Matrix C(8,8) stored in A(64), row location.
DET	Determinant value of C(I,J)
SIGMA	Longitudinal compressive stress (lb./in.^{2})
E	Young's modulus (lb./in.^{2})
XMUE	Poisson's ratio
XLAMBDA	Half buckling wave length (ins.)
ZETA	$\pi^2 K/w^2$
T	Component flat thickness (ins.)
DEL	Increment in value of λ (arbitrary) (ins.)
VAL	Maximum value of λ (arbitrary) (ins.)
L,KX,N,MC) NC,M,NN)	Count labels.
BETA/ANGLE 1	Inclination of core slant flat to horizontal (rads./degrees)
ETA/ANGLE 2	Inclination of core bend flat to horizontal (rads./degrees)
AVS/AVA	A_{V5}/A_{VA} , See Eqns. 13/27
APSIS/APSIA	A_{ψ_5}/A_{ψ_A} , See Eqns. 14/18

FO	Initial value of σ (lb./in.^{2})
DELSIG	Increment in value of σ (lb./in.^{2})
S_{MM} S_{MF} S_{FF}) F_{MM} F_{MF} F_{FF})	Influence coefficients.
P	Longitudinal compressive load (lbs.)
XI	Second moment of area of bend flat (in.^{4})
BB	Width of bend flat (in.)
TS1,TS2,) TS3,TS4)	Terms of A_{115} in Eqn. 20
TA1,TA2,) TA3,TA4)	Terms of A_{11A} in Eqn. 34
A115, A125, A225	Elements of Eqn.21
A11A, A12A, A22A	Elements of Eqn.35
XKC	See Eqn. 10
THETA	Ratio of deflections e.g. $\frac{r_7}{r_8}$, $\frac{r_5}{r_8}$ etc.

DELTA	δ)	See list of notations in the main text.
OMEGA	ω)	
ALPHA	α)	
GAMA	γ)	
ZSTAR	z^*)	

<u>Suffices</u>

B	Core bend flat
S	Core slant flat
P	Face-plate flat (unbonded)
J	Face-plate/core bonded flat

1.2 Simplified Flowchart

The basic computation cycles are shown. Where further details are desired, the actual program (see para. 1.3) must be consulted.

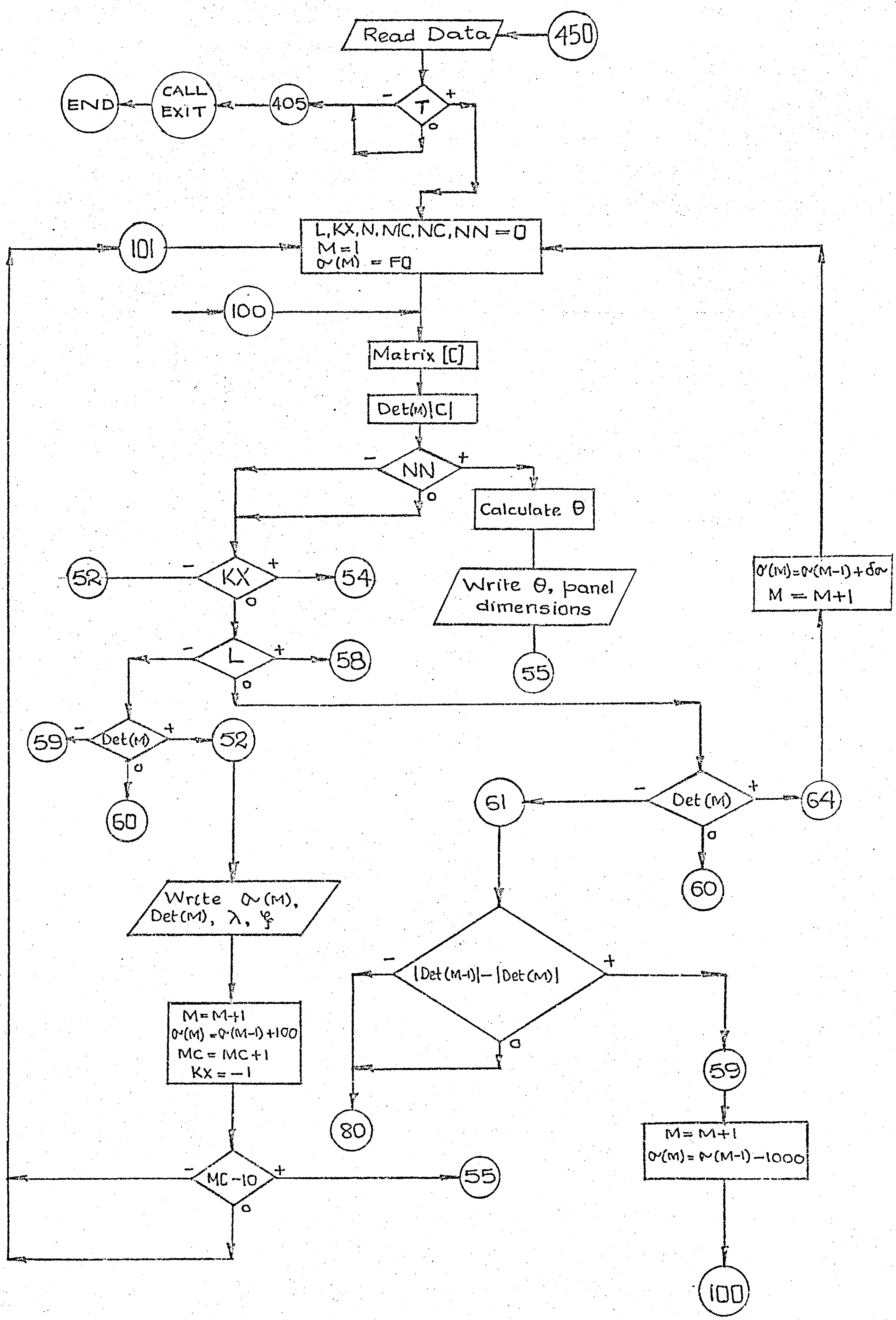

FLOWCHART CONTINUED.../
OVERLEAF /

FLOWCHART CONTINUED FROM PAGE No.: 126

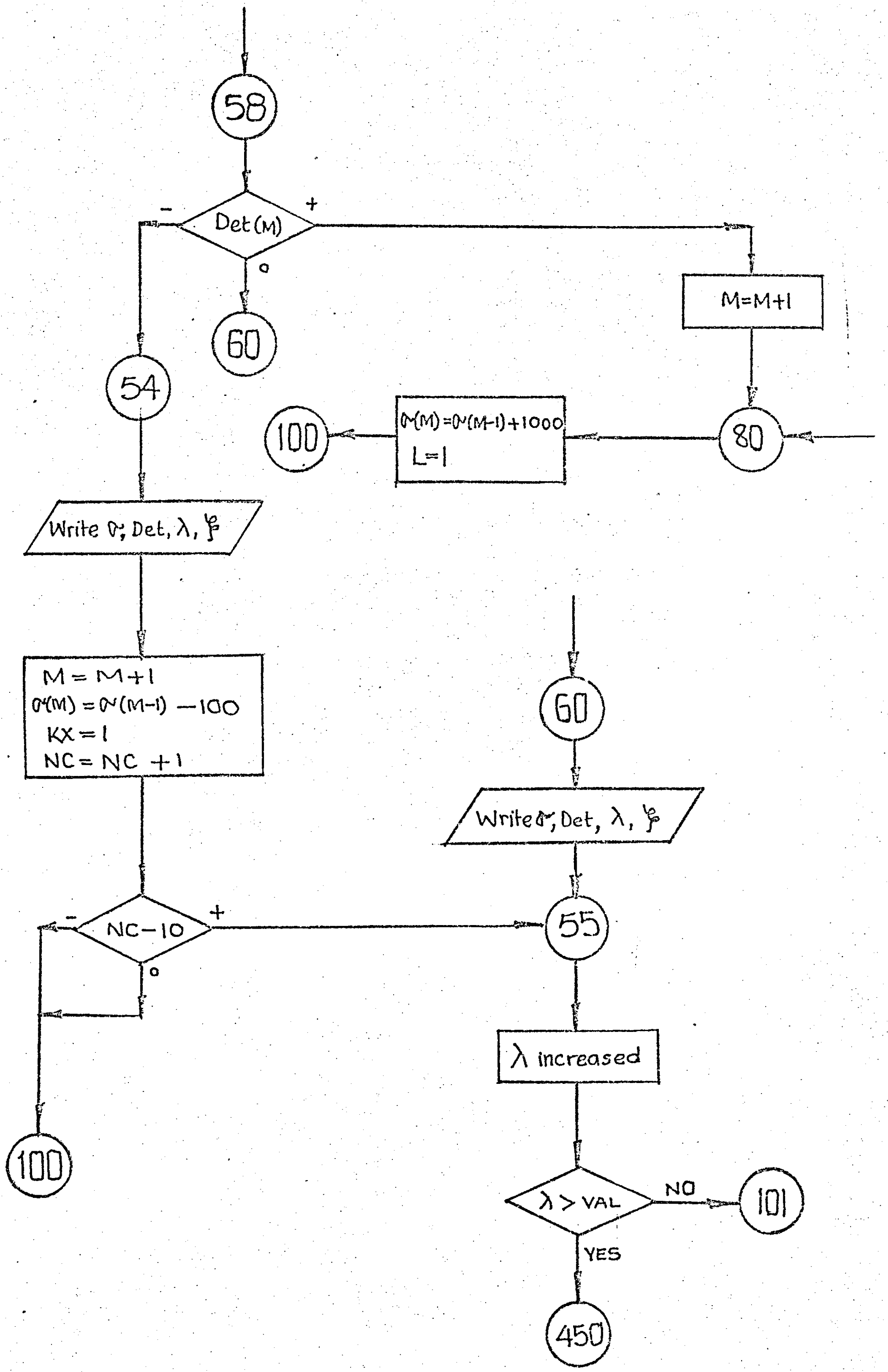

Simplified Flowchart Showing the Basic Computation Cycles.

1.3 Master Segment.

```
      MASTER NG1
      DIMENSION F(8,8),B(8,8),C(8,8),DET(50),SIGMA(50),A(64),U(8,8),
     1THETA(8),REINT(8)
      COMMON/E/E/XMUE/XMUE/XLAMBDA/XLAMBDA/SIGMA/SIGMA/M/M/ZETA/ZETA
      COMMON/A11S/A11S/A12S/A12S/A22S/A22S/A11A/A11A/A12A/A12A/A22A/A22A
     1/B/B
```

Program name, store allocation and Common statement.

```
  450 READ(1,402)T,TP,BB,BS,BJ,BP,ANGLE1,ANGLE2,E
  402 FORMAT(9F0.0)
      READ(1,451)FO,DELSIG,XLAMBDA,DEL,VAL
  451 FORMAT(5F0.0)
      READ(1,406)MODE
  406 FORMAT(I1)
```

Read for input information data.

```
      IF(T.EQ.0.0)GO TO 405
```

End of data logic statement.

```
      TJ=T+TP
      XMUE=0.30
      DEL=0.05
      VAL=1.3
      XLAMBDA=1.05
```

Bonded flat thickness, ν, increment in value of λ, initial value of λ and final value of λ.

```
  103 WRITE(2,202)
  202 FORMAT(1H1///23X,5HSIGMA,12X,3HDET,13X,7HXLAMBDA,9X,4HZETA/)
```

Write Title on new page.

```
  101 CONTINUE
      L,KX,N,MC,NC=0
      M=1
      NN=0
      N=N+1
```

Initial values for count lable instructions.

```
      SIGMA(M)=FO
100   CONTINUE
      K=0
```

Set initial value of stress and lable instruction.

```
       CALL WITTRICK(T,    BB,  SBMM,SBMF,SBFF,FBMM,FBMF,FBFF)
       CALL WITTRICK(T,    BS,   SSMM,SSMF,SSFF,FSMM,FSMF,FSFF)
```

Subroutine Wittrick call up for calculating core bend and slant flat influence coefficients.

```
      ETA=(ANGLE2*3.1416)/180.
      BETA=(ANGLE1*3.1416)/180.
```

Core geometric angles converted to radians from degrees.

```
      AVS=-((SSMF+FSMF)*SIN(ETA)/(-SIN(BETA-ETA))+FBMF*COS(ETA)+SBMF*SIN
     1(ETA)*COT(BETA-ETA))/(SSMM+FSMM+SBMM)
      TS1=(SBFF*COS( ETA)+FBMF*AVS+FBFF*SIN( ETA)*COT(BETA- ETA))*COS( E
     1TA)
      P=T*BB*SIGMA(M)
      XI=(T*BB**3.)/12.
      XKC=((E*XI*3.1416**2./XLAMBDA**2.-P)*3.1416**2.*SIN(ETA))/(XLAMBDA
     1**2.)
      TS2=XKC*SIN(ETA)
      TS3=(FBFF*COS( ETA)+SBMF*AVS+SBFF*SIN( ETA)*COT(BETA- ETA))*COT(BE
     1TA- ETA)*SIN( ETA)
      TS4=(((SSMF+FSMF)*AVS+(SSFF+FSFF)*SIN(ETA)/(-SIN(BETA-ETA)))*SIN(
     1ETA))/SIN(BETA- ETA)
      A11S=TS1+TS2+TS3-TS4
      A12S=SBMF*COS( ETA)+FBMM*AVS+FBMF*SIN( ETA)*COT(BETA- ETA)
      A21S=A12S
      APSIS=-FBMM/(SSMM+FSMM+SBMM)
      A22S=SBMM+FBMM*APSIS
```

Calculation of elements of corrugation flat stiffness matrix for Symmetric case.

```
      AVA=-((SSMF-FSMF)*SIN(ETA)/(-SIN(BETA-ETA))-FBMF*COS(ETA)+SBMF*SI
     1N( ETA)*COT(BETA- ETA))/(SSMM-FSMM+SBMM)
      TA1=(SBFF*COS( ETA)-FBMF*AVA-FBFF*SIN( ETA)*COT(BETA- ETA))*COS( E
     1TA)
      TA2=TS2
      TA3=(-FBFF*COS( ETA)+SBMF*AVA+SBFF*SIN( ETA)*COT(BETA- ETA))*COT(B
     1ETA- ETA)*SIN( ETA)
      TA4=(((SSMF+FSMF*AVA+SSFF-FSFF)*SIN(ETA)/(-SIN(BETA-ETA)))*SIN(ET
     1A))/SIN(BETA- ETA)
      A11A=TA1+TA2+TA3+TA4
      A12A=SBMF*COS( ETA)-FBMM*AVA-FBMF*SIN( ETA)*COT(BETA- ETA)
      A21A=A12A
      APSIA=FBMM/(SSMM-FSMM+SBMM)
      A22A=SBMM-FBMM*APSIA
```

Calculation of elements of corrugation flat stiffness matrix for Antisymmetric Case.

```
      IF(MODE.EQ.1)GO TO 407
      IF(MODE.EQ.2)GO TO 408
      IF(MODE.EQ.3)GO TO 409
      IF(MODE.EQ.4)GO TO 410
  407 CALL XMODE1
      GO TO 411
  408 CALL XMODE2
      GO TO 411
  409 CALL XMODE3
      GO TO 411
  410 CALL XMODE4
  411 CONTINUE
```

Subroutine XMODE call up for forming $A_2^T K_2 A_2$.
Subroutine call up dependent on the input data.

```
      CALL WITTRICK(TJ,   BJ, SJMM,SJMF,SJFF,FJMM,FJMF,FJFF)
      CALL WITTRICK(TP,   BP, SPMM,SPMF,SPFF,FPMM,FPMF,FPFF)
```

Subroutine Wittrick call up for calculating face-plate bonded and unbonded flat influence coefficients.

```
      F(1,5),F(1,6),F(2,5),F(3,7),F(3,8),F(4,8),F(2,6),F(4,7)=0.0
      F(1,1),F(3,3),F(5,5),F(7,7)=SJFF+SPFF
      F(2,2),F(4,4),F(6,6),F(8,8)=SJMM+SPMM
      F(1,2),F(5,6)=-SJMF+SPMF
      F(1,3),F(5,7)=-FJFF
      F(1,4),F(5,8)=-FJMF
      F(1,7),F(3,5)=-FPFF
      F(1,8),F(4,5)=FPMF
      F(2,3),F(6,7)=FJMF
      F(2,4),F(6,8)=FJMM
      F(2,7),F(3,6)=-FPMF
      F(2,8),F(4,6)=FPMM
      F(3,4),F(7,8)=SJMF-SPMF
      DO 5 I=1,8
      DO 5 J=2,8
    5 F(J,I)=F(I,J)
```

Formation of matrix $A_1' K_1 A_1$

```
C     MATRIX C IS (A1DASH K1 A1 + A2DASH K2 A2)
      DO 8 I=1,8
      DO 8 J=1,8
      K=K+1
      C(I,J)=F(I,J)+B(I,J)
    8 A(K)=C(I,J)/1000.
```

Formation of matrix $C(8,8) = A_1' K_1 A_1 + A_2' K_2 A_2$. Storing C(8,8) into A(64). Each element being divided by 1000. as a precaution against overflow. Conversion of C(8,8) into A(64) is necessary for use of Subroutine F4DET

```
      N=8
      NA=64
      CALL F4DET(A,N,NA,D,ID,REINT,IT)
```

Input instructions for F4DET, and call up for solving the determinant of A(64).

```
      IF(NN)33,33,34
```

Instruction for calculating θ, when the panel has buckled.

```
35 DET(M)=D*2.**ID
```

Numerical value of determinant.

```
    WRITE(2,201)SIGMA(M),DET(M),XLAMBDA,ZETA
201 FORMAT(20X,E12.5,3E16.5)
```

Write instructions.

```
    IF(KX)52,53,54
```

Lable instruction for stress increment of ± 100 lb/in^2

```
52  M=M+1
    SIGMA(M)=SIGMA(M-1)+100.
    MC=MC+1
    KX=-1
    IF(MC-10)100,100,55
```

Stress increased by 100 lb/in^2

```
54  M=M+1
    SIGMA(M)=SIGMA(M-1)-100.
    KX=1
    NC=NC+1
    IF(NC-10)100,100,55
```

Stress decreased by 100 lb/in^2

```
53  IF(L)56,57,58
```

Label instruction for stress increment of ± 1000 lb/in^2

```
56  IF(DET(M))59,60,52
```

Check on sign of determinant.

```
59  M=M+1
    SIGMA(M)=SIGMA(M-1)-1000.
    L=-1
    GO TO 100
```

Stress decreased by 1000 lb/in^2

```
57 IF(DET(M))61,60,64
61 IF(ABS(DET(M-1))-ABS(DET(M)))62,62,59
```

Comparision of magnitude of determinant values to decide whether to increase or decrease the stress value.

```
62 SIGMA(M)=SIGMA(M-1)
80 M=M+1
   SIGMA(M)=SIGMA(M-1)+1000.
   L=1
   GO TO 100
```

Stress increased by 1000 lb/in^2

```
64 M=M+1
   SIGMA(M)=SIGMA(M-1)+DELSIG)
   GO TO 100
```

Stress increased by DELSIG. lb/in^2

```
58 IF(DET(M))54,60,80
60 WRITE(2,201)SIGMA(M),DET(M),XLAMBDA,ZETA
```

Write results if determinant value is equal to zero.

```
 55 M=M-1
    DO 50 I=1,20
    RAT=DET(M)/DET(M-1)
    IF(RAT)30,30,50
 50 M=M-1
 30 CONTINUE
 30 WRITE(2,400)
400 FORMAT(/23X, 7HXLAMBDA,7X,8HSIGMA(M),6X,6HDET(M),8X,8HDET(M 1),5X,
   110HSIGMA(M-1))
    WRITE(2,204)XLAMBDA,SIGMA(M),DET(M),DET(M-1),SIGMA(M-1)
204 FORMAT(/5X,5(2X,E12.5)/)
    IF(ABS(DET(M-1))-ABS(DET(M)))31,31,32
 31 SIGMA(49)=SIGMA(M-1)
    NN=1
    GO TO 100
 32 SIGMA(49)=SIGMA(M)
    NN=1
    GO TO 100
```

Scanning of values of determinant for the last 10 values of stress to determine the stress at which the determinant achieves change of sign. When determinant changes sign, output of values of stress and determinant on either side of the zero.

```
 34 THETA(8)=1.
    DO 74 IO=1,7
    I=8-IO
    THETA(I)=0.
    DO 74 J=I+1,8
 74 THETA(I)=THETA(I)-A(I+8*(J-1))*THETA(J)
    WRITE(2,401)
401 FORMAT(20X,12HTHETA 1 TO 8/)
 75 WRITE(2,203)THETA
203 FORMAT(18X,8(2X,F7.4))
```

Calculation of Θ, the ratios of deflections and output of results.

```
    WRITE(2,404)
404 FORMAT(/23X,1HT,6X,2HTJ,6X,2HTP,6X,2HBB,6X,2HBS,6X,2HBJ,6X,2HBP,
   18X,1HE,5X,4HMODE/)
    WRITE(2,403)T,TJ,TP,BB,BS,BJ,BP,E,MODE
403 FORMAT(18X,7(2X,F6.3),2X,F10.0,2X,I1)
```

Output of core geometry, and mode.

```
 35 XLAMBDA=XLAMBDA+DEL
    IF(XLAMBDA-VAL)103,103,405
```

Increment in value of λ.

```
405 CONTINUE
    STOP
    END
```

End of Master Segment.

1.4 Wittrick Subroutine.

```
SUBROUTINE WITTRICK (T,B,SMM,SMF,SFF,FMM,FMF,FFF)
DIMENSION SIGMA(50)
COMMON/E/E/XMUE/XMUE/XLAMBDA/XLAMBDA/SIGMA/SIGMA/M/M/ZETA/ZETA
```

Subroutine title, store location and common statement.

```
D=(E*T**3.)/(12.*(1.-XMUE**2.))
XK=(SIGMA(M)*B*B*T)/(3.1416*3.1416*D)
ZETA=XK*(XLAMBDA/B)**2.
OMEGA=3.1416*B/XLAMBDA
```

Calculation of D, K, φ and ω.

```
IF(ZETA-1.)1,2,3
```

Check to determine whether φ is less than one, greater than one or equal to one.

```
1 ALPHA=OMEGA*(1.+ZETA**.5)**.5
  GAMA=OMEGA*(1.-ZETA**.5)**.5
  Z=SINH(ALPHA)*SINH(GAMA)+(ALPHA*GAMA/OMEGA**2.)*(1.-COSH(ALPHA)*CO
 1SH(GAMA))
  R=ZETA**.5/Z
  SMM=D*R/B*(ALPHA*COSH(ALPHA)*SINH(GAMA)-GAMA*COSH(GAMA)*SINH(ALPH
 1A))
  SMF=D*OMEGA**2./B**2.*(1.-XMUE-ZETA*SINH(ALPHA)*SINH(GAMA)/Z)
  SFF=R*D*ALPHA*GAMA/B**3.*(ALPHA*SINH(ALPHA)*COSH(GAMA)-GAMA*SINH(G
 1AMA)*COSH(ALPHA))
  FMM=R*D/B*(GAMA*SINH(ALPHA)-ALPHA*SINH(GAMA))
  FMF=-R*ALPHA*GAMA*D/B**2.*(COSH(ALPHA)-COSH(GAMA))
  FFF=R*ALPHA*GAMA*D/B**3.*(ALPHA*SINH(ALPHA)-GAMA*SINH(GAMA))
  GO TO 4
```

Calculation of plate influence coefficients for $\varphi \angle 1$.

```
2 ALPHA=OMEGA*2.**.5
  ZSTAR=SINH(ALPHA)+(2.**.5*(1.-COSH(ALPHA)))/OMEGA
  R=1./ZSTAR
  SMM=R*D/B*(ALPHA*COSH(ALPHA)-SINH(ALPHA))
  SMF=(OMEGA/B)**2.*D*(1.-XMUE-R*SINH(ALPHA))
  SFF=R*D/B**3.*ALPHA**2.*SINH(ALPHA)
  FMM=R*D/B*(SINH(ALPHA)-ALPHA)
  FMF=-(ALPHA*D)/(ZSTAR*B*B)*(COSH(ALPHA)-1.)
  FFF=SFF
  GO TO 4
```

Calculation of plate influence coefficients for $\varphi=1$.

```
3 DELTA=OMEGA*(ZETA**.5-1.)**.5
  ALPHA=OMEGA*(1.+ZETA**.5)**.5
  Z=SINH(ALPHA)*SIN(DELTA)+(ALPHA*DELTA*(1.-COSH(ALPHA)*COS(DELTA)))
 1/OMEGA**2.
  R=ZETA**.5/Z
  SMM=D*R/B*(ALPHA*COSH(ALPHA)*SIN(DELTA)-DELTA*COS(DELTA)*SINH(ALPH
 1A))
  SMF=D*OMEGA**2./B**2.*(1.-XMUE-ZETA*SINH(ALPHA)*SIN(DELTA)/Z)
  SFF=R*D*ALPHA*DELTA/B**3.*(ALPHA*SINH(ALPHA)*COS(DELTA)+DELTA*SIN(
 1DELTA)*COSH(ALPHA))
  FMM=R*D/B*(DELTA*SINH(ALPHA)-ALPHA*SIN(DELTA))
  FMF=-R*ALPHA*DELTA*D/B**2.*(COSH(ALPHA)-COS(DELTA))
  FFF=R*ALPHA*DELTA*D/B**3.*(ALPHA*SINH(ALPHA)+DELTA*SIN(DELTA))
  GO TO 4
```

Calculation of plate influence coefficients for $\varphi>1$.

```
4 CONTINUE
  RETURN
  END
```

End of subroutine and return to master segment.

1.5 Subroutines IN XMODE series.

Example is illustrated by XMODE4.

```
      SUBROUTINE XMODE4
      DIMENSION B(8,8)
      COMMON/A11S/A11S/A12S/A12S/A22S/A22S/A11A/A11A/A12A/A12A/A22A/A22A
     1/B/B
```

subroutine title, store allocation and common statement.

```
      DO 7 I=1,8
      DO 7 J=1,8
    7 B(I,J)=0.0
```

Filling the matrix B(8,8) by zero elements.

```
      B(1,1),B(3,3),B(5,5),B(7,7)=(A11S+A11A)
      B(2,2),B(4,4),B(6,6),B(8,8)=(A22S+A22A)
      B(1,3),B(1,7),B(3,5),B(5,7)=(A11S-A11A)*.5
      B(2,8),B(2,4),B(4,6),B(6,8)=(A22S-A22A)*.5
      B(1,8),B(2,7),B(3,6),B(4,5)=(A12S-A12A)*.5
      B(1,4),B(2,3),B(5,8),B(6,7)=-(A12S-A12A)*.5
```

Filling the upper triangle of the matrix B(8,8)

```
      DO 9 I=1,8
      DO 9 J=2,8
    9 B(J,I)=B(I,J)
```

As the matrix B(8,8) is symmetric, the lower triangle can be filled by this loop with appropriate elements from the upper triangle.

```
      RETURN
      END
```

End of subroutine and return to master segment.

APPENDIX 2.

EXPERIMENTAL ANALYSIS

APPENDIX 2

EXPERIMENTAL ANALYSIS

2.0 Introduction

Buckling load is taken as the load at which a change in slope of the load/deflection graph occurs. Where one or more 'contractometers' are mounted on the same face, mean value is taken. Cross-sectional areas used in computing buckling stresses are obtained from Table 3.4.

2.1 Strain Conversion Factor

2.1.1 Strain gauge readings

$$\text{Strain, } e = (\text{Strain gauge reading}) \times \frac{10^{-5}}{2.06}$$

2.1.2 Contractometer (dial gauge) readings)

$$\text{Strain, } e = \frac{\text{Dial gauge reading (ins.)}}{(\text{Lever ratio}) \times (\text{Gauge Length})}$$

where Lever ratio = 2 : 1

Gauge length = 10 ins.

2.2 Panels in 5B Configuration

Panel 5B/1

For the first and second 'setting-up' runs, the readings of strain gauges 0, 9, 10 and 19 are plotted in Figs.A2.1 and A2.2 respectively. These runs were made to ensure even loading of the specimen.

Outer face-plates

Taking mean value for strain gauges 1 to 8 (See Figs. A2.4 and A2.6).

Buckling load = 67 tons

Buckling stress = 32,700 lb./in.^{2}

Inner face-plates:

Taking mean value for strain gauges 11 to 18 (See Figs. A2.5 and A2.7).

Buckling load = 68.5 tons

Buckling stress = 33,400 lb./in.^{2}

Dial gauges mounted on the inner face-plate do not yield any information. (See Fig.A2.8).

Panel 5B/2

This panel had a defective adhesive joint. To enable the panel to be tested, the defective joint was 'cut-away', thus, the width of the panel at inner face-plate was reduced to three pitch. (See Fig.3.4).

For deflection measurement, three contractometers were used. (See Fig.3.4).

Outer face-plate:

Taking mean value for dial gauges A and B, (See Fig.A2.9)

Buckling load = 45 tons

Buckling stress = 30,200 lb./in.^{2}

Inner face-plate:

From Fig.A2.9, for dial gauge C

Buckling load = 46 tons

Buckling stress = 30,900 lb./in.^{2}

Panel 5B/3

Buckling load was determined by studying the reflections of an'illuminated grid' on the polished specimen.

Outer face-plate:

Buckling load = 69 tons

Buckling stress = 33,600 lb./in.^{2}

Inner face-plate:

Buckling load = 70 tons

Buckling stress = 34,100 lb./in.^{2}

Cire slant-flat:

Buckling load = 50 tons

Buckling stress = 24,400 lb./in.^{2}

2.3 Panels in 2A, 2B, and 2C Series

Buckling loads are determined from Figs.A2.10 - 16.

	Buckling Load (tons)			
Panel No.	2A/1	2B/1	2C/1	2C/2
Outer face-plate	+	14.8	11.0	14.0
Inner face-plate	13.8	11.0	+	13.7
Core slant flat	13.1	14.5	13.0	15.8

	Buckling Stress (lb./in.^{2})			
Panel No.	2A/1	2B/1	2C/1	2C/2
Outer face-plate	+	12,000	8,600	11800
Inner face-plate	11,200	8,900	+	10700
Core slant flat	10,700	11,800	10,100	12400

+ Buckling loads can not be determined.

Note. Panel 2B/1 had faulty adhesive joint at the outer face-plate. To avoid 'weak-spots' two rows of 1/8 dia. Avdel rivets at 0.5 in. staggered pitch were used.

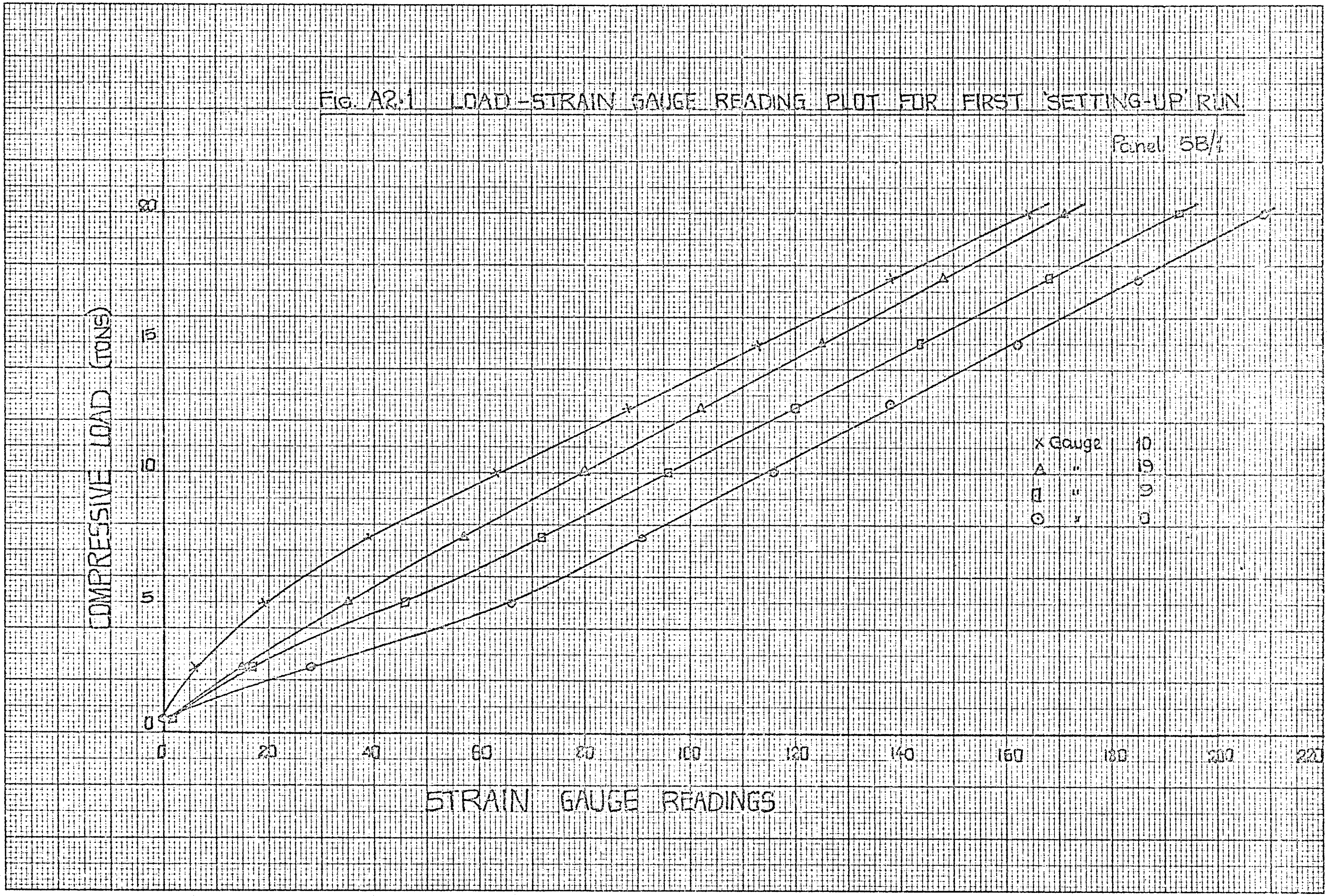

FIG. A2.1 LOAD-STRAIN GAUGE READING PLOT FOR FIRST 'SETTING-UP' RUN

FIG. A2.2 LOAD-STRAIN GAUGE READING PLOT FOR SECOND 'SETTING-UP' RUN

Panel 53/1

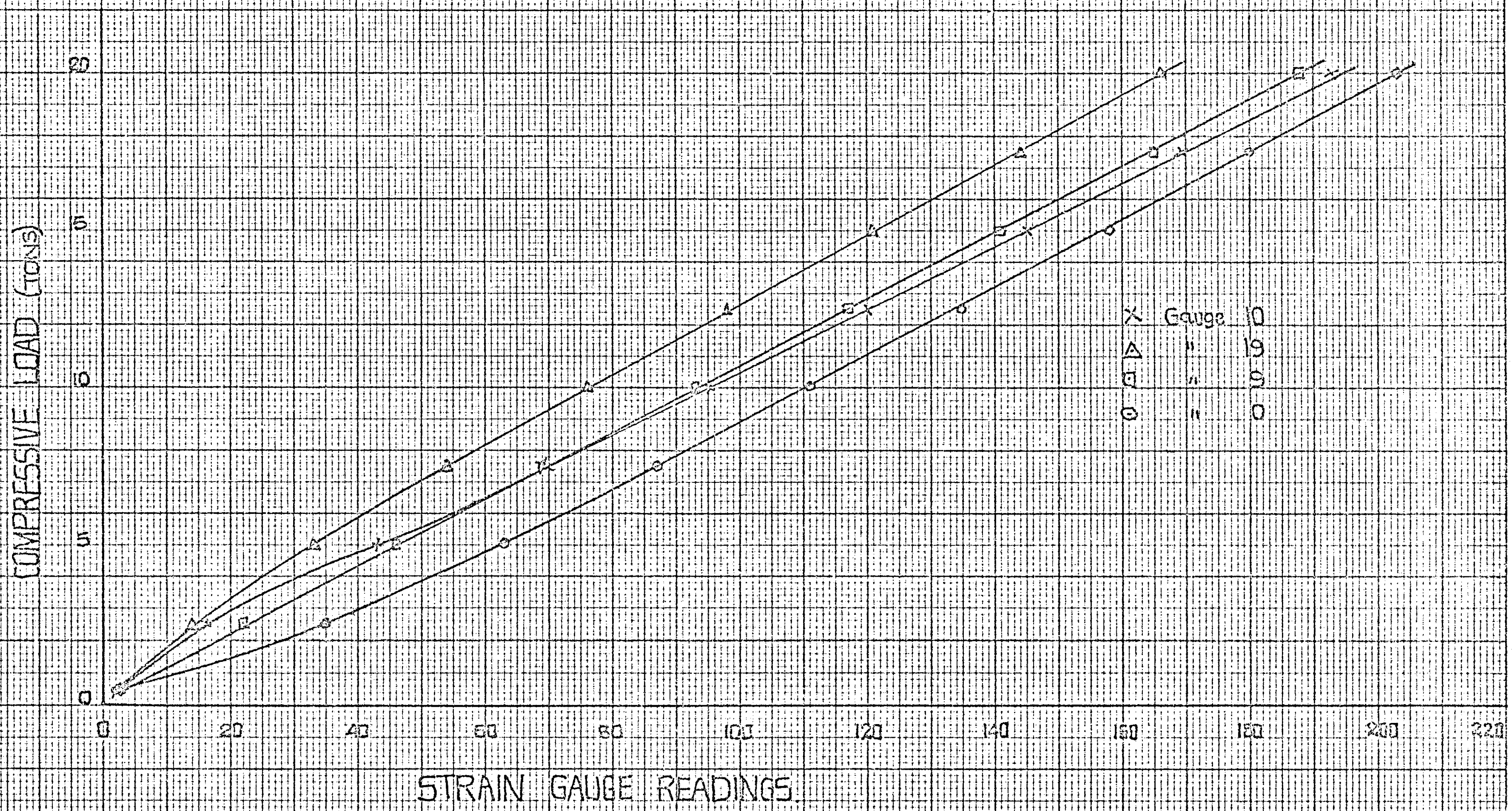

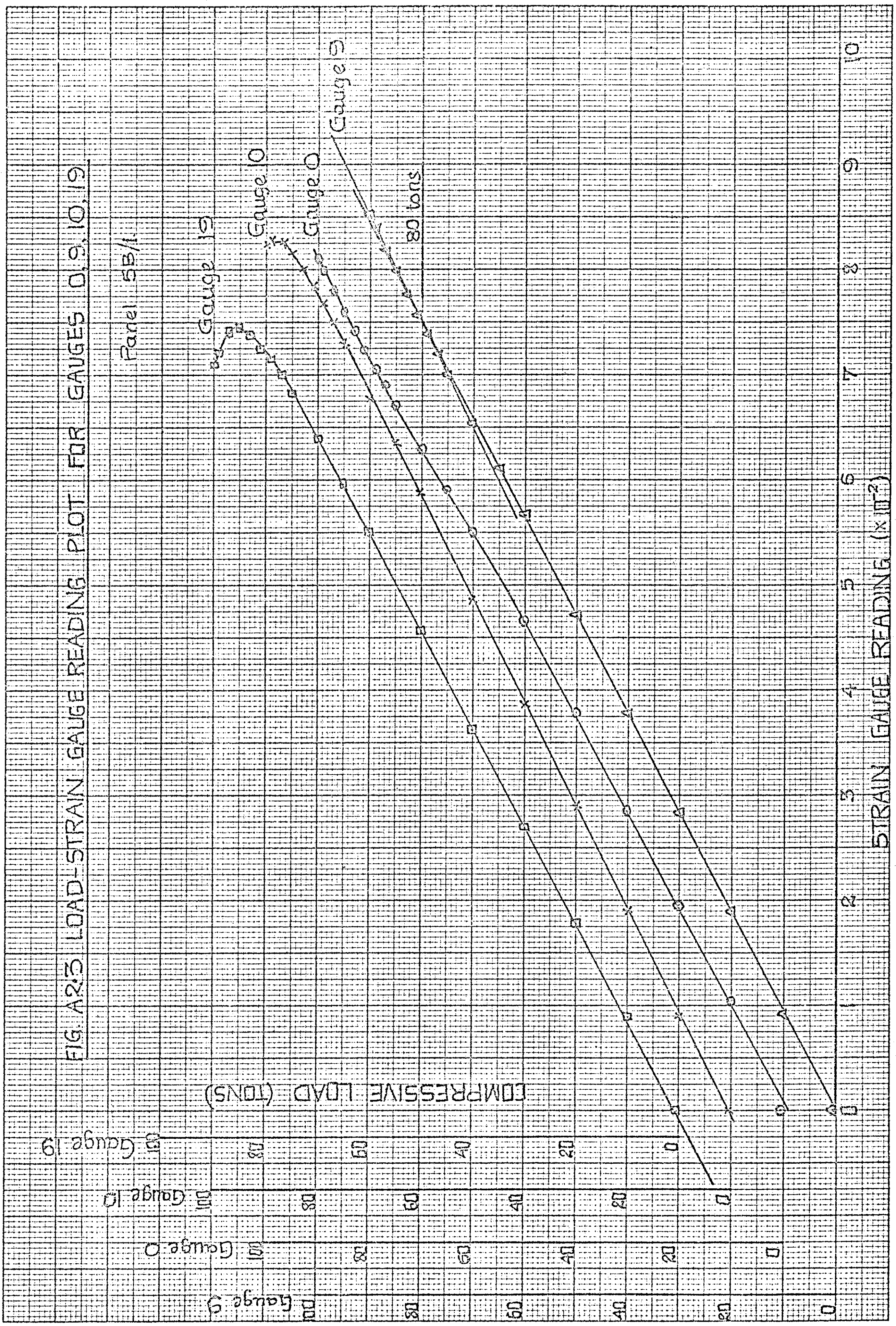

FIG. A2.3 LOAD-STRAIN GAUGE READING PLOT FOR GAUGES 0,9,10,19

FIG. AR.4 PLOT FOR STRAIN GAUGES 6,7 & 8 Panel 53/1

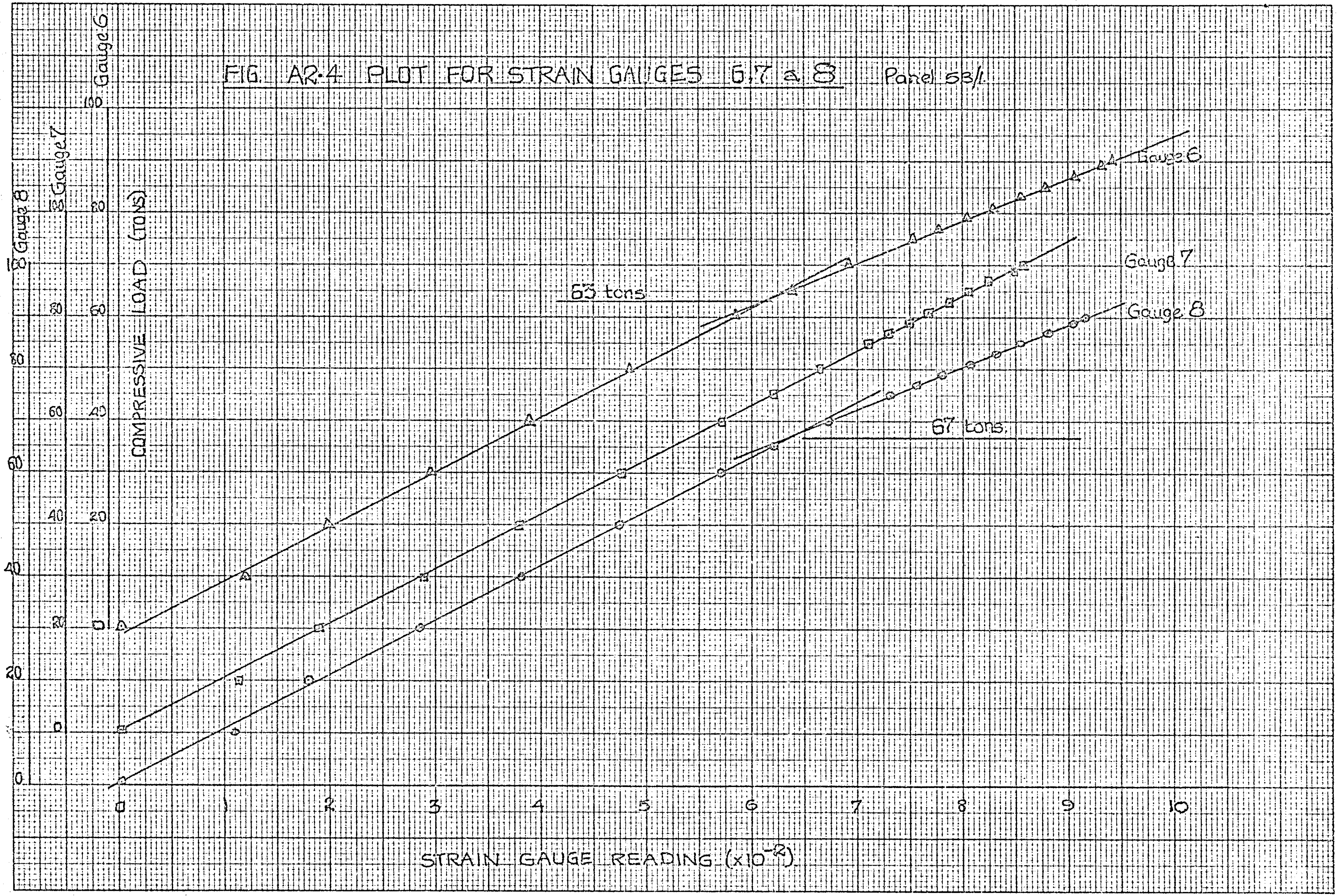

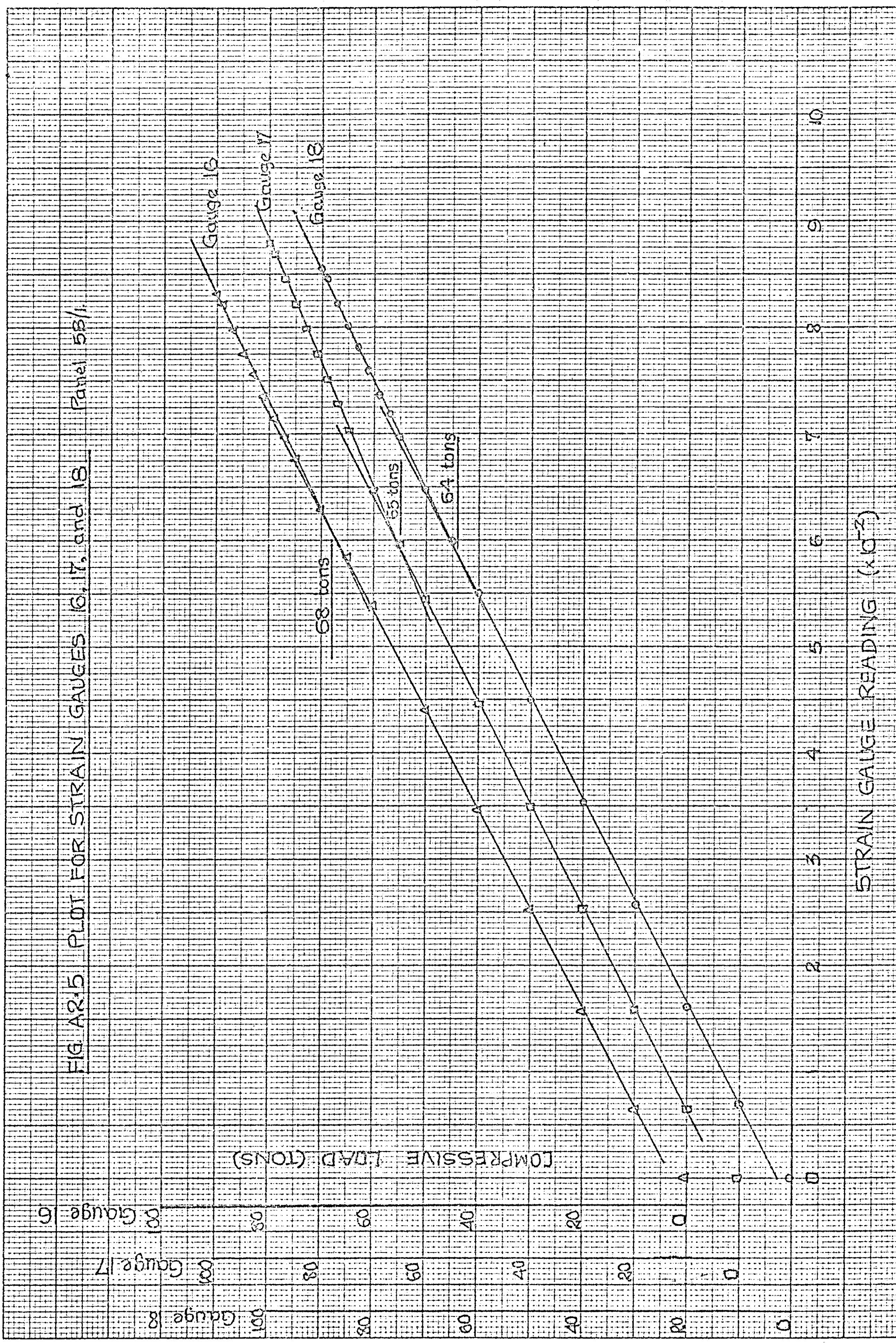

FIG A2.5 PLOT FOR STRAIN GAUGES 16, 17, and 18 Panel 5B/1

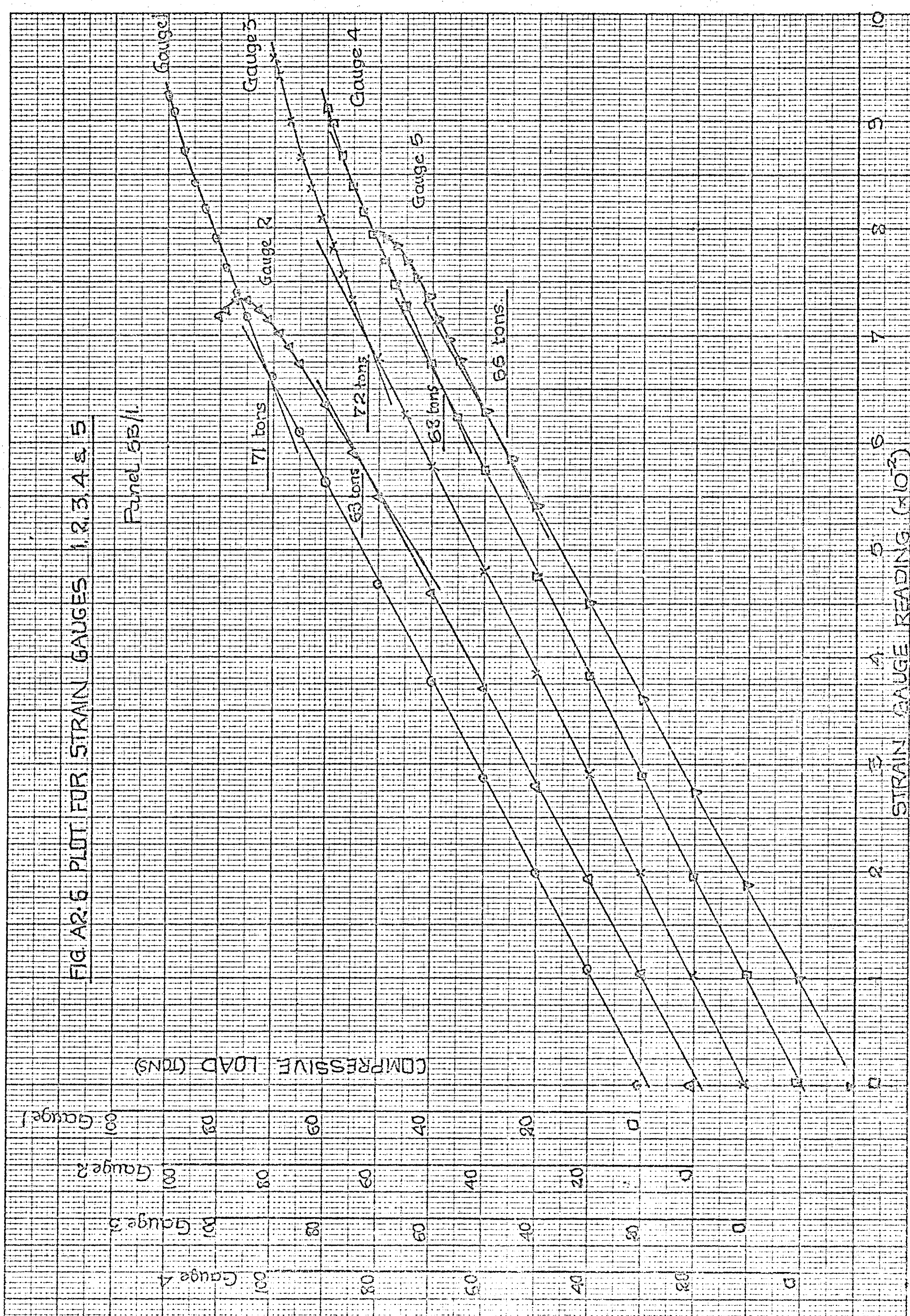

FIG. A2.6 PLOT FOR STRAIN GAUGES 1,2,3,4 & 5

FIG. AP.7 PLOT FOR STRAIN GAUGES 15, 14, 13, 12 & 11

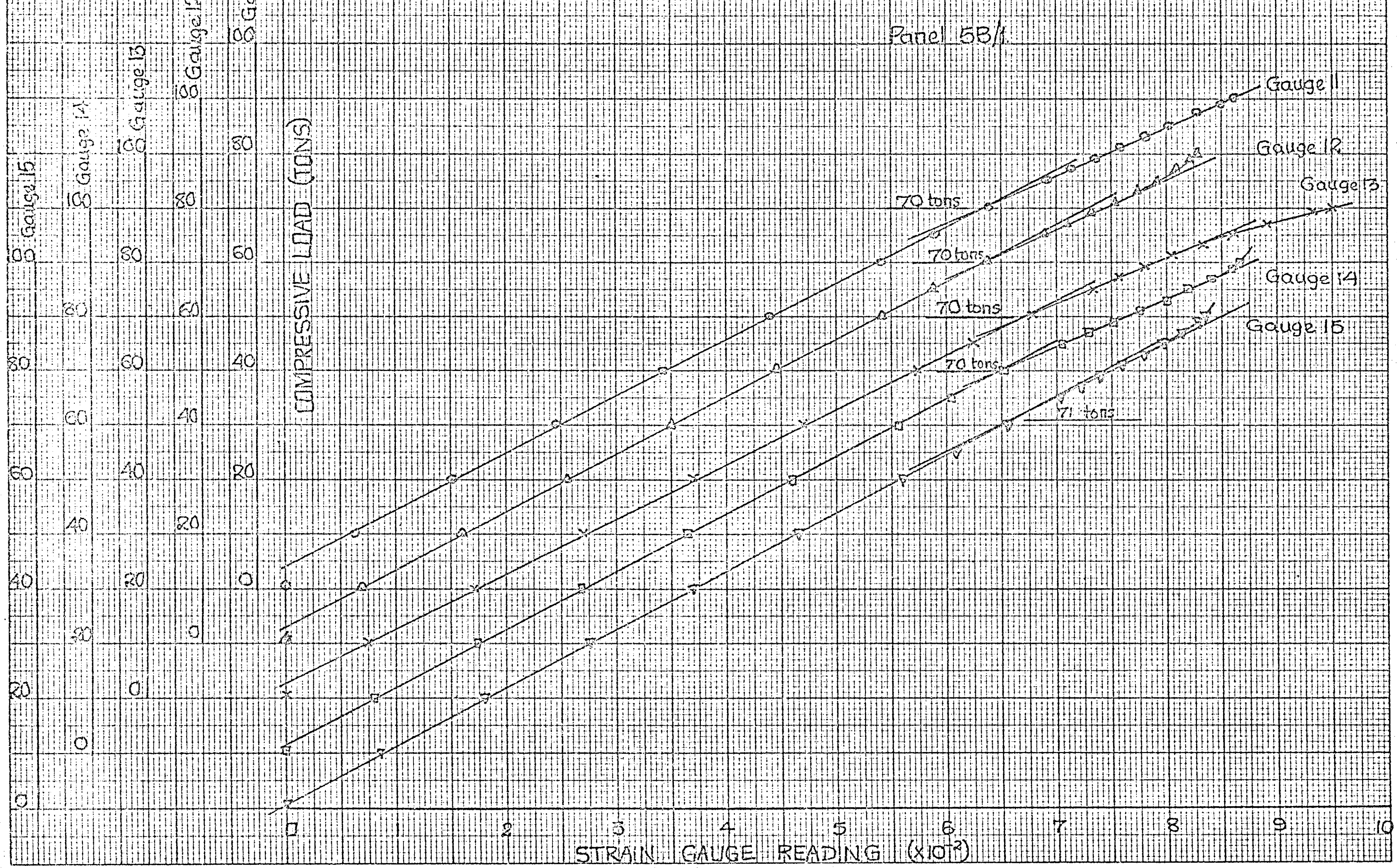

FIG A2.8 PLOT OF DIAL GAUGE READINGS

PANEL 58/1

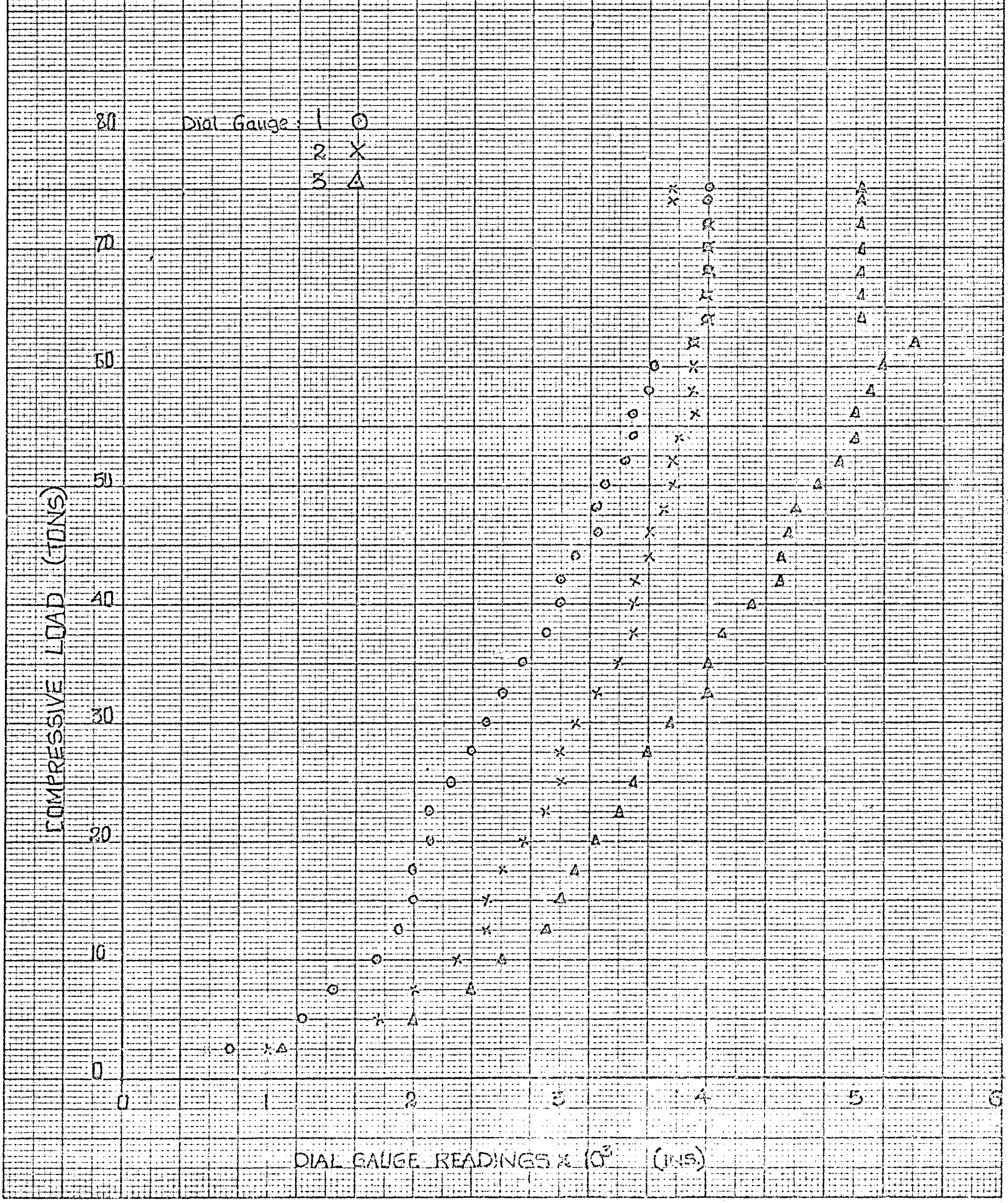

Fig A2.9 LOAD-DEFLECTION PLOT FOR PANEL 5B/2

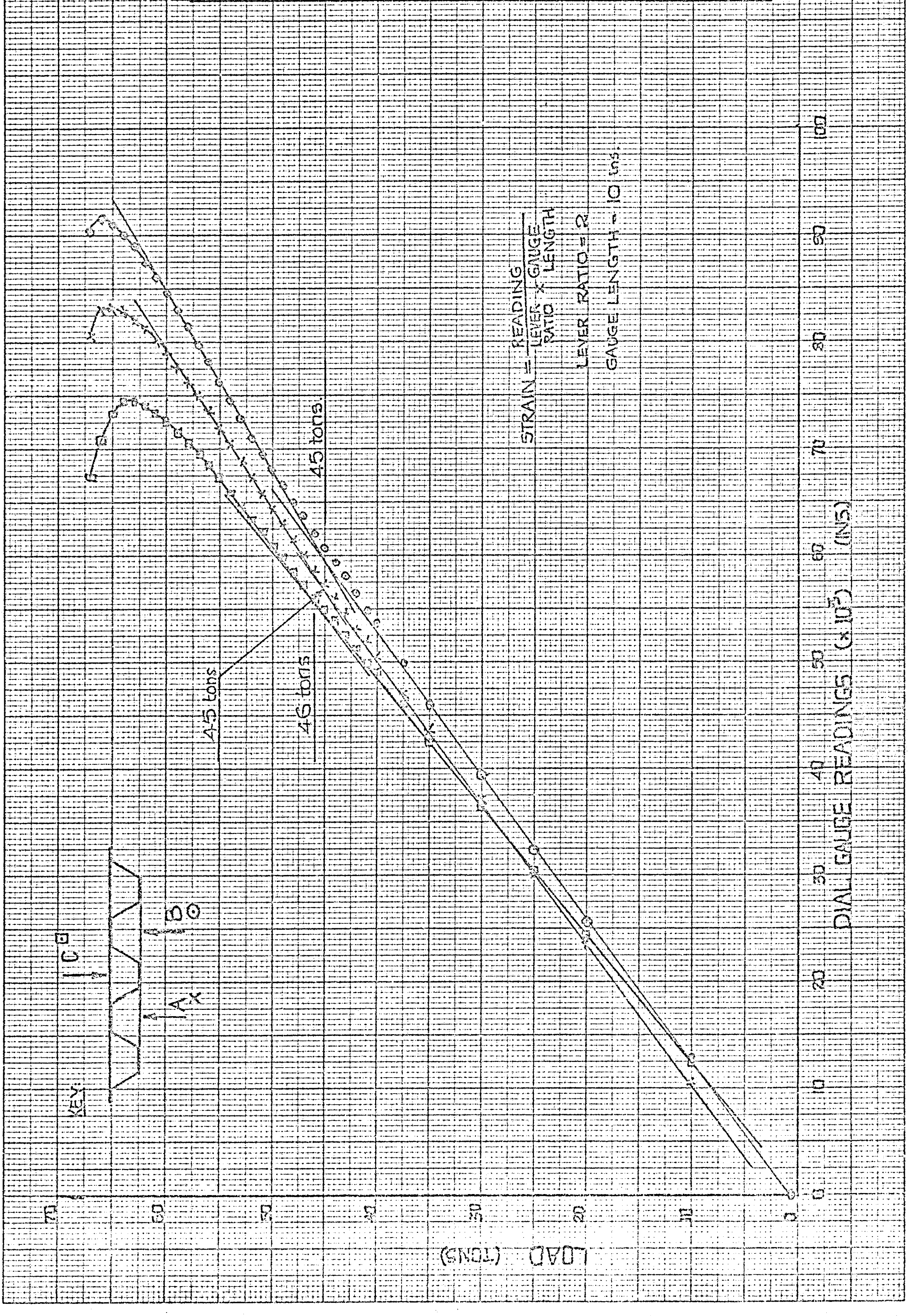

Fig. A2.10 LOAD-DEFLECTION PLOT FOR PANEL 2A/1

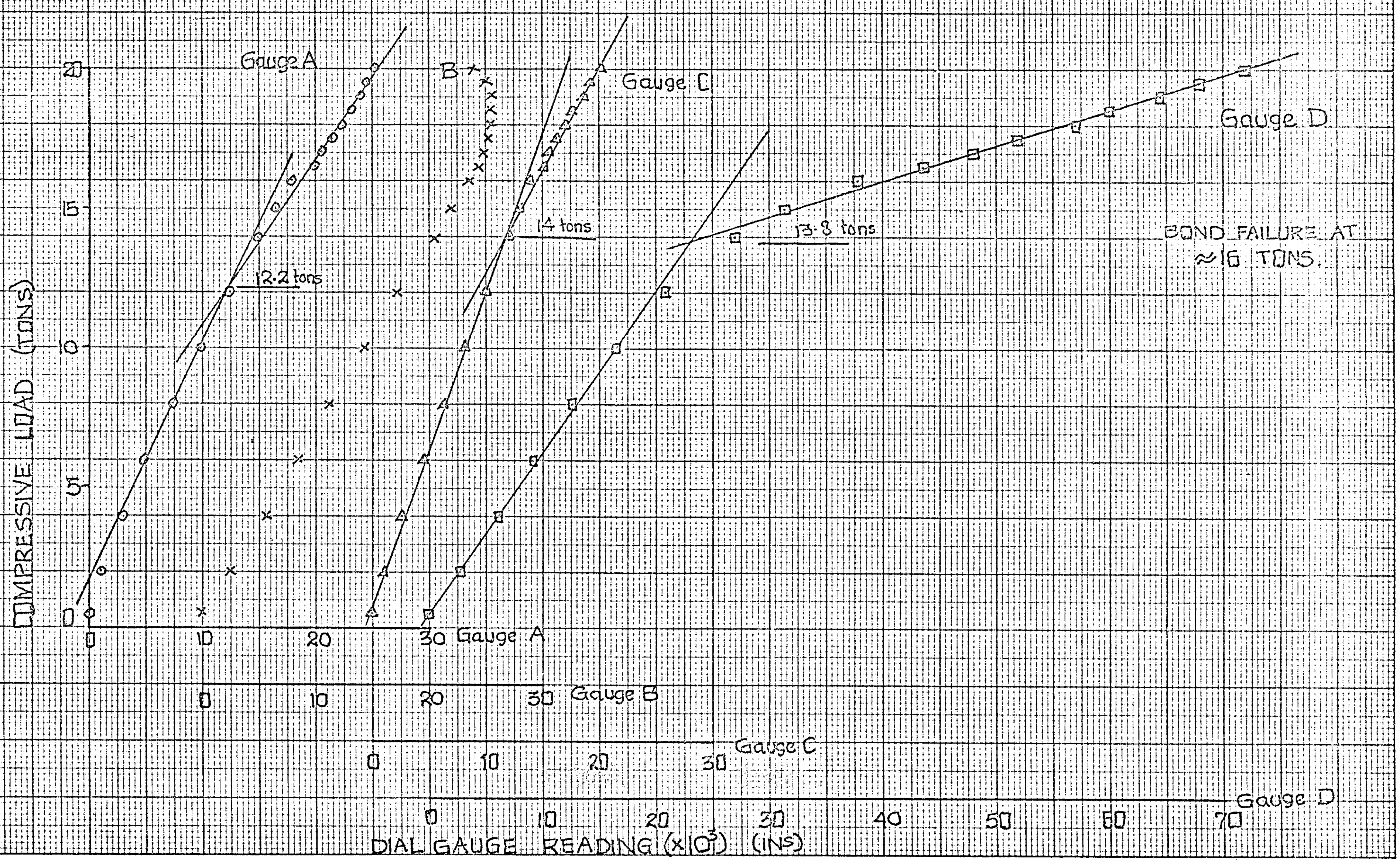

FIG. A2·1 LOAD-DEFLECTION PLOT FOR PANEL 2B/1

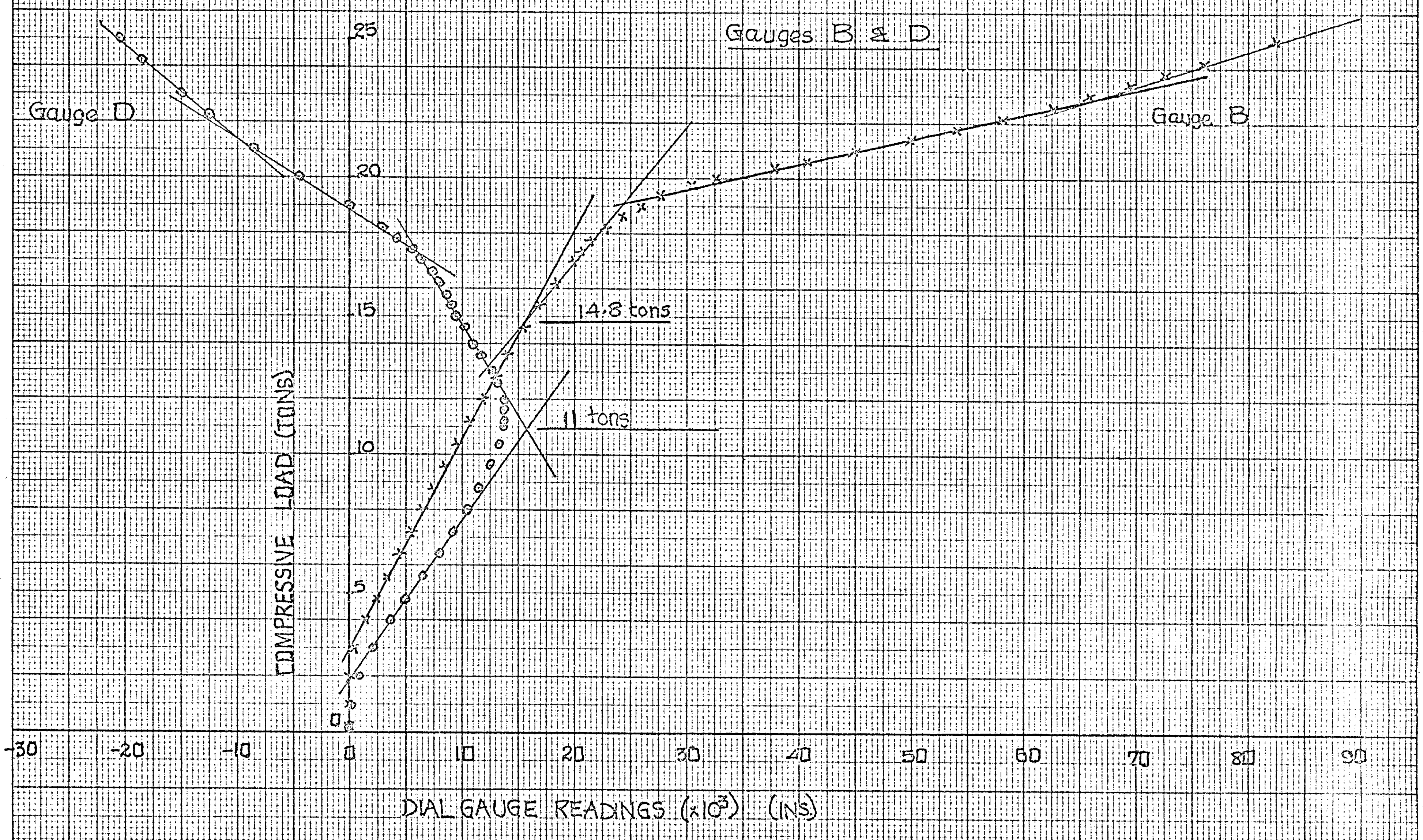

FIG. A2.12 LOAD-DEFLECTION PLOT FOR PANEL 2B/1

Gauges A & C

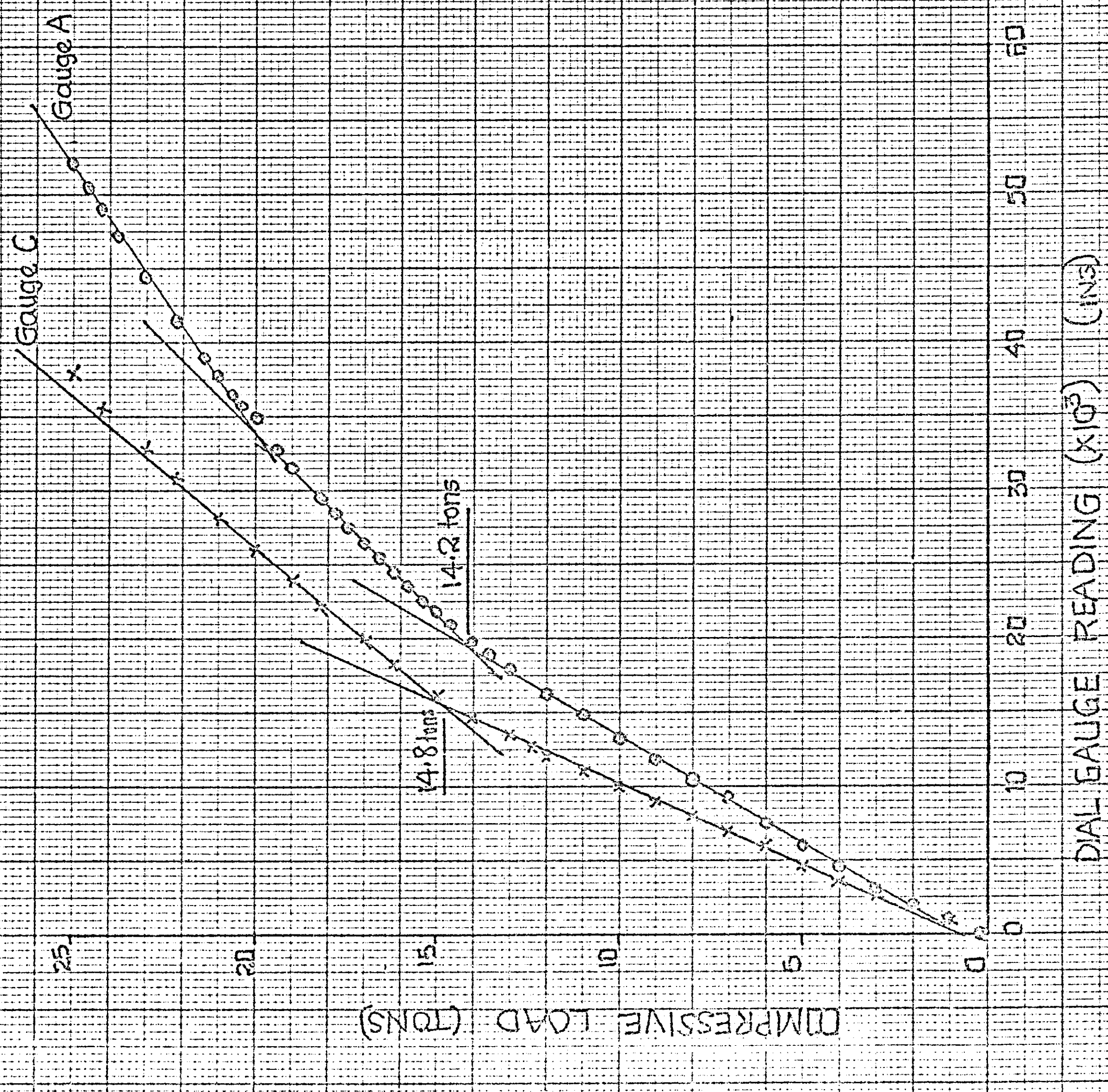

FIG. A2.13 LOAD-DEFLECTION PLOT FOR PANEL RC/1

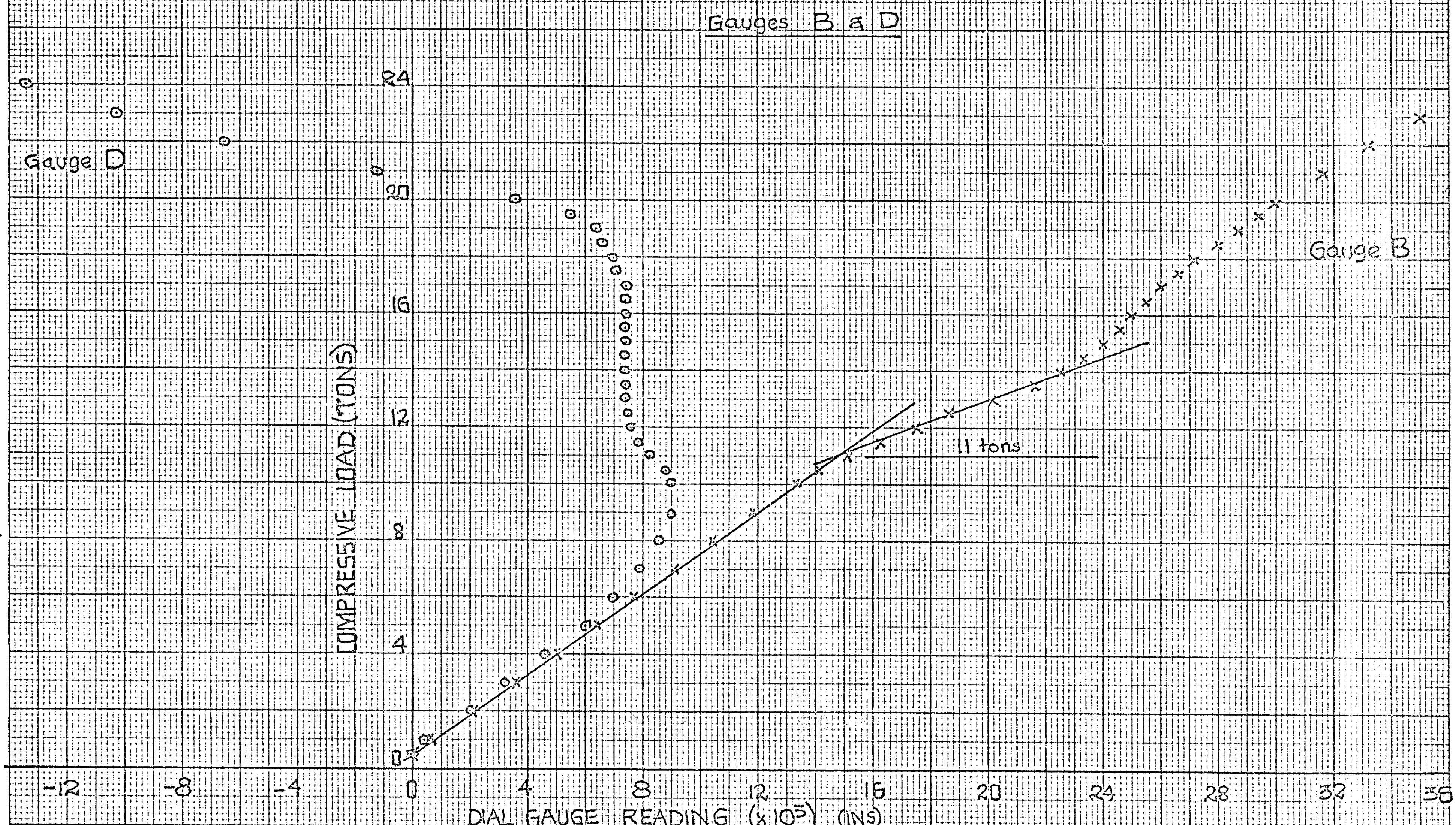

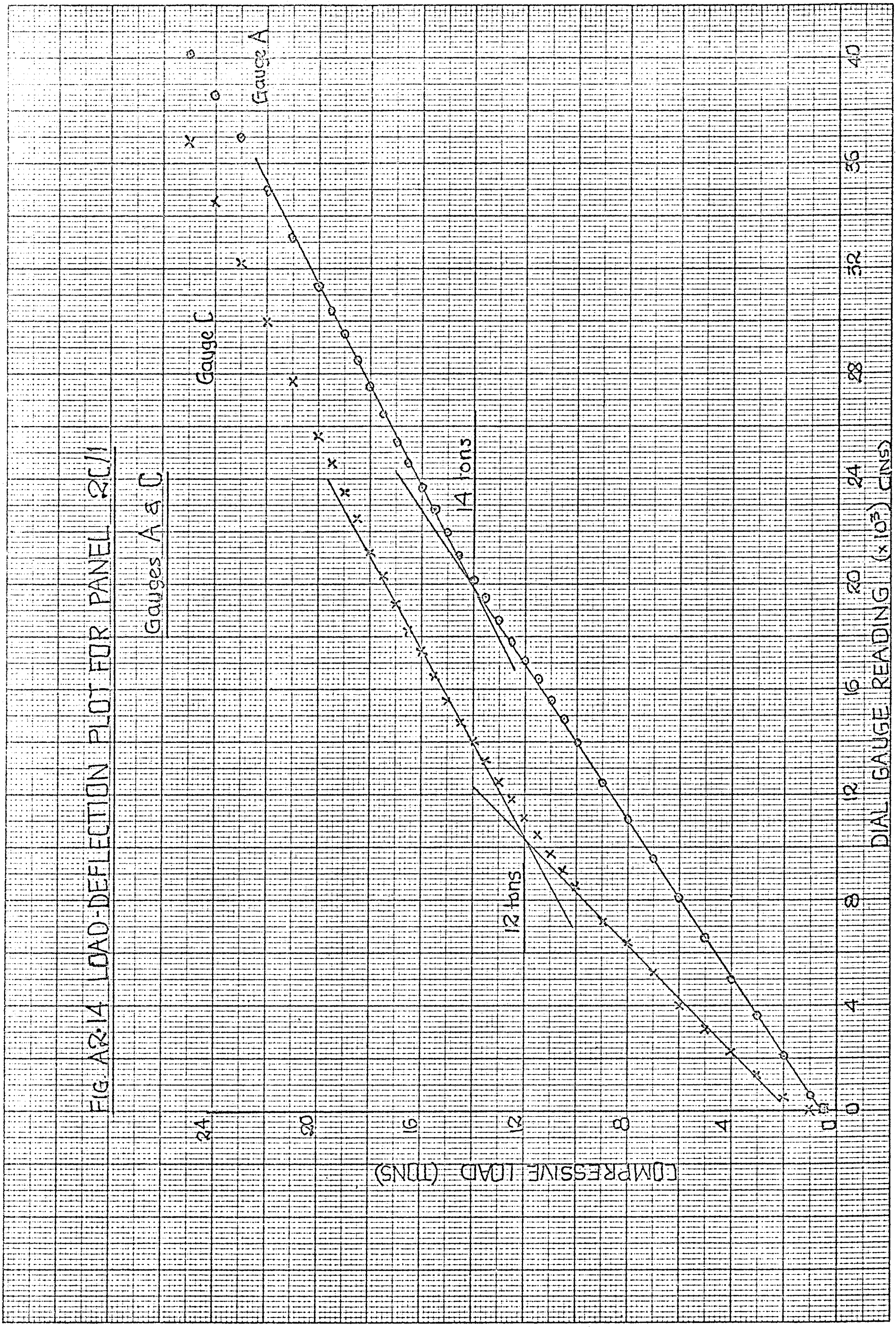
FIG. AR.14 LOAD-DEFLECTION PLOT FOR PANEL 2C/1
Gauges A & C
Gauge A
Gauge C
14 tons
12 tons
COMPRESSIVE LOAD (TONS)
0
4
8
12
16
20
24
DIAL GAUGE READING (×10⁻³) (INS)
0
4
8
12
16
20
24
28
32
36
40

FIG. A2·15 LOAD-DEFLECTION PLOT FOR PANEL 2C/2

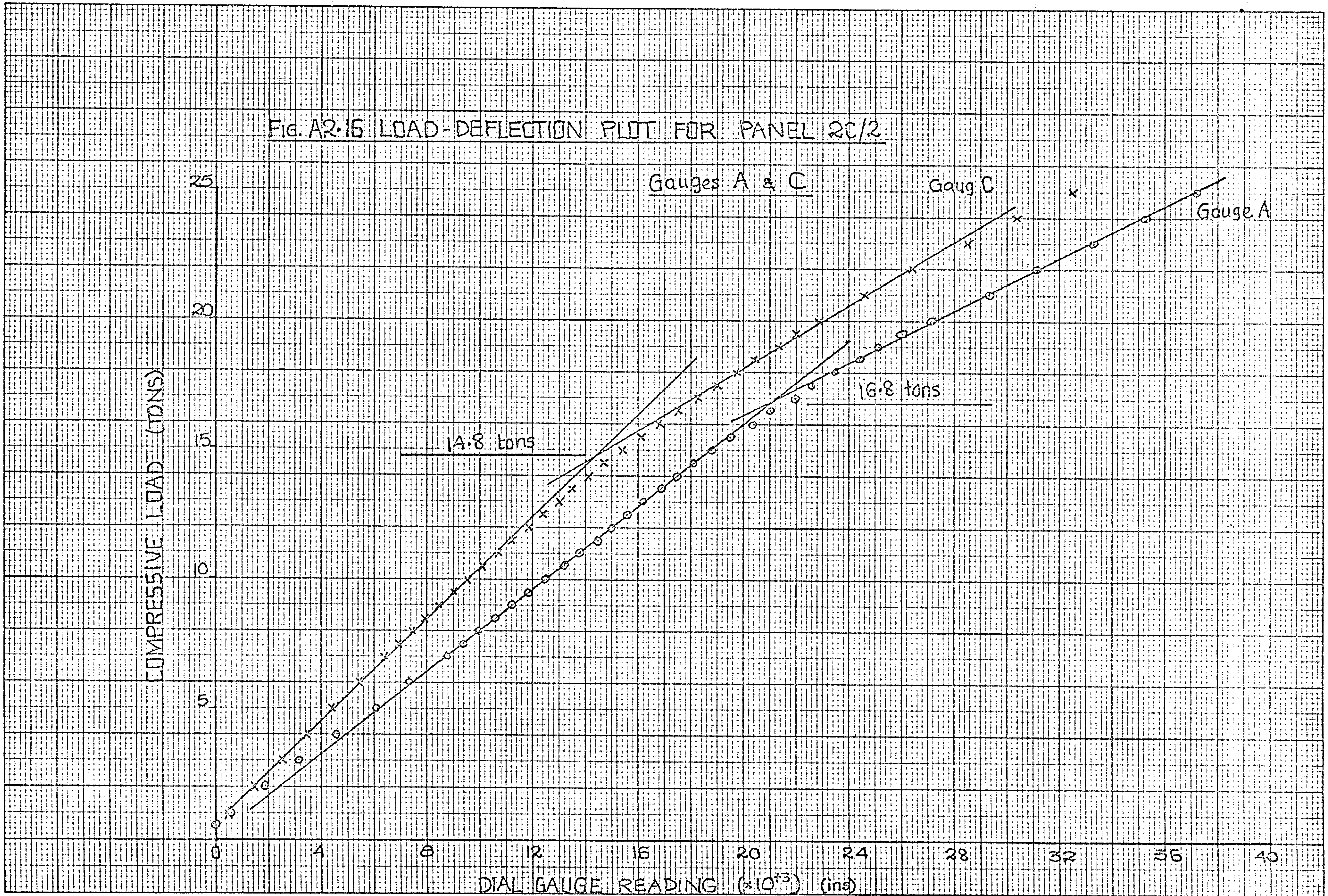
FIG. A2.16 LOAD-DEFLECTION PLOT FOR PANEL 2C/2
Gauges A & C
Gaug C
Gauge A
14.8 tons
16.8 tons
COMPRESSIVE LOAD (TONS)
DIAL GAUGE READING ($\times 10^{-3}$) (ins)
0
4
8
12
16
20
24
28
32
36
40
5
10
15
20
25

APPENDIX 3.

THEORETICAL PREDICTION OF BUCKLING STRESS USING DATA SHEETS

APPENDIX 3

THEORETICAL RREDICTION OF BUCKLING STRESS USING DATA SHEETS (Ref.5)

3.0 Introduction

The basic theory behind this method of calculating buckling stress for corrugated core sandwich panels is outlined in detail in ref.5.

In this appendix the general method adapted for measuring flat widths (required for predicting the buckling stresses) is explained.

A specimen calculation is included for specimen No.1. Theoretical values of buckling stresses for the Handley Page test specimens (see Table 3.1) and the test program specimens (see Table 3.3) are tabulated in Table 4.3 and 4.4 respectively.

3.1 Flat Dimensions

Notations used for identifying the flats of the sandwich panel are shown in Fig.A3.1. The figure also indicates the method used in measuring the flat widths.

3.2 Specimen Calculation (Specimen No.1)

Flat	A	B	D	F
b	1.125	1.24	0.58	0.58
t	.048	.064	.048	.064
$E't^3/3b$	348	750	675	1610
$f_o (\times 10^{-3})$	64	93	241	426

where $E' = \dfrac{E}{(1-\nu^2)}$ (lb./in.^{2})

$$f_o = \frac{\pi^2 E'}{3} \left(\frac{t}{b} \right)^2 \text{ lb./in.}^2$$

and other notations are as defined in the main text.

Using the Data Sheets 02.01.31-2 (Ref.5), stiffness of the flats, μ_2, is obtained for various values of b/λ and fx/fo. f_x is the longitudinal compressive stress in the flat.

λ (ins.)	f_x ($\times 10^{-3}$) (lb.in^2)	μ_2 (lb.in./in.) A	B	D	F	Total + Stiffness (lb.in/in.)	Critical $f_x \times 10^{-3}$ (lb./in.^{2})
0.7	100.0	-2020	937	534	1500	951	103.0
	102.3	-2610	900	526	1480	296	
	104.0	-3390	825	513	1465	-587	
0.8	100.0	-2160	375	459	1280	- 46	100.0
1.0	93.0	- 905	8	418	1100	621	98.7
	98.0	-1290	-150	405	1100	65	
	100.0	-1460	-150	398	1100	-112	
1.2	98.0	-784	-150	378	1009	453	104.4
	100.0	-800	-187	371	965	349	
	105.8	-1044	-375	367	950	-102	
1.4	100.0	-397	- 94	364	934	807	111.0
	105.8	-505	-188	358	917	582	
	110.0	-870	-278	350	900	100	

+ $(A + B + D + F)\mu_2$

Minimum critical f_x = 98700 lb./in.^{2} at $\lambda \approx 1.0"$

(Buckling stress)

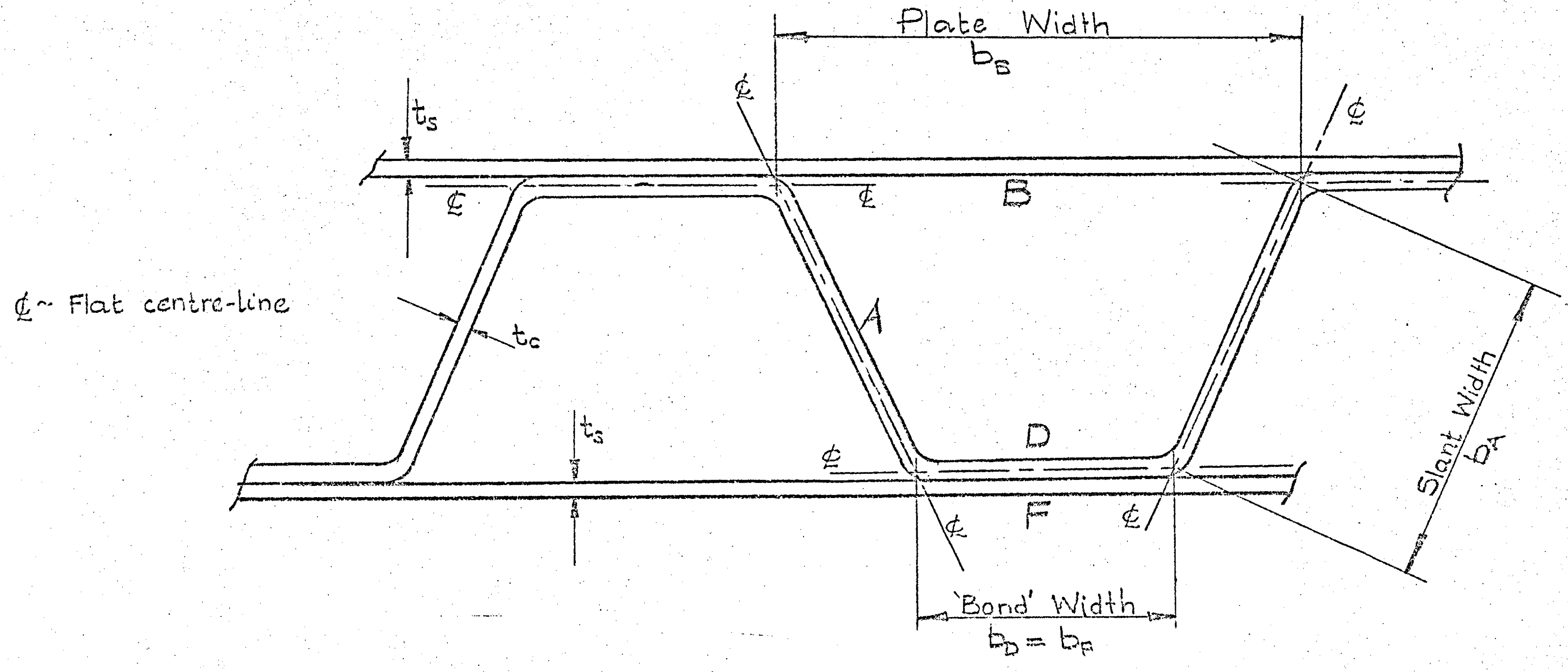

Fig. A3·1 Component Flat Notations and Width Measurements.

APPENDIX 4.

EXPERIMENTAL RECORDS

4.0 Introduction

Tables : A 4.1 - A 4.7

APPENDIX 4

EXPERIMENTAL RECORDS

4.0 Introduction

In this appendix, the experimental deflection readings taken during the testing of the panels are presented. Titles of the tables are self-explanatory.

Readings taken during the initial 'setting-up' runs for each of the specimens are not included.

Though deflection readings were taken at small load increments, all of them are not necessarily plotted on the load-deflection graphs. (See Appendix 2.)

Load (Tons)	Strain Gauge Readings.									
	0	1	2	3	4	5	6	7	8	9
00.5	001	001	-001	-001	002	000	000	000	000	000
10.0	105	109	103	104	100	104	103	103	102	92
20.0	197	198	193	198	196	187	200	198	196	189
30.0	287	287	281	291	289	273	295	291	288	283
40.0	378	378	371	385	382	361	390	385	382	378
50.0	466	468	458	479	476	448	486	479	475	472
60.0	550	563	548	578	575	540	587	575	573	566
65.0	589	610	591	626	624	584	639	621	622	610
70.0	629	661	633	678	674	629	693	666	673	653
75.0	671	716	674	733	727	677	753	712	732	699
77.0	689	739	689	757	748	696	778	730	757	719
79.0	706	763	702	781	769	715	804	748	781	737
81.0	723	791	714	810	794	735	830	768	807	757
83.0	742	818	725	837	817	753	855	788	832	777
85.0	760	843	733	865	840	769	880	807	855	798
87.0	779	874	734	898	867	783	906	827	881	818
89.0	800	910	724	941	898	791	933	849	906	841
90.0	810	924	717	959	911	793	944	859	917	852

Table A 4.1 : Strain Gauge Readings for Panel 5B/1.

.......(/contd. overleaf)...

.......(continued)..

Load (tons)	Strain Gauge Readings.									
	10	11	12	13	14	15	16	17	18	19
00.5	001	000	000	-001	001	000	001	000	000	002
10.0	90	63	69	75	80	86	64	65	69	90
20.0	190	151	161	172	175	180	157	158	162	179
30.0	288	246	255	270	270	275	252	253	257	271
40.0	387	343	350	370	365	370	347	349	354	364
50.0	486	440	445	469	460	465	441	446	450	457
60.0	587	541	542	574	557	562	538	546	550	552
65.0	635	590	588	625	205	609	584	596	599	596
70.0	677	639	637	678	652	656	628	647	647	640
75.0	729	691	688	734	706	704	676	703	697	683
77.0	750	713	710	757	729	723	695	728	718	701
79.0	767	735	731	780	752	740	714	751	737	716
81.0	784	758	753	806	776	760	735	776	758	726
83.0	801	781	773	832	799	779	756	799	781	738
85.0	816	803	792	859	820	796	776	822	802	745
87.0	826	827	809	891	841	813	797	846	823	741
89.0	827	851	822	932	859	828	821	870	846	721
90.0	826	861	828	950	866	835	831	881	856	710

Table A 4.1

Load (Tons)	Dial Gauge Readings (x 10^3) ins.		
	1	2	3
0.5	0.00	0.00	0.00
2.5	0.75	1.00	1.10
5.0	1.25	1.75	2.00
7.5	1.50	2.00	2.40
10.0	1.75	2.30	2.60
12.5	1.90	2.50	2.90
15.0	2.00	2.50	3.00
17.5	2.00	2.60	3.10
20.0	2.10	2.75	3.25
22.5	2.10	2.80	3.40
25.0	2.25	3.00	3.50
27.5	2.40	3.00	3.60
30.0	2.50	3.10	3.75
32.5	2.60	3.25	4.00
35.0	2.75	3.40	4.00
37.5	2.90	3.50	4.10
40.0	3.00	3.50	4.30
42.0	3.00	3.50	4.50
44.0	3.10	3.60	4.50
46.0	3.25	3.60	4.55
48.0	3.25	3.70	4.60
50.0	3.30	3.75	4.75
52.0	3.45	3.75	4.90
54.0	3.50	3.80	5.00
56.0	3.50	3.90	5.00
58.0	3.60	3.80	5.10
60.0	3.65	3.90	5.20
62.0	3.90	3.90	5.40
64.0	4.00	4.00	5.05
66.0	4.00	4.00	5.06
68.0	4.00	4.00	5.06
70.0	4.00	4.00	5.07
72.0	4.00	4.00	5.07
74.0	4.00	3.75	5.07
75.0	4.00	3.75	5.07

Table A 4.2 Dial Gauge Readings for Panel 5B/1

Load (Tons)	Contractometer Readings ($x10^3$) ins.		
	A	B	C
00.5	00.0	00.0	00.0
10.0	10.5	13.0	12.5
20.0	23.5	25.7	24.4
25.0	30.0	32.5	30.5
30.0	37.0	39.5	36.5
35.0	43.5	46.0	42.6
37.5	47.0	50.0	46.0
40.0	50.5	53.7	49.0
41.0	51.8	55.0	50.0
42.0	53.2	56.5	51.3
43.0	54.6	58.2	52.6
44.0	56.0	59.4	53.8
45.0	57.3	60.75	55.0
46.0	58.6	62.2	56.1
47.0	60.1	63.6	57.3
48.0	61.5	65.0	58.5
49.0	63.0	66.7	60.0
50.0	64.4	68.0	61.0
51.0	65.8	69.5	62.3
52.0	67.4	71.1	63.5
53.0	68.9	72.9	64.6
54.0	70.4	74.5	65.9
55.0	71.8	76.3	67.2
56.0	73.5	78.2	68.5
57.0	75.0	79.8	69.5
58.0	76.2	81.5	70.5
59.0	77.6	83.0	71.5
60.0	79.0	84.6	72.5
61.0	80.2	86.1	73.2
62.0	81.3	87.6	74.0
63.0	82.1	89.0	74.4
64.0	82.9	90.1	74.1
65.0	83.2	91.0	73.3
66.0	83.0	91.5	70.8
67.0	80.6	90.5	67.4

Table : A 4.3 : Contractometer Readings for Panel 5B/2

Load (Tons)	Contractometer Readings ($x\ 10^3$) ins.			
	A	B	C	D
0.5	00.0	00.0	00.0	00.0
2.0	1.0	2.3	1.0	2.7
4.0	3.0	5.5	2.6	6.2
6.0	5.0	8.4	4.5	9.3
8.0	7.4	11.2	6.3	12.7
10.0	10.0	14.3	8.1	16.5
12.0	12.5	17.2	10.0	20.8
14.0	15.0	20.4	12.0	27.0
15.0	16.4	21.8	13.0	31.4
16.0	18.0	23.6	14.0	38.0
16.5	20.0	24.4	15.0	43.5
17.0	20.6	24.8	15.6	48.0
17.5	21.5	25.2	16.2	52.0
18.0	22.4	25.5	17.0	57.0
18.5	23.2	25.5	17.6	60.0
19.0	24.0	25.4	18.5	64.5
19.5	24.6	24.9	19.3	67.8
20.0	25.2	24.0	20.2	71.8

Table A 4.4 : Contractometer Readings for Panel 2A/1.

Load (Tons)	Contractometer Readings ($x10^3$) ins.			
	A	B	C	D
00.2	00.0	00.0	00.0	00.0
1.0	0.9	0.0	1.0	0.1
2.0	2.0	0.0	1.8	0.9
3.0	3.1	0.6	2.6	2.1
4.0	4.5	1.6	3.5	3.75
4.2	4.9	1.85	3.75	4.0
4.4	5.1	2.1	4.0	4.5
4.6	5.4	2.25	4.1	4.75
4.8	5.6	2.5	4.25	5.0
5.0	6.0	2.7	4.5	5.4
5.2	6.2	3.0	4.7	5.75
5.4	6.5	3.15	5.0	6.0
5.6	6.8	3.4	5.1	6.5
5.8	7.4	3.8	5.7	7.25
6.0	7.6	4.0	5.9	7.5
6.2	7.9	4.2	6.1	7.8
6.4	8.15	4.4	6.3	8.1
6.6	8.5	4.6	6.5	8.5
6.8	8.75	4.9	6.65	8.75
7.0	9.1	5.4	7.0	9.1
7.2	9.25	5.4	7.1	9.25
7.4	9.5	5.6	7.25	9.5
7.6	9.8	5.9	7.5	9.9
7.8	10.1	6.15	7.6	10.1
8.0	10.4	6.4	7.85	10.5
8.2	10.7	6.6	8.0	10.75
8.4	11.0	7.0	8.2	11.0
8.6	11.25	7.25	8.4	11.25
8.8	11.5	7.5	8.6	11.5

Table A 4.5 : Contractometer Readings for Panel 2B/1

.......(/contd. overleaf)...

.... (continued)..

Load (Tons)	Contractotmeter Readings (x 10^3) ins.			
	A	B	C	D
9.0	11.75	7.75	8.8	11.75
9.2	12.0	8.0	9.0	12.0
9.4	12.4	8.25	9.25	12.4
9.6	12.65	8.5	9.5	12.5
9.8	13.0	8.75	9.7	12.75
10.0	13.25	9.0	10.0	13.0
10.2	13.6	9.3	10.2	13.1
10.4	13.9	9.6	10.4	13.3
10.6	14.2	9.9	10.5	13.0
10.8	14.5	10.1	10.8	13.5
11.0	14.8	10.4	11.0	13.6
11.2	15.1	10.7	11.2	13.75
11.4	15.4	11.0	11.5	13.75
11.6	15.7	11.2	11.6	13.75
11.8	16.0	11.5	12.0	13.75
12.0	16.3	11.8	12.0	13.75
12.2	16.6	12.1	12.4	13.75
12.4	17.0	12.4	12.5	13.75
12.6	17.3	12.65	12.8	13.4
12.8	17.6	13.0	13.0	13.2
13.0	18.0	13.4	13.4	12.75
13.2	18.7	13.9	13.9	12.0
13.4	19.1	14.1	14.0	11.7
13.6	19.4	14.4	14.3	11.5
13.8	19.8	14.65	14.5	11.0
14.0	20.2	15.0	14.85	10.75
14.2	21.0	15.6	15.5	10.2
14.6	21.8	16.25	16.0	9.5
15.0	22.5	16.8	16.6	9.0

Table A 4.5

....(/contd. overleaf).

.........(continued)....

Load (Tons)	Contractometer Readings (x 10^3) ins.			
	A	B	C	D
15.4	22.5	16.8	16.6	9.0
15.8	23.6	17.5	17.4	8.5
16.2	24.5	18.4	18.2	8.0
16.6	25.5	19.0	19.0	7.4
17.0	26.6	19.9	19.8	6.4
17.4	27.5	20.7	20.6	5.5
17.8	28.5	21.7	21.5	4.2
18.2	29.6	22.8	22.1	3.0
18.6	30.5	24.4	23.0	1.5
19.0	31.6	25.9	23.9	0.0
19.4	32.8	27.7	24.6	- 1.9
19.8	35.0	30.4	25.5	- 3.5
20.0	35.0	32.7	26.0	- 4.5
20.2	35.2	35.0	26.4	- 5.0
20.4	35.8	37.8	26.9	- 6.0
20.6	36.5	40.0	27.4	- 7.0
20.8	37.1	42.9	27.8	- 7.75
21.0	37.7	45.0	28.1	- 8.5
21.4	39.0	50.0	29.0	- 10.0
21.8	40.3	54.2	30.0	- 11.4
22.2	41.5	58.0	30.8	- 12.5
22.6	43.0	62.5	31.8	- 14.0
23.0	44.4	66.0	32.8	- 15.1
23.4	46.0	69.4	33.6	- 16.25
23.8	47.3	72.7	34.6	- 17.5
24.2	49.0	76.1	35.6	- 18.5
24.6	50.5	79.4	36.7	- 19.4
25.0	52.2	82.5	37.9	- 20.5
26.0	56.7	90.0	40.5	-

Table A 4.5

Load (tons)	Contractometer Readings ($\times 10^3$) ins.			
	A	B	C	D
00.5	00.0	00.0	00.0	00.0
1.0	0.6	0.6	0.0	0.4
2.0	2.1	2.1	0.5	2.0
3.0	3.6	3.6	1.4	3.25
4.0	5.0	5.0	2.25	4.6
5.0	6.6	6.5	3.1	6.0
6.0	8.1	7.7	4.0	7.0
7.0	9.6	9.1	5.25	7.9
8.0	11.1	10.4	6.4	8.6
9.0	12.5	11.8	7.25	9.0
10.0	14.0	13.3	8.5	9.0
10.5	14.9	14.15	9.1	8.8
11.0	15.6	15.15	9.8	8.25
11.5	16.4	16.25	10.5	7.9
12.0	17.1	17.5	11.1	7.6
12.5	17.8	18.6	11.8	7.5
13.0	18.65	20.15	12.5	7.4
13.5	19.5	21.6	13.3	7.4
14.0	20.0	22.5	14.0	7.4
14.5	21.1	23.3	14.75	7.4
15.0	22.0	24.0	15.6	7.4
15.5	22.9	24.6	16.5	7.4
16.0	23.7	25.0	17.4	7.4
16.5	24.6	25.5	18.2	7.4
17.0	25.5	26.0	19.25	7.4
17.5	26.5	26.6	20.3	7.1
18.0	27.5	27.0	21.2	7.0
18.5	28.5	28.0	22.5	6.6
19.0	29.5	28.0	23.5	6.4
19.5	30.4	28.7	24.6	5.5
20.0	31.4	29.4	25.6	3.6
21.0	33.2	30.0	27.75	- 1.2
22.0	35.0	31.6	30.0	- 6.5
23.0	37.0	33.2	32.2	-10.25
24.0	38.6	35.0	34.5	-18.4
25.0	40.2	37.0	36.8	-16.0

Table A 4.6 : Contractometer Readings For

Panel 2C/1

Load (Tons)	Contractometer Reading (x 10^3) ins.			
	A	B	C	D
00.5	00.0	00.0	00.0	00.0
1.0	0.6	0.4	0.5	0.5
2.0	1.9	1.4	1.4	2.0
3.0	3.15	2.5	2.5	3.0
4.0	4.6	3.5	3.4	4.4
5.0	6.1	4.65	4.4	5.5
6.0	7.35	5.9	5.4	6.6
7.0	8.8	7.3	6.4	7.75
7.5	9.4	7.9	6.9	8.25
8.0	10.0	8.5	7.4	8.75
8.5	10.6	9.2	7.9	9.1
9.0	11.2	10.0	8.5	9.6
9.5	11.9	10.9	9.0	10.2
10.0	12.5	11.6	9.5	10.6
10.5	13.2	12.4	10.1	11.0
11.0	13.8	13.25	10.7	11.4
11.5	14.5	14.0	11.2	11.9
12.0	15.0	14.8	11.85	12.25
12.5	15.6	15.5	12.4	12.5
13.0	16.2	16.5	13.0	12.75
13.5	16.9	17.4	13.5	12.75
14.0	17.5	18.6	14.1	12.9
14.5	18.1	20.1	14.5	12.4
15.0	18.8	23.1	15.4	10.75
15.5	19.5	27.6	16.1	8.4
16.0	20.4	32.4	16.8	6.0
16.5	21.0	36.4	17.5	4.1
17.0	22.0	41.6	18.25	1.5
17.5	22.6	45.6	19.0	- 0.0
18.0	23.5	50.5	19.7	- 2.5
18.5	24.4	54.6	20.4	- 4.5
19.0	25.1	59.5	21.3	- 6.6
19.5	26.0	63.6	22.0	- 8.25
20.0	27.1	68.1	22.9	-10.25
21.0	29.3	76.6	24.6	-13.5
22.0	31.1	84.4	26.4	-16.5
23.0	33.3	92.5	28.5	-19.1
24.0	35.3	99.8	30.4	-21.5
25.0	37.25	106.9	32.3	-23.6

Table A 4.7 : Contractometer Readings for Panel 2C/2.

APPENDIX 5.

VARIATION OF STIFFNESS DETERMINANT WITH COMPRESSIVE STRESS.

APPENDIX 5

VARIATION OF STIFFNESS DETERMINANT WITH COMPRESSIVE STRESS

5. Introduction

When the graph of buckling stress, σ , against half buckling wave-length, λ , was being plotted, it was found that a couple of values did not fall on the curve traced by the rest.

Study of the program output (See Tables A5.1 - A5.4) indicated that the computer program failed to locate "zero" stiffness determinant corresponding to the buckling stress of the panel in its primary buckling mode because the increment in stress was very big. However, the program did locate the "zero" stiffness determinant when λ was 1.25 ins. (See Fig.A5.1).

In the successive program runs, the increment in stress was kept small. Further study of the program output revealed that just prior to the "stiffness determinant" becoming negative, there was a small increase in the value of the determinant. Therefore, it was decided to study in detail the behaviour of stiffness determinant with increase in stress.

5.1 Detail Study

The computer program was modified to list the values of determinant against stress for λ = 1.25 ins. The program was run with data for panel 5B.

The variation of stiffness determinant with stress is shown by Fig.A5.2. Behaviour of stiffness determinant around 31,600 lb./in.^{2} and 35,200 lb./in.^{2} is shown in greater detail in Figs. A5.3 and A5.4 respectively.

5.1.2 Possible explanation for the behaviour of the stiffness determinant

To give an explanation for this behaviour, with authority, is not possible without further study. (See Section 7).

It is possible that one of the terms in the denominator of the determinant becomes zero, whilst other terms are slightly less than zero, thus giving a large but finite stiffness.

Other possibility is the existence of two buckling modes at approximately the same stress value. The inter-action between the two modes - one being symmetric and the other antisymmetric - could give rise to fluctuations in the stiffness determinant value.

5.2 Effect of λ on the Relationship Between the Stiffness Determinant and Stress

It is found that at higher values of λ, the variation of the value of stiffness determinant with stress is linear. (See Fig.A5.5).

5.3 Effect of Determinant Value on Deflections

The deflections are obtained for the case when unit rotation is introduced at point D. (See Section 2, para. 2.4.6).

From Table A5.5, it can be seen that at the buckling stress the value of the determinant becomes very large; this corresponds to a very large moment applied at point D to produce the unit rotation at the same point. Other deflections are nearly zero.

This suggests a buckling of a plate with one clamped edge and the other simply supported. This is just guessing at what is happening. Further work is necessary to determine what actually is happening. (See Section 7).

For this reason, the values of deflections computed for the specimens at low buckling wave-lengths cannot be relied upon.

SIGMA	DET	XLAMBDA	ZETA
0.30000E 05	0.72901E 15	0.11000E 01	0.10109E 01
0.45000E 05	0.50384E 15	0.11000E 01	0.15163E 01
0.60000E 05	0.13999E 15	0.11000E 01	0.20217E 01
0.75000E 05	0.11906E 16	0.11000E 01	0.25272E 01
0.90000E 05	0.21060E 16	0.11000E 01	0.30326E 01
0.10500E 06	0.11497E 16	0.11000E 01	0.35380E 01
0.12000E 06	0.87497E 15	0.11000E 01	0.40435E 01
0.13500E 06	0.73541E 15	0.11000E 01	0.45489E 01
0.15000E 06	0.65394E 15	0.11000E 01	0.50544E 01
0.16500E 06	0.61093E 15	0.11000E 01	0.55598E 01
0.18000E 06	0.60422E 15	0.11000E 01	0.60652E 01
0.19500E 06	0.64513E 15	0.11000E 01	0.65707E 01
0.21000E 06	0.76258E 15	0.11000E 01	0.70761E 01
0.22500E 06	-0.22318E 16	0.11000E 01	0.75815E 01
0.21100E 06	0.77283E 15	0.11000E 01	0.71098E 01
0.21200E 06	0.78274E 15	0.11000E 01	0.71435E 01
0.21300E 06	0.79189E 15	0.11000E 01	0.71772E 01
0.21400E 06	0.79962E 15	0.11000E 01	0.72109E 01
0.21500E 06	0.80495E 15	0.11000E 01	0.72446E 01
0.21600E 06	0.80634E 15	0.11000E 01	0.72783E 01
0.21700E 06	0.80138E 15	0.11000E 01	0.73120E 01
0.21800E 06	0.78618E 15	0.11000E 01	0.73457E 01
0.21900E 06	0.75430E 15	0.11000E 01	0.73794E 01
0.22000E 06	0.69463E 15	0.11000E 01	0.74131E 01
0.22100E 06	0.58711E 15	0.11000E 01	0.74468E 01
0.22200E 06	0.39327E 15	0.11000E 01	0.74804E 01
0.22300E 06	0.33314E 14	0.11000E 01	0.75141E 01
0.22400E 06	-0.67694E 15	0.11000E 01	0.75478E 01
0.22390E 06	-0.58038E 15	0.11000E 01	0.75445E 01
0.22380E 06	-0.49086E 15	0.11000E 01	0.75411E 01
0.22370E 06	-0.40778E 15	0.11000E 01	0.75377E 01
0.22360E 06	-0.33060E 15	0.11000E 01	0.75344E 01
0.22350E 06	-0.25881E 15	0.11000E 01	0.75310E 01
0.22340E 06	-0.19197E 15	0.11000E 01	0.75276E 01
0.22330E 06	-0.12968E 15	0.11000E 01	0.75243E 01
0.22320E 06	-0.71587E 14	0.11000E 01	0.75209E 01
0.22310E 06	-0.17354E 14	0.11000E 01	0.75175E 01
0.22300E 06	0.33314E 14	0.11000E 01	0.75141E 01

XLAMBDA	SIGMA(M)	DET(M)	DET(M-1)	SIGMA(M-1)
0.11000E 01	0.22300E 06	0.33314E 14	-0.17354E 14	0.22310E 06

THETA 1 TO 8

0.0924	0.4778	0.0768	-1.0070	-0.0956	-0.5214	-0.0911	1.0000

T	TJ	TP	BB	BS	BJ	BP	E
0.048	0.112	0.064	0.190	0.875	0.400	1.800	9700000.

Table A5.1 Failure of the Computer Program to Locate Zero Stiffness.

SIGMA	DET	XLAMBDA	ZETA
0.30000E 05	0.57135E 15	0.11500E 01	0.11049E 01
0.45000E 05	0.37806E 15	0.11500E 01	0.16573E 01
0.60000E 05	0.55332E 14	0.11500E 01	0.22097E 01
0.75000E 05	0.27999E 16	0.11500E 01	0.27621E 01
0.90000E 05	0.18171E 16	0.11500E 01	0.33146E 01
0.10500E 06	0.99387E 15	0.11500E 01	0.38670E 01
0.12000E 06	0.75211E 15	0.11500E 01	0.44194E 01
0.13500E 06	0.62751E 15	0.11500E 01	0.49719E 01
0.15000E 06	0.55171E 15	0.11500E 01	0.55243E 01
0.16500E 06	0.50579E 15	0.11500E 01	0.60767E 01
0.18000E 06	0.48448E 15	0.11500E 01	0.66291E 01
0.19500E 06	0.48964E 15	0.11500E 01	0.71816E 01
0.21000E 06	0.53117E 15	0.11500E 01	0.77340E 01
0.22500E 06	0.61441E 15	0.11500E 01	0.82864E 01
0.24000E 06	-0.25420E 17	0.11500E 01	0.88389E 01
0.22600E 06	0.61736E 15	0.11500E 01	0.83233E 01
0.22700E 06	0.61808E 15	0.11500E 01	0.83601E 01
0.22800E 06	0.61542E 15	0.11500E 01	0.83969E 01
0.22900E 06	0.60766E 15	0.11500E 01	0.84337E 01
0.23000E 06	0.59209E 15	0.11500E 01	0.84706E 01
0.23100E 06	0.56446E 15	0.11500E 01	0.85074E 01
0.23200E 06	0.51776E 15	0.11500E 01	0.85442E 01
0.23300E 06	0.43999E 15	0.11500E 01	0.85811E 01
0.23400E 06	0.30965E 15	0.11500E 01	0.86179E 01
0.23500E 06	0.85485E 14	0.11500E 01	0.86547E 01
0.23600E 06	-0.31832E 15	0.11500E 01	0.86915E 01
0.23590E 06	-0.26564E 15	0.11500E 01	0.86879E 01
0.23580E 06	-0.21625E 15	0.11500E 01	0.86842E 01
0.23570E 06	-0.16992E 15	0.11500E 01	0.86805E 01
0.23560E 06	-0.12641E 15	0.11500E 01	0.86768E 01
0.23550E 06	-0.85534E 14	0.11500E 01	0.86731E 01
0.23540E 06	-0.47093E 14	0.11500E 01	0.86694E 01
0.23530E 06	-0.10921E 14	0.11500E 01	0.86658E 01
0.23520E 06	0.23139E 14	0.11500E 01	0.86621E 01
0.23510E 06	0.55230E 14	0.11500E 01	0.86584E 01
0.23500E 06	0.85485E 14	0.11500E 01	0.86547E 01

XLAMBDA	SIGMA(M)	DET(M)	DET(M-1)	SIGMA(M-1)
0.11500E 01	0.23520E 06	0.23139E 14	-0.10921E 14	0.23530E 06

THETA 1 TO 8

0.0937	0.4936	0.0794	-1.0076	-0.0964	-0.5353	-0.0927	1.0000

T	TJ	TP	BB	BS	BJ	BP	E
0.048	0.112	0.064	0.190	0.875	0.400	1.800	9700000.

Table A5.2 Failure of the Computer Program to Locate Zero Stiffness.

SIGMA	DET	XLAMBDA	ZETA
0.30000E 05	0.45738E 15	0.12000E 01	0.12030E 01
0.45000E 05	0.28942E 15	0.12000E 01	0.18045E 01
0.60000E 05	0.37309E 13	0.12000E 01	0.24060E 01
0.75000E 05	0.34390E 16	0.12000E 01	0.30076E 01
0.90000E 05	0.16425E 16	0.12000E 01	0.36091E 01
0.10500E 06	0.88484E 15	0.12000E 01	0.42106E 01
0.12000E 06	0.66398E 15	0.12000E 01	0.48121E 01
0.13500E 06	0.55002E 15	0.12000E 01	0.54136E 01
0.15000E 06	0.47919E 15	0.12000E 01	0.60151E 01
0.16500E 06	0.43325E 15	0.12000E 01	0.66166E 01
0.18000E 06	0.40589E 15	0.12000E 01	0.72181E 01
0.19500E 06	0.39582E 15	0.12000E 01	0.78196E 01
0.21000E 06	0.40548E 15	0.12000E 01	0.84211E 01
0.22500E 06	0.44148E 15	0.12000E 01	0.90227E 01
0.24000E 06	0.48151E 15	0.12000E 01	0.96242E 01
0.25500E 06	-0.26766E 19	0.12000E 01	0.10226E 02
0.24100E 06	0.47588E 15	0.12000E 01	0.96643E 01
0.24200E 06	0.46580E 15	0.12000E 01	0.97044E 01
0.24300E 06	0.44921E 15	0.12000E 01	0.97445E 01
0.24400E 06	0.42295E 15	0.12000E 01	0.97846E 01
0.24500E 06	0.38198E 15	0.12000E 01	0.98247E 01
0.24600E 06	0.31806E 15	0.12000E 01	0.98648E 01
0.24700E 06	0.21699E 15	0.12000E 01	0.99049E 01
0.24800E 06	0.53026E 14	0.12000E 01	0.99450E 01
0.24900E 06	-0.22400E 15	0.12000E 01	0.99851E 01
0.24890E 06	-0.18887E 15	0.12000E 01	0.99811E 01
0.24880E 06	-0.15569E 15	0.12000E 01	0.99770E 01
0.24870E 06	-0.12433E 15	0.12000E 01	0.99730E 01
0.24860E 06	-0.94676E 14	0.12000E 01	0.99690E 01
0.24850E 06	-0.66620E 14	0.12000E 01	0.99650E 01
0.24840E 06	-0.40058E 14	0.12000E 01	0.99610E 01
0.24830E 06	-0.14896E 14	0.12000E 01	0.99570E 01
0.24820E 06	0.89525E 13	0.12000E 01	0.99530E 01
0.24810E 06	0.31568E 14	0.12000E 01	0.99490E 01
0.24800E 06	0.53026E 14	0.12000E 01	0.99450E 01

XLAMBDA	SIGMA(M)	DET(M)	DET(M-1)	SIGMA(M-1)
0.12000E 01	0.24820E 06	0.89525E 13	-0.14896E 14	0.24830E 06

THETA 1 TO 8

0.0946	0.5158	0.0836	-1.0045	-0.0958	-0.5376	-0.0904	1.0000

T	TJ	TP	BB	BS	BJ	BP	E
0.048	0.112	0.064	0.190	0.875	0.400	1.800	9700000.

Table A5.3 Failure of the Computer Program to Locate Zero Stiffness.

SIGMA	DET	XLAMBDA	ZETA
0.30000E 05	0.37315E 15	0.12500E 01	0.13054E 01
0.45000E 05	0.22588E 15	0.12500E 01	0.19580E 01
0.60000E 05	-0.26301E 14	0.12500E 01	0.26107E 01
0.59000E 05	-0.26748E 13	0.12500E 01	0.25672E 01
0.58000E 05	0.19584E 14	0.12500E 01	0.25237E 01
0.58100E 05	0.17417E 14	0.12500E 01	0.25280E 01
0.58200E 05	0.15237E 14	0.12500E 01	0.25324E 01
0.58300E 05	0.13044E 14	0.12500E 01	0.25368E 01
0.58400E 05	0.10838E 14	0.12500E 01	0.25411E 01
0.58500E 05	0.86188E 13	0.12500E 01	0.25455E 01
0.58600E 05	0.63868E 13	0.12500E 01	0.25498E 01
0.58700E 05	0.41415E 13	0.12500E 01	0.25542E 01
0.58800E 05	0.18829E 13	0.12500E 01	0.25585E 01
0.58900E 05	-0.38921E 12	0.12500E 01	0.25629E 01
0.59000E 05	-0.26748E 13	0.12500E 01	0.25672E 01

XLAMBDA	SIGMA(M)	DET(M)	DET(M−1)	SIGMA(M−1)
0.12500E 01	0.58900E 05	-0.38921E 12	0.18829E 13	0.58800E 05

THETA 1 TO 8

-0.0293	-0.8700	-0.3712	-1.0000	0.0292	0.8697	0.3711	1.0000

T	TJ	TP	BB	BS	BJ	BP	E
0.048	0.112	0.064	0.190	0.875	0.400	1.800	9700000.

Table A5.4 Failure of the Computer Program to Locate Zero Stiffness.

Det. value $x10^{-16}$	α $x10^{-3}$ p.s.i.	Deflections, θ							
		1	2	3	4	5	6	7	8
00.069	30.20	-.0004	-.0077	-.0074	-.0162	-.0869	-.0721	.0682	1
00.072	30.40	.0012	-.0042	-.0030	-.0113	-.0888	-.0757	.0641	1
00.075	30.60	.0031	.0002	.0002	-.0103	-.0911	-.0800	.0591	1
00.080	30.80	.0057	.0058	.0089	-.0074	-.0939	-.0856	.0528	1
00.087	31.00	.0093	.0133	.0175	-.0058	-.0977	-.0930	.0444	1
00.099	31.20	.0148	.0242	.0291	-.0093	-.1030	-.1034	.0327	1
00.119	31.40	.0251	.0427	.0460	-.0333	-.1112	-.1197	.0143	1
00.141	31.60	.0627	.0977	.0773	-.2355	-.1308	-.1585	-.0295	1
00.131	31.62	.0752	.1142	.0833	-.3188	-.1258	-.1683	-.0407	1
00.108	31.64	.0952	.1400	.0914	-.4585	-.1434	-.1830	-.0576	1
00.053	31.66	.2197	.3499	.2704	-.8414	-.1138	-.1240	.0091	1
-00.090	31.68	.2073	.3274	.2513	-.8064	-.0780	-.0515	.0900	1
-00.528	31.70	.2953	.5417	.5547	-.4030	.1034	.3086	.4971	1
-02.606	31.72	-.0142	.0138	.0843	.4449	-.1145	-.1285	.0061	1
-54.039	31.74	-.0713	-.0569	.0684	.8702	-.0954	-.0915	.0486	1
-18.724	31.76	-.0634	-.0465	.0720	.8165	-.0985	-.0976	.0417	1
-03.488	31.78	-.0403	-.0163	.0824	.6593	-.1076	-.1153	.0214	1
-01.557	31.80	-.0261	.0032	.0909	.5701	-.1139	-.1276	.0074	1
-00.124	32.00	.0278	.1005	.1809	.4489	-.1571	-.2150	-.0900	1
-00.038	32.20	-.0117	-.1182	-.2314	-.7461	.1818	.4788	.6786	1
-00.009	32.40	-.1849	-.4999	-.7100	-1.0826	.1295	.3826	.5645	1
00.006	32.60	-.1538	-.4241	-.6026	-.9394	.1945	.5100	.7092	1
00.015	32.80	-.1338	-.3573	-.5331	-.8460	.2374	.5933	.8402	1

Table A 5.5 : Variation of Deflections with Stress.

(Panel 5B, λ =1.25 ins.)

FIG. A5.1 FAILURE OF COMPUTER PROGRAM TO LOCATE 'ZERO' STIFFNESS IF INCREMENT IN STRESS IS TOO LARGE

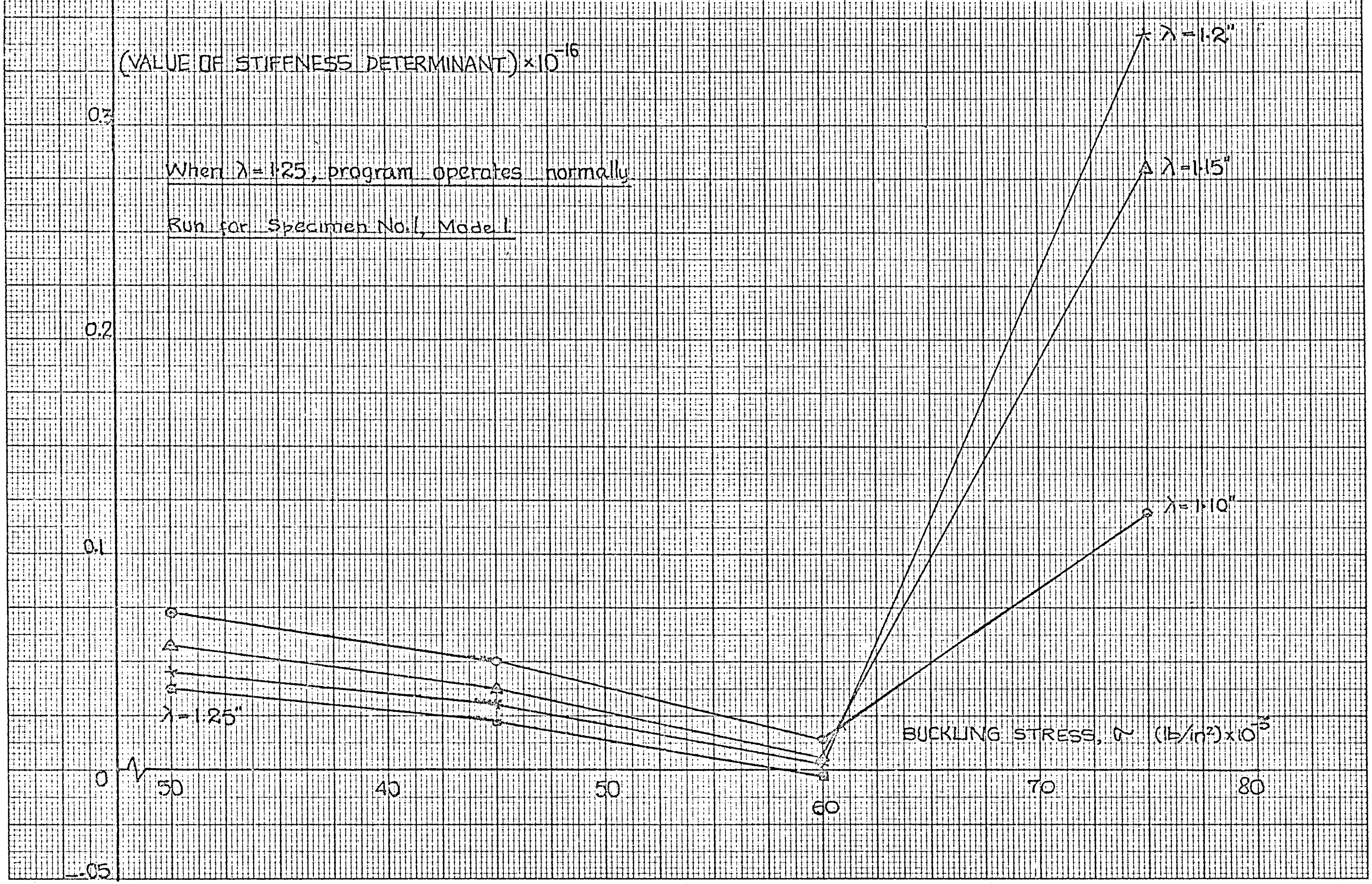

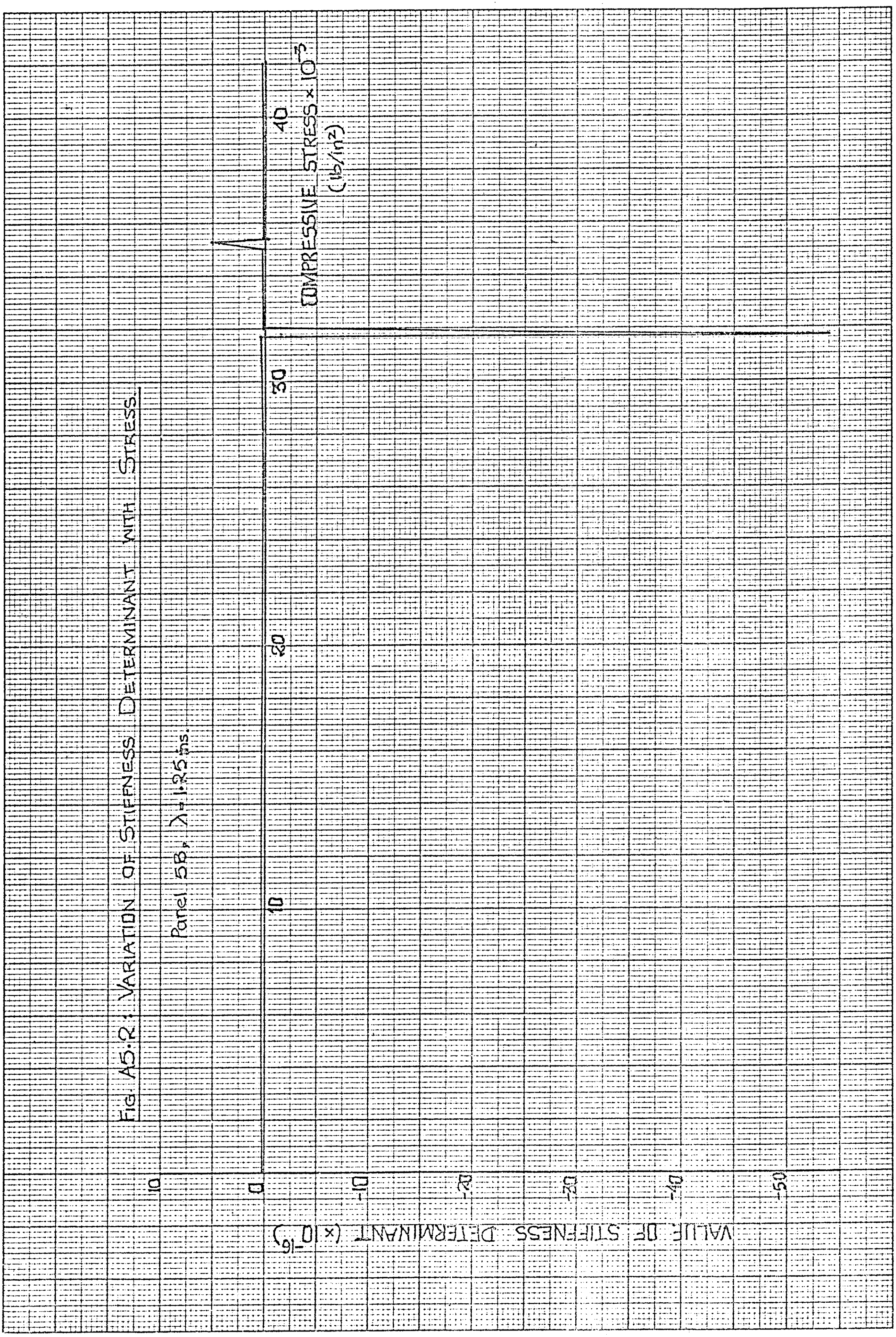

Fig. A5.2: Variation of Stiffness Determinant with Stress.

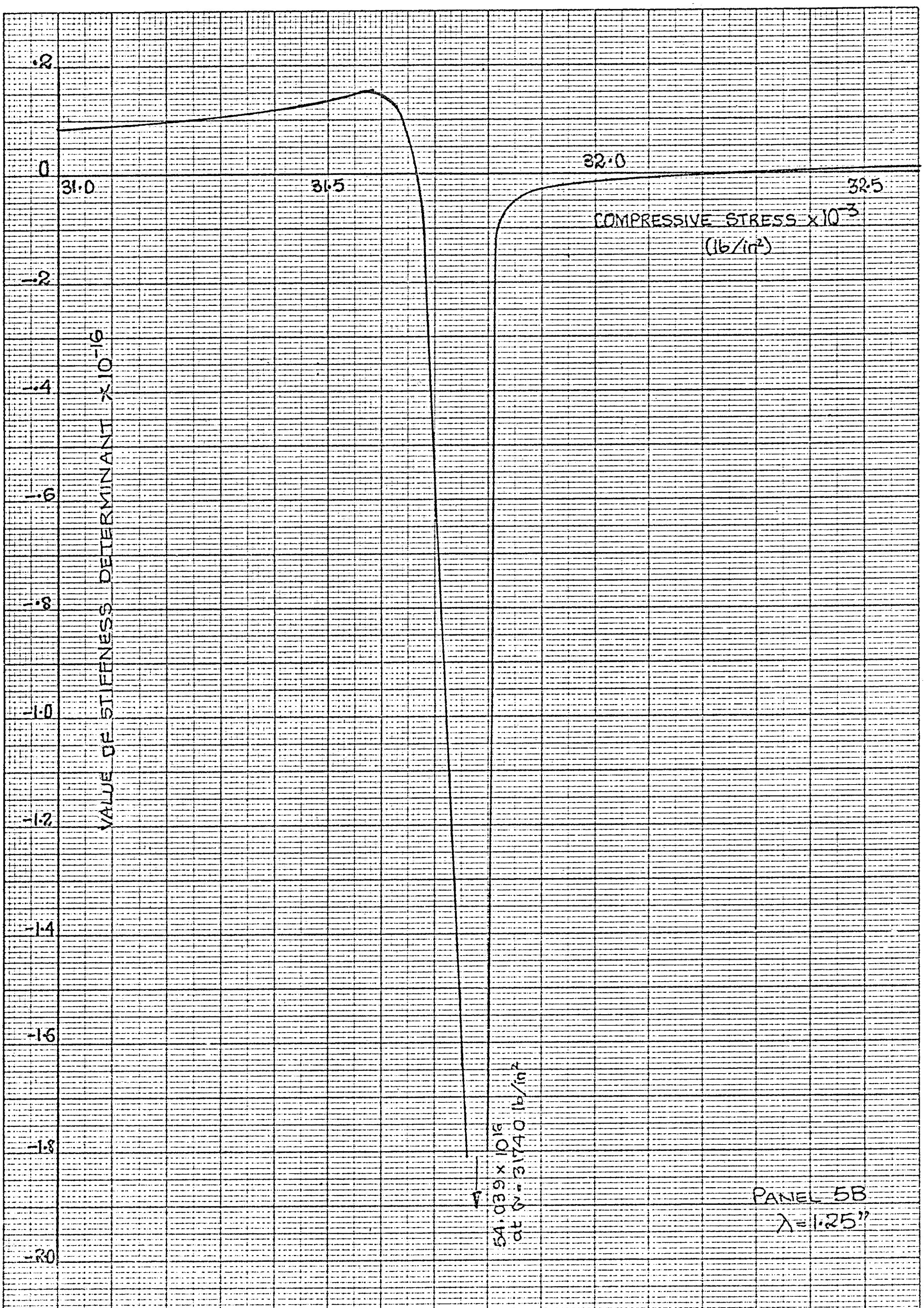

FIG. A5·3 : VARIATION OF STIFFNESS DETERMINANT WITH STRESS.

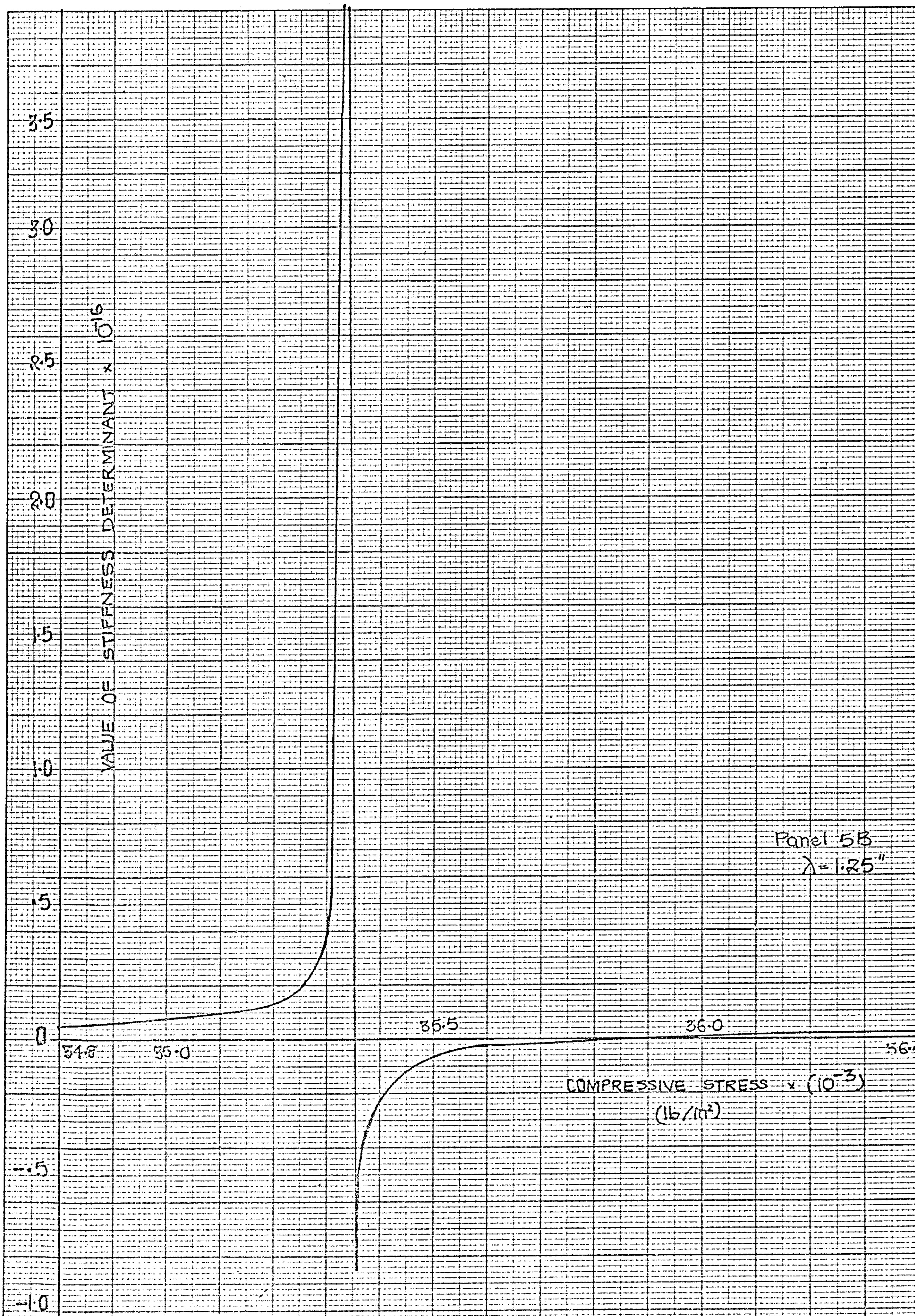

FIG. A5.4: VARIATION OF STIFFNESS DETERMINANT WITH STRESS

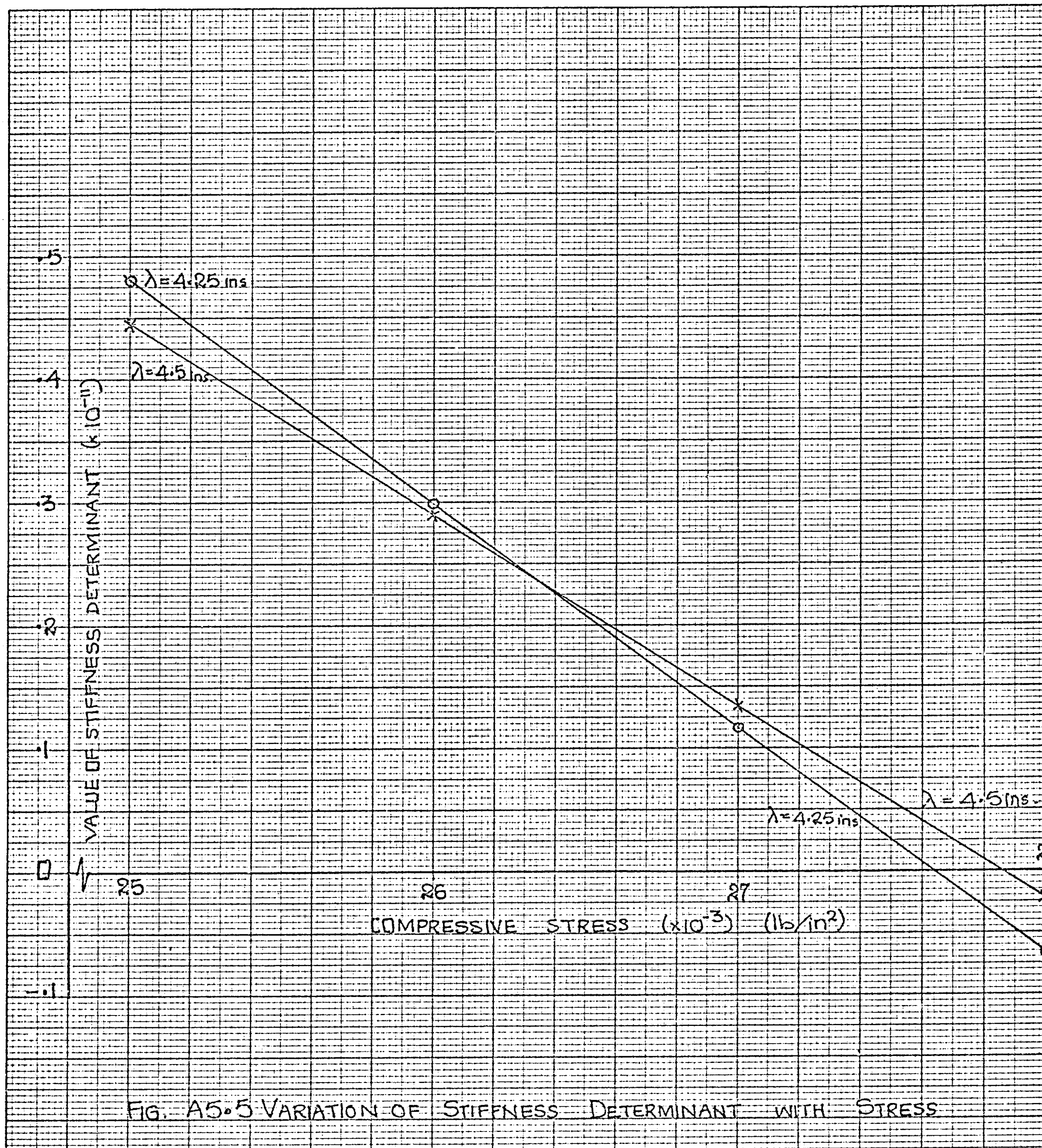

FIG. A5·5 VARIATION OF STIFFNESS DETERMINANT WITH STRESS